Space-time Spectral Methods for PDEs on Irregular Domains

by

C.P. Wilegoda Liyanage

A thesis submitted to the Faculty of Graduate Studies of
The University of Manitoba
in partial fulfilment of the requirements of the degree of

DOCTOR OF PHILOSOPHY

Department of Mathematics
University of Manitoba
Winnipeg

Abstract

Spectral methods are used to solve partial differential equations numerically. When the solution is analytic, the rate of convergence of the numerical solution is exponential; that is, the error decays exponentially. In time-dependent PDEs, low-order finite difference schemes and spectral schemes have traditionally been used for the time and spatial derivatives, respectively. However, applying spectral schemes in both space and time has been thought of recently. These methods have spectral convergence in both spatial and temporal domains. This study consists of two main parts.

The first part focuses on the analysis of space-time spectral methods for the stream function formulation of the unsteady Stokes equations. In this part, proofs of the condition number estimate and convergence analysis of the Stokes operator are discussed.

The second part of this study focuses on solving PDEs in irregular domains using space-time spectral collocation methods. One major drawback of classical spectral methods is their inability to handle irregularly shaped domains, which is why they have only been used sparingly in many engineering problems. In order to overcome this, we propose a numerical method to approximate the solution of PDEs in irregular domains using space-time spectral collocation methods. The main idea here is to embed the irregular domain in a regular one and extend the data from the physical domain to the larger regular domain. To achieve this, Huybrechs' method was implemented for 1D Fourier extension of the non-homogeneous term with

exponential accuracy. Further, we also successfully implemented a one-dimensional non-periodic extension by modifying the Huybrechs' method. For 2D domains, a new method named 'Alternating Non-periodic Extension' was developed. This algorithm uses non-periodic extensions combined with domain embedding to achieve a practical solution methodology. Implementations for the 2D Poisson, Heat, Wave, unsteady Stokes, Allen–Cahn, Schrödinger and Navier–Stokes equations on convex and non-convex domains demonstrate spectral convergence. Convergence analysis of this non-periodic extension is also discussed in this part.

Acknowledgements

I take this opportunity to express my gratitude to the people who have been instrumental in the successful completion of this project. I would like to extend my appreciation especially to the following.

First and foremost, my heartfelt gratitude and sincere thanks go to my supervisor Prof. Shaun Lui, Dept. of Mathematics, University of Manitoba, who helped me through this project consistently and, I highly appreciate his constant guidance, motivation, enthusiasm, immense knowledge and dedication to help me to understand this project profoundly. I am also very thankful to him for giving me much of his precious time carefully supervising and guiding me throughout my study. Without his guidance and help, this research would not be possible, and for that, I am forever grateful.

I am also sincerely grateful to my advisory committee members, Prof. Mikael Slevinsky and Prof. Parimala Thulasiraman, for their valuable advice and guidance, which significantly improved the quality of this work.

In addition, I extend my sincere thanks to my external examiner, Prof. Raymond Spiteri, for taking the time to carefully review my thesis and for his insightful questions, comments, and suggestions, all of which were invaluable in improving and strengthening this work.

I also wish to thank the financial support provided by UMGF, Department of Mathematics, and the Faculty of Graduate Studies at the University of Manitoba as

well as my supervisor's NSERC grant throughout my years of study.

I further extend my appreciation to my parents, brothers and sisters for their endless support even after I moved across the world to pursue my studies. Last but not least, my deepest appreciation goes to my loving husband, who has been a true pillar of strength, providing constant support and encouragement throughout my academic journey.

I dedicate this thesis to my beloved husband, my parents and to my family. For the blessings, encouragement, and support they have given me throughout this endeavour, I am truly grateful.

Contributions of Author

The work of this thesis is based on manuscripts in preparation.

Chapter 2 is a part of a manuscript in preparation co-authored with Prof. Shaun Lui. The condition number estimate of the space-time spectral scheme of the Stokes operator, as well as proof of spectral convergence, are new in the literature.

Chapter 3 is a version of a manuscript in preparation co-authored with Prof. Shaun Lui. The one-dimensional non-periodic extension and two-dimensional Alternating non-periodic extension are new methods. We are not aware of any papers proving spectral convergence of solutions of time-dependent PDEs using domain embedding methods.

Some parts of Chapter 3 are a part of a conference article submitted and accepted for publication coauthored with Prof. Shaun Lui, Dr. Sarah Nataj and Dr. Avleen Kaur.

Contents

List of Figures

List of Tables

1

Introduction

Time-dependent partial differential equations (PDEs), such as the unsteady Stokes, Navier–Stokes, and diffusion equations, are used to model many real-world physical phenomena. In particular, accurate and stable solutions to these equations are critical in areas like fluid dynamics, heat transfer, and biomedical flow simulations. Spectral methods are well known for their high accuracy when applied to problems with analytic solutions. In such cases, the error in the numerical solution decays exponentially with respect to the number of basis functions. This makes spectral methods especially attractive in scientific computing applications where high precision is required.

Traditionally, time-dependent PDEs are solved using a combination of low-order finite-difference methods for time derivatives and spectral methods for spatial discretization. However, this mismatch in discretization accuracy often leads to the temporal error dominating the overall solution error, limiting the benefits of using spectral methods in space. To overcome this, there has been growing interest in space-time spectral methods that apply spectral discretization in both space and time. These methods aim to address the limitations of the traditional approach by using spectral schemes for both spatial and temporal derivatives. This advance-

ment allows for more efficient and accurate numerical solutions, particularly for time-dependent problems, by ensuring that both spatial and temporal errors decay exponentially, leading to higher overall convergence rates.

Despite these advantages, one major drawback of classical spectral methods is their inability to handle irregularly shaped domains, which is why they have only been used sparingly in engineering problems. In practice, many physical and engineering problems involve irregular domains, which may include curved boundaries, holes, or non-convex shapes. Classical spectral schemes struggle in these settings because they rely on global basis functions defined on standard shapes like rectangles or disks. While there have been many attempts to use classical spectral methods for elliptic PDEs in irregular domains, there are far fewer studies on spectral collocation methods for time-dependent PDEs in complex geometries. Therefore, the development of a method that combines the high accuracy of space-time spectral schemes with the flexibility to handle irregular domains represents a significant and timely advancement in the numerical solution of time-dependent PDEs.

The goal of this thesis is to develop, analyze, and validate a high-order accurate space-time spectral collocation method for solving time-dependent partial differential equations on irregular domains. By an irregular domain, we mean a domain that is neither a square nor a disk, so that standard spectral methods cannot be applied directly. In the first part of the thesis, we establish the numerical stability of the space-time spectral scheme by analyzing the condition number of the discrete unsteady Stokes operator. We then prove spectral convergence of the Stokes operator using Chebyshev collocation in both space and time. These results ensure that the space-time spectral methods are both stable and accurate on regular domains. A central contribution of the thesis is the development of a new non-periodic extension algorithm, which enables the approximation of solutions to time-dependent PDEs in irregular domains using space-time spectral collocation. Finally, we demonstrate the

accuracy and robustness of the proposed method through a broad set of numerical experiments covering a variety of domain shapes and model equations.

The main idea of our proposed method is to embed the irregular domain in a regular one. Initially, we assume the non-homogeneous term is analytic and periodic in the extended domain. We use the Fourier spectral method to solve the PDE on regular geometry and observe spectral error convergence in both linear and nonlinear PDEs. Then we assume that the non-homogeneous term is only known in the physical domain and perform an extension of the non-homogeneous term to the extended domain. We implemented Boyd's technique [15] for this Fourier extension and observed super-algebraic convergence only.

Next we applied the method introduced by Huybrechs [58, 59] to extend the non-homogeneous term of the PDE from the physical domain to the regular domain with exponential accuracy. In the 1D case, the fundamental idea is to achieve a spectrally accurate Fourier series by extending a non-periodic analytic function f, defined on the interval $[-1, 1]$, into a periodic function over a larger interval $[-T, T]$, for some $T > 1$. Huybrechs [58] extended his Fourier extension from the domain $[-1, 1]$ to $[-2, 2]$. The periodic extension of f from an arbitrary domain $[-a, b]$ to $[-T, T]$ can be achieved by applying a scaling to the Huybrechs method. We have implemented 1D Poisson and Heat equations using this Fourier extension and observed spectral error convergence. To solve these PDEs we can use either Chebyshev or Fourier spectral collocation methods.

Next we introduced an algorithm, Alternating Fourier Extension, that can be used for the two-dimensional Fourier extension. In this method, we combine both techniques; 1D Fourier extension and domain embedding. The basic idea of this algorithm is to embed the complex geometry in a larger, regular (rectangular) domain and then apply the Fourier extension in both the x and y directions separately until the periodicity error in both directions is very small. We implemented the 2D Poisson

equation defined in the square physical domain $(-1,1)^2$, embedded it in a larger domain $(-2,2)^2$, and then applied Alternating Fourier Extension. Here we observed spectral error convergence.

However, we observed spikes appearing in corners of the extended domain when applying the Alternating Fourier Extension for a non-rectangular physical domain. We were able to overcome this issue by implementing a non-periodic extension, which we termed the Alternating Non-Periodic Extension. The basic concept of this new algorithm is similar to the Alternating Fourier Extension. Here, we combined both techniques; 1D non-periodic extension and domain embedding. The basic idea of this algorithm is to embed the complex geometry in a larger, regular (rectangular) domain $(-1,1)^2$ and then apply only one non-periodic extension in both the x and y directions. We have implemented the 2D Poisson equation, Heat equation, steady and unsteady Stokes equations, Allen–Cahn equation, Schrödinger equation and Navier–Stokes equations defined in convex as well as non-convex irregular domains. Spectral error convergence is observed in each instance. Further, convergence analysis of the non-periodic extension for the one-dimensional and two-dimensional Poisson, Heat, Stokes and Wave equations is discussed.

An outline of the thesis is given in the remainder of this introductory chapter.

In Chapter 2, we present the necessary mathematical preliminaries, space-time spectral methods for solving the stream function formulation of unsteady Stokes equations and proofs of the condition number estimate and convergence analysis of the Stokes operator.

In Chapter 3, we introduce methods to approximate the solution of PDEs in irregular domains using space-time spectral collocation. Alternating Fourier Extension and Alternating Non-Periodic Extension are introduced for the two-dimensional periodic and non-periodic extensions, respectively. Further, the convergence analysis of the non-periodic extension, as well as the uniqueness of the solution on the

extended domain, are discussed.

In Chapter 4, numerical experiments done in MATLAB are shown to demonstrate the accuracy and efficiency of space-time spectral methods for solving PDEs in irregular geometry.

This thesis concludes in Chapter 5 with discussions of future directions.

The main contributions of the thesis are as follows:

- Condition number analysis: We derive a condition number estimate of the space-time spectral scheme of the 2D unsteady Stokes operator, using its stream function formulation.

- Spectral convergence: We prove spectral convergence for the 2D unsteady Stokes equation using Chebyshev collocation in both space and time.

- Non-periodic extension algorithm: We propose a new algorithm for non-periodic extension from irregular domains to regular ones, extending and improving on existing methods by Boyd and Huybrechs. We also prove spectral convergence of solutions of time-dependent PDEs using domain embedding methods.

- Numerical validation: Numerical experiments confirm exponential convergence on both convex and non-convex irregular domains, demonstrating the robustness and accuracy of the method.

2

Space-Time Spectral Methods

2.1 Literature Review

Spectral methods are among the most important and dominant methods that are used to solve ODEs and PDEs relating to various physical phenomena. They apply global smooth functions to approximate solutions of ODEs and PDEs. The main advantage is that, for elliptic differential equations which have an analytic solution, the rate of convergence of the numerical solution is an exponential function of the number of basis functions that are used. While Legendre or Chebyshev polynomials could be used as basis functions for non-periodic boundary conditions, it is more practical to use trigonometric polynomials when boundary conditions are periodic. In spectral collocation, an interpolating polynomial is used to approximate a given ODE or PDE at a set of interior collocation points, called Gauss-Lobatto points.

Two of the early studies on space-time spectral methods are [88] and [87]. These works explain how to apply space-time spectral methods for PDEs with periodic boundary conditions. Other references include [85, 67, 96, 97] and the references therein. These works use Gauss-Lobatto quadrature and Gaussian quadrature based collocations for space and time, respectively.

Space-time spectral methods employ spectral discretization in both space and time. See [89, 73, 75] and [74]. When the solution is analytic, exponential decay of the numerical error can be observed as the number of spectral modes increases. Numerical spectral convergence of space-time spectral methods has been demonstrated by some researchers. The first rigorous condition number estimate for the heat equation first appeared in [73], where a simpler time discretization was also proposed. In [74], they analyzed the method replacing Legendre polynomials by Chebyshev polynomials. They further analyzed this scheme for various time-dependent PDEs in [75].

One major drawback of space-time spectral methods is that time stepping cannot be implemented. Unknowns have to be solved for all times simultaneously. There have been many works that attempted to overcome the inability of time stepping. See [30, 39, 57] and references therein for such attempts thereof. See [37] to obtain an overview of four different time parallel methods. Moreover, references [9, 15], [43] and [51] are some excellent works that review theory and practice of spectral methods.

2.2 Basic notation and preliminaries

Let us briefly summarize the matrix notations that frequently appear in space-time spectral methods. The $n \times n$ identity matrix is denoted by I_n. Consider a square matrix M of size $n \times n$. Another matrix $[M]$ of size $(n-1) \times (n-1)$ is obtained by removing the last row and column of M. Similarly, $[[M]]$ of size $(n-2) \times (n-2)$ is obtained by removing the first and last rows and columns of M. The transpose and complex conjugate transpose of M is denoted by M^T and M^* respectively. Also, let $\overline{a}$ denote the complex conjugate for any complex number a and, $\Re(a)$ and $\Im(a)$ denotes real and imaginary parts of the complex number a thereof. Two vector/matrix norms,

namely, the 2-norm and the ∞-norm, are denoted by $|\cdot|$ and $|\cdot|_\infty$ respectively. Let $diag(v)$ denote a diagonal matrix whose diagonal entries comprise of elements from vector v. Let $\mathbb{M}$ denote $\mathbb{R}$ or $\mathbb{C}$.

Definition 2.1. The Kronecker (tensor) product of the matrix $A \in \mathbb{M}^{p\times q}$ with the matrix $B \in \mathbb{M}^{r\times s}$ is defined as

$$A \otimes B = \begin{bmatrix} a_{11}B & \cdots & a_{1q}B \\ \vdots & \vdots & \vdots \\ a_{p1}B & \cdots & a_{pq}B \end{bmatrix} \in \mathbb{M}^{pr\times qs}.$$

Two theorems that will be instrumental for this study are given below.

Theorem 2.2. Let $A \in \mathbb{M}^{m\times m}$ and $B \in \mathbb{M}^{n\times n}$. Furthermore, let $\lambda \in \Lambda(A)$ with corresponding eigenvector x, and $\mu \in \Lambda(B)$ with corresponding eigenvector y. Then $\lambda\mu$ is an eigenvalue of $A \otimes B$ with corresponding eigenvector $x \otimes y$. Any eigenvalue of $A \otimes B$ arises as such a product of eigenvalues of A and B.

It follows directly that if $A \in \mathbb{M}^{m\times m}$ and $B \in \mathbb{M}^{n\times n}$ are positive (semi) definite matrices, then $A \otimes B$ is also positive (semi) definite.

Theorem 2.3. Let $A \in \mathbb{M}^{m\times m}$ and $B \in \mathbb{M}^{n\times n}$. Furthermore, let $\lambda \in \Lambda(A)$ with corresponding eigenvector x, and $\mu \in \Lambda(B)$ with corresponding eigenvector y. Then $\lambda + \mu$ is an eigenvalue of $(I_n \otimes A) + (B \otimes I_m)$ with corresponding eigenvector $y \otimes x$. Any eigenvalue of $(I_n \otimes A) + (B \otimes I_m)$ arises as such a sum of eigenvalues of A and B.

Definition 2.4. For any matrix $A \in \mathbb{M}^{m\times n}$ define

$$vec(A) = (a_{11}, \cdots, a_{m1}, a_{12}, \cdots, a_{m2}, \cdots, a_{1n}, \cdots, a_{mn})^T.$$

That is, columns of matrix A are ordered one below the other to construct a vector of length mn. The Kronecker product can be utilized to transform a linear

matrix equation to an equation which is a combination of matrices and vectors. For example,

$$AX + YB = C \quad \Leftrightarrow \quad (I \otimes A)vec(X) + (B^T \otimes I)vec(Y) = vec(C).$$

Further, $(X \otimes Y)z = vec(YZX^T)$ for matrices $X \in \mathbb{M}^{n\times n}$, $Y \in \mathbb{M}^{m\times m}$ and $z \in \mathbb{M}^{mn}$. Here $vec(Z) = z$, is the vector representation of Z.

Let N be some positive integer and P_N denote the space of polynomials of degree at most N. For polynomials in two variables x and t, P_N denotes polynomials in x of degree at most N for a fixed t, and in t of degree at most N for a fixed x. Let T_N denote the Nth degree Chebyshev polynomial and x_j be the zeros of the polynomial $(1-x^2)T_N'(x)$. We shall take $x_0 = 1$, $x_N = -1$ and $x_1, \ldots, x_{N-1}$ as the descending zeros of the function thereof. The set $x_0, \ldots, x_N$ is defined as Chebyshev Gauss-Lobatto nodes in space. Similarly, the Chebyshev Gauss-Lobatto nodes along the t axis are denoted by $\{t_k\}$. Let

$$x_h = \begin{bmatrix} x_1 \\ \vdots \\ x_{N-1} \end{bmatrix} \qquad t_h = \begin{bmatrix} t_0 \\ \vdots \\ t_{N-1} \end{bmatrix}$$

Note that x_h excludes both boundary points x_0 and x_N, while t_h excludes only the initial point $t_N = -1$. For $0 \le j \le N$, let ℓ_j be the Lagrange polynomial interpolant in x_j and degree N so that $\ell_j(x_k) = \delta_{jk}$. It will be worth remembering that D, the Chebyshev pseudospectral derivative matrix is defined as,

$$D_{jk} = \frac{d\ell_k(x_j)}{dx}, \quad 0 \le j, k \le N.$$

Further, let d_h denote the first N entries of the last column of D. That is, $d_h = D(0 : N-1, N)$. For any continuous u in x, the Chebyshev interpolation operator

is defined as,

$$\mathcal{L}_N u = \sum_{j=0}^{N} u(x_j)\ell_j. \tag{2.1}$$

Let us also briefly remember a property of the Chebyshev quadrature. Consider any polynomial of degree less than or equal to $2N-1$. We may write,

$$\int_{-1}^{1} v(x)w(x)dx = \sum_{k=0}^{N} v(x_k)\rho_k, \qquad w(x) = \frac{1}{\sqrt{1-x^2}},$$

where ρ_k is the set of weights pertaining to Chebyshev Gauss-Lobatto quadrature. The $(N+1)\times(N+1)$ diagonal matrix W_h has $\{\rho_k\}$ as its diagonal entries. A continuous function v on $\Omega := (-1,1)^2$ will have the weighted L^2-norm of

$$\|v\| := \left(\int_{\Omega} |v(x,t)|^2 w(x)w(t)dxdt\right)^{1/2}.$$

The discrete norm corresponding to v is,

$$\|v\|_N := \left(\sum_{j,k=0}^{N} \rho_j\rho_k |v(x_j,t_k)|^2\right)^{1/2}.$$

For all such polynomials v of degree at most N, it is observed that discrete and weighted L^2-norms are equivalent:

$$\|v\| \le \|v\|_N \le 2\|v\|. \tag{2.2}$$

If v is a single variable function, the weighted L^2-norm is also denoted by

$$\|v\| := \left(\int_{-1}^{1} |v(x)|^2 w(x)dx\right)^{1/2}.$$

2.3 Space-time collocation method

Let us discuss a space-time spectral collocation to one of the simplest PDEs, the one-dimensional heat equation. The spatial and temporal domains are taken as $(-1, 1)$. While $(-1, 1)$ may seem unorthodox for a temporal domain, there is no loss of generalization and it is evident that a simple transformation would suffice to accomplish this. Now consider the 1D heat equation

$$u_t = u_{xx} + f(x, t) \ \ on \ \ (-1, 1)^2, \tag{2.3}$$

with boundary conditions $u(\pm 1, t) = 0$ and initial condition $u(x, -1) = u_0(x)$. We will calculate a numerical solution $u \in P_N$ at $t = 1$. The spectral equations are

$$(I_{N+1} \otimes D)u_h = (D^2 \otimes I_{N+1})u_h + f_h,$$

where u_h and f_h are the vectors of u and f, respectively, evaluated at the collocation points. We obtain two vectors $\hat{u}_h$ and $\hat{f}_h$ by removing the corresponding boundary and initial points from u_h and f_h, respectively. The linear equation can now be written as

$$A_h\hat{u}_h = \hat{f}_h - (u_{0h} \otimes d_h), \quad A_h = (I_{N-1} \otimes [D]) - ([[D^2]] \otimes I_N). \tag{2.4}$$

Let U_h and F_h be $N \times (N-1)$ matrices and, $vec(U_h) = \hat{u}_h$ and $vec(F_h) = \hat{f}_h - (u_{0h} \otimes d_h)$. Then equation (2.4) is equivalent to the Sylvester equation $[D]U_h - U_h[[D^2]]^T = F_h$ which can be solved by the algorithm of Bartels and Stewart in $O(N^3)$ operations. Observe that all unknowns over all times must be solved simultaneously.

Next, the spectral condition number estimate and spectral convergence of the heat

equation will be briefly discussed. The spectral condition number is defined by,

$$\kappa(M) = \frac{max_{\lambda \in \Lambda(M)}|\lambda|}{min_{\lambda \in \Lambda(M)}|\lambda|},$$

where $\Lambda(M)$ is the spectrum of matrix M. A few important lemmas (see [74]) relating to the condition number are mentioned below.

Lemma 2.5. Let $N \geq 1$. Then the real part of every eigenvalue of $[D]$ is larger than some positive constant independent of N.

Lemma 2.6. Let $N \geq 1$ and λ be an eigenvalue of $[D]$. Then $|\lambda| \leq cN^2$.

The next lemma is well known; see [91].

Lemma 2.7. Let $N \geq 2$. Then the eigenvalue of $-[[D^2]]$ are real, bounded below by c and above by CN^4, where c and C are positive and independent of N.

The following theorem gives an estimation of spectral condition number of the discrete spectral differentiation operator A_h. The proof relies on the above Lemmas.

Theorem 2.8. [75] Let $N \geq 2$. Let A_h be the Chebyshev spectral collocation matrix defined by (2.4) and λ be an eigenvalue of A_h. Then

$$c \leq |\lambda| \leq CN^4.$$

Consequently,

$$\kappa(A_h) \leq CN^4.$$

Further, below theorem shows the spectral convergence of the heat equation.

Theorem 2.9. [75] For any integer $N \geq 2$, let u be the solution of the heat equation (2.3). Assume that $u(x,t)$ is separately analytic in each variable. Define the error

vector E_h as the difference of u evaluated at the collocation points and $\hat{u}_h$. Then

$$\left|W^{1/2}E_h\right|_2 \leq cN^{3.5}e^{-CN}.$$

Spectral convergence and condition number estimates for other linear PDEs are shown in [75], [74].

2.4 Stokes Problem

The Stokes equations are a linearized version of the Navier–Stokes equations and model incompressible viscous fluid flow with low Reynolds number. The typical approach to solve such time-dependent PDEs is to use a low order scheme such as a finite difference method for the time derivative and a spectral scheme for the spatial derivative. In this study, we analyze a space-time spectral method for the stream function form of the unsteady Stokes equations, which converges exponentially in both space and time. The main objectives of the research are estimating the condition number of the unsteady Stokes operator and proving the spectral convergence of this scheme in space and time.

Let Ω be a bounded domain in $\mathbb{R}^2$ with a Lipschitz boundary. The velocity field, denoted by u, is a vector quantity. We consider $u \in V := (H_0^1(\Omega))^2 = H_0^1(\Omega) \times H_0^1(\Omega)$. The pressure, denoted by p, is a scalar quantity. We consider $p \in L_0^2(\Omega)$, where

$$L_0^2(\Omega) := \left\{ q \in L^2(\Omega) | \int_\Omega q = 0 \right\}.$$

The norm of p is given as,

$$\|p\|_0 = \left[\int_\Omega |p|^2 \right]^{1/2}, \tag{2.5}$$

and the inner product on the space $L_0^2(\Omega)$ is defined to be the same as that for $L^2(\Omega)$,

which is given by

$$(u, v)_0 := \int_\Omega uv, \quad \forall u, v \in L^2(\Omega).$$

The following two bilinear forms are defined for $u, v \in V$ and $q \in L^2_0(\Omega)$,

$$a(u, v) : = \int_\Omega \nabla u \cdot \nabla v = \sum_{i=1}^{2} \int_\Omega \nabla u_i \cdot \nabla v_i \tag{2.6}$$

$$b(q, v) : = - \int_\Omega q(\nabla \cdot v). \tag{2.7}$$

The bilinear form $a(u, v)$, for all $u = (u_1, u_2), v = (v_1, v_2) \in V$, is an inner product on the space V. The norm on the space V is denoted by $\|\cdot\|$ and it is defined for all $u = (u_1, u_2) \in V$ as,

$$\|u\| := \sqrt{a(u, u)} = \left[\int_\Omega |\nabla u_1|^2 + |\nabla u_2|^2 \right]^{1/2}. \tag{2.8}$$

Definition 2.10 (Inverse Laplacian)**.** The inverse Laplacian is denoted by $\Delta^{-1} : (H^{-1}(\Omega))^2 \to V$. Let $u \in (H^{-1}(\Omega))^2$, we say $\Delta^{-1}u = v \in V$ if

$$\begin{aligned} \Delta v &= u \quad \text{in} \quad \Omega, \\ v &= 0 \quad \text{on} \quad \partial\Omega. \end{aligned}$$

Here, Δ is the vector Laplacian as $v \in V$ is a vector having two components. Now, we define $V^{'}$ as the dual of the space V, thus, $V^{'} := (H^{-1}(\Omega))^2$. The norm on $V^{'}$ is denoted as $\|\cdot\|^{'}$. For any $f \in V^{'}$, the norm is defined as

$$\|f\|^{'} := \sup_{\substack{v \in V \\ v \neq 0}} \frac{\langle f, v \rangle_{V^{'}, V}}{\|v\|}, \tag{2.9}$$

or equivalently

$$\|f\|'^2 = \int_\Omega \nabla((-\Delta)^{-1}f) \cdot \nabla((-\Delta)^{-1}f). \tag{2.10}$$

Definition 2.11 (Stokes problem)**.** On a bounded domain Ω with a Lipschitz boundary and for $(u, p) \in V \times L_0^2(\Omega), f \in V'$ the Stokes problem is given as,

$$-\Delta u + \nabla p = f \quad \text{in} \quad \Omega, \tag{2.11}$$

$$\nabla \cdot u = 0 \quad \text{in} \quad \Omega, \tag{2.12}$$

$$u = 0 \quad \text{on} \quad \partial\Omega. \tag{2.13}$$

The weak formulation of the Stokes problem for all $v \in V$ and $q \in L_0^2(\Omega)$ is

$$a(u, v) + b(p, v) = f(v),$$
$$b(q, u) = 0.$$

We now convert equations (2.11)-(2.13) into stream function form. Here, we treat u and f as vectors with two components: $u = [u_1, u_2]^T$ and $f = [f_1, f_2]^T$. Now we define a stream function ψ such that $u_1 = \frac{\partial \psi}{\partial y}, u_2 = -\frac{\partial \psi}{\partial x}$.

When considering a sufficiently smooth scalar function f, one may write

$$\nabla \times \nabla f = \nabla \times [f_x, f_y, f_z] = [f_{zy} - f_{yz}, f_{xz} - f_{zx}, f_{yx} - f_{xy}] = \mathbf{0}.$$

This speaks to the fact that the curl annihilates the gradient. Thus, a model absent of the pressure term can be obtained by taking the curl of (2.11).

$$\nabla \times (-\Delta u + \nabla p) = \nabla \times f.$$

The other advantage of the stream function formulation is that the number of un-

knowns reduces to one from three (u_1, u_2, p). This is a fourth-order PDE and more difficult to solve than second order ones. Now, our new model is

$$\Delta^2 \psi = f_{2x} - f_{1y} \quad \text{in} \quad \Omega, \tag{2.14}$$

$$\psi = \frac{\partial \psi}{\partial \nu} = 0 \quad \text{on} \quad \partial\Omega. \tag{2.15}$$

Here $f_{2x} = \frac{\partial f_2}{\partial x}$ and $f_{1y} = \frac{\partial f_1}{\partial y}$. Similarly to the above calculation, it can be shown that a stream function model can be obtained for the unsteady Stokes equation as well.

$$\begin{aligned} u_t - \Delta u + \nabla p &= f \quad \text{in} \quad \Omega, \\ \nabla \cdot u &= 0 \quad \text{in} \quad \Omega, \\ u &= 0 \quad \text{on} \quad \partial\Omega, \\ u(x, y, -1) &= u_0(x, y) \quad \text{in} \quad \Omega. \end{aligned}$$

We take the initial time at $t = -1$.

Now, by taking the curl and using $u = \frac{\partial \psi}{\partial y}\underline{i} - \frac{\partial \psi}{\partial x}\underline{j}$, we have

$$-\Delta \psi_t + \Delta^2 \psi = f_{2x} - f_{1y} \quad \text{in} \quad \Omega, \tag{2.16}$$

$$\psi = \frac{\partial \psi}{\partial \nu} = 0 \quad \text{on} \quad \partial\Omega, \tag{2.17}$$

$$\psi(x, y, -1) = \psi_0(x, y) \quad \text{in} \quad \Omega. \tag{2.18}$$

2.4.1 Space-time spectral methods for the Stokes problem

In this section, we discuss a space-time spectral method for the stream function form of the unsteady Stokes equations. Here, we will consider the simplest case where the spatial and temporal domains are both $(-1, 1)$.

Consider the stream function formulation for the 1D unsteady Stokes equation

$$(\psi_t)_{xx} = \psi_{xxxx} + f,$$

with initial condition $\psi(x, -1) = \psi_0(x)$ and homogeneous Dirichlet boundary conditions. Now, a space-time spectral collocation scheme for the 1D unsteady Stokes equation can be written as

$$(D^2 \otimes D)\psi_h = (D^4 \otimes I_{N+1})\psi_h + f_h,$$

where ψ_h and f_h are the vectors of ψ and f respectively, evaluated at the collocation points. A spectral approximation of the second derivative can be derived by considering the corresponding boundary conditions.

Let $\psi = \psi(x)$ be a polynomial so that $\psi(\pm 1) = \psi^{'}(\pm 1) = 0$. Let Z vanish at ± 1 so that $\psi(x) = (1 - x^2)Z(x)$. That is, ψ automatically satisfies the boundary conditions if Z vanishes at the boundary. By differentiating ψ twice, we obtain the following.

$$\psi^{''}(x) = (1 - x^2)Z^{''}(x) - 4xZ^{'}(x) - 2Z(x). \tag{2.19}$$

Let M be a $(N-1) \times (N-1)$ diagonal matrix with diagonal entries $1 - x_j^2$. Also, take X to be a diagonal matrix of the same size but with diagonal entries x_j. Here $1 \leq j \leq N - 1$. Therefore, the spectral approximation of the second derivative (denoted by B_2) satisfying the four boundary conditions can be written as,

$$B_2 := (M[[D^2]] - 4X[[D]] - 2I)M^{-1}. \tag{2.20}$$

Similarly, the spectral approximations of third and fourth derivative can be defined as:

$$\psi'''(x) = (1-x^2)Z'''(x) - 6xZ''(x) - 6Z'(x). \tag{2.21}$$

$$\psi''''(x) = (1-x^2)Z''''(x) - 8xZ'''(x) - 12Z''(x). \tag{2.22}$$

Then, the spectral approximations of third and fourth derivatives satisfying the four boundary conditions are

$$B_3 := (M[[D^3]] - 6X[[D^2]] - 6[[D]])M^{-1}. \tag{2.23}$$

$$B_4 := (M[[D^4]] - 8X[[D^3]] - 12[[D^2]])M^{-1}. \tag{2.24}$$

The resulting spectral equation for the Stokes equation is

$$(B_2 \otimes [D])\hat{\psi}_h - (B_4 \otimes I_N)\hat{\psi}_h = \hat{f}_h - (\psi_{0h} \otimes d_h),$$

where ψ_{0h} is ψ_0 evaluated at the (interior spatial) collocation points. The two vectors $\hat{\psi}_h$ and $\hat{f}_h$ are obtained by removing the corresponding boundary and initial points from ψ_h and f_h, respectively. The linear equation now can be written as

$$A_h\hat{\psi}_h = \hat{f}_h - (\psi_{0h} \otimes d_h),$$

where

$$A_h = (B_2 \otimes [D]) - (B_4 \otimes I_N). \tag{2.25}$$

Now, consider the stream function formulation for the 2D unsteady Stokes equation

$$(\psi_t)_{xx} + (\psi_t)_{yy} = \psi_{xxxx} + \psi_{yyyy} + 2\psi_{xxyy} + f,$$

with initial condition $\psi(x, y, -1) = \psi_0(x, y)$ and homogeneous Dirichlet boundary

conditions. The space-time spectral scheme is

$$\Big\{\Big((D^2 \otimes I_{N+1}) + (I_{N+1} \otimes D^2)\Big) \otimes D\Big\}\psi_h = \Big\{\Big((D^4 \otimes I_{N+1}) + (I_{N+1} \otimes D^4) + 2(D^2 \otimes D^2)\Big) \otimes I_{N+1}\Big\}\psi_h + f_h,$$

where ψ_h and f_h are the vectors of ψ and f, respectively, evaluated at the collocation points. Let B_2 be the spectral second derivative (2.20) and B_4 be the spectral fourth derivative (2.24) defined for the 1D Stokes problem. Finally, we may write

$$\Big\{\Big((B_2 \otimes I_{N-1}) + (I_{N-1} \otimes B_2)\Big) \otimes [D] - \Big((B_4 \otimes I_{N-1}) + (I_{N-1} \otimes B_4) + 2(B_2 \otimes B_2)\Big) \otimes I_N\Big\}\hat{\psi}_h = \hat{f}_h - (\psi_{0h} \otimes d_h),$$

where ψ_{0h} is ψ_0 evaluated at the interior collocation points. Here, the known boundary and initial values have been removed. Thus, the linear equation to be solved becomes

$$A_h\hat{\psi}_h = \hat{f}_h - (\psi_{0h} \otimes d_h), \tag{2.26}$$

where

$$A_h = \Big((B_2 \otimes I_{N-1}) + (I_{N-1} \otimes B_2)\Big) \otimes [D] - \Big((B_4 \otimes I_{N-1}) + (I_{N-1} \otimes B_4) + 2(B_2 \otimes B_2)\Big) \otimes I_N, \tag{2.27}$$

is the space-time Stokes operator.

2.4.2 Analysis

In this section, we estimate the condition number of the unsteady Stokes operator and also prove the spectral convergence of this scheme in space and time. The analysis presented here is original and constitutes a key contribution of this thesis.

The condition number estimate is established for the Legendre discrete spectral operator A_h, as deriving a lower bound is more challenging in the Chebyshev case. For the spectral convergence analysis, however, we employ the Chebyshev spectral collocation matrix.

We begin with some properties and a couple of well-known inequalities ([73]) which will be needed to estimate the bounds on the eigenvalues. An important property is that for a polynomial v of degree at most $2N-1$,

$$\int_{-1}^{1} v(x)dx = \sum_{k=0}^{N} v(x_k)\rho_k,$$

where ρ_k is the set of weights associated with the Legendre Gauss-Lobatto quadrature. Let

$$x_h = \begin{bmatrix} x_1 \\ \vdots \\ x_{N-1} \end{bmatrix}, \quad t_h = \begin{bmatrix} t_0 \\ \vdots \\ t_{N-1} \end{bmatrix}.$$

For any continuous function v on $(-1,1)^2$, define the discrete norm

$$\|v\|_N := \left(\sum_{j,k=0}^{N} \rho_j \rho_k \left| v(x_j, t_k) \right|^2 \right)^{1/2}.$$

Recall the Poincaré inequality for any $v \in H_0^1(-1,1)$,

$$\frac{\pi^2}{4} \int_{-1}^{1} |v(x)|^2 \, dx \leq \int_{-1}^{1} |v'(x)|^2 \, dx,$$

inverse estimate for any polynomial v of degree N or lower

$$\int_{-1}^{1} |v'(x)|^2 \, dx \leq CN^4 \int_{-1}^{1} |v(x)|^2 \, dx,$$

trace inequality for any polynomial v of degree N or lower:

$$|v(-1)|^2 + |v(1)|^2 \leq (N+1)^2 \int_{-1}^{1} |v(x)|^2 \, dx,$$

and finally the equivalence of the $L^2(-1,1)$ norm and a discrete norm:

$$\int_{-1}^{1} |v(x)|^2 \, dx \leq \sum_{j=0}^{N} |v(x_j)|^2 \, \rho_j \leq 3 \int_{-1}^{1} |v(x)|^2 \, dx$$

for any polynomial v of degree N or lower.

Theorem 2.12. Let $N \geq 2$. Let A_h be the Legendre spectral collocation matrix defined by (2.27) and λ be an eigenvalue of A_h. Then

$$c \leq |\lambda| \leq CN^8,$$

where c and C are positive and independent of N.

Proof. Let $A_h v_h = \lambda v_h$, and $v \in P_N \otimes P_N$ such that $v(\pm 1, y_l, t_q) = 0 = v_x(\pm 1, y_l, t_q)$, $v(x_p, \pm 1, t_q) = 0 = v_y(x_p, \pm 1, t_q)$, $v(x, y, -1) = 0$ and $v(x_i, y_j, t_k) = v_{ijk}, 1 \leq i, j \leq N-1$, where v_{ijk} is a component of v_h corresponding to (x_i, y_j, t_k).

The eigenvalue problem is equivalent to finding $v \in P_N \otimes P_N$ and eigenvalue λ so that

$$\begin{aligned}
(v_t)_{xx}(x_i, y_j, t_k) + (v_t)_{yy}(x_i, y_j, t_k) - v_{xxxx}(x_i, y_j, t_k) - v_{yyyy}(x_i, y_j, t_k) \\
-2v_{xxyy}(x_i, y_j, t_k) = \lambda v(x_i, y_j, t_k), \quad 1 \leq i, j \leq N-1, 0 \leq k \leq N-1 \\
v(\pm 1, y_l, t_q) = 0 = v_x(\pm 1, y_l, t_q) \\
v(x_p, \pm 1, t_q) = 0 = v_y(x_p, \pm 1, t_q) \\
v(x_p, y_l, -1) = 0
\end{aligned}$$

for $0 \leq p, q, l \leq N$ satisfying the normalization $\|v\|_N = 1$. There is no condition on v

at $t = 1$. There are exactly $N(N-1)^2$ collocation equations in $N(N-1)^2$ unknowns.

Multiply the eigenvalue problem by $\bar{v}(x_i, y_j, t_k)\rho_i\rho_j\rho_k$ and then sum to obtain

$$\begin{aligned}
&\lambda \sum_{i=1}^{N-1}\sum_{j=1}^{N-1}\sum_{k=0}^{N-1} |v(x_i, y_j, t_k)|^2 \rho_i\rho_j\rho_k \\
&= \sum_{i=1}^{N-1}\sum_{j=1}^{N-1}\sum_{k=0}^{N-1} v_{txx}(x_i, y_j, t_k)\bar{v}(x_i, y_j, t_k)\rho_i\rho_j\rho_k + \sum_{i=1}^{N-1}\sum_{j=1}^{N-1}\sum_{k=0}^{N-1} v_{tyy}(x_i, y_j, t_k)\bar{v}(x_i, y_j, t_k)\rho_i\rho_j\rho_k \\
&\quad - \sum_{i=1}^{N-1}\sum_{j=1}^{N-1}\sum_{k=0}^{N-1} v_{xxxx}(x_i, y_j, t_k)\bar{v}(x_i, y_j, t_k)\rho_i\rho_j\rho_k - \sum_{i=1}^{N-1}\sum_{j=1}^{N-1}\sum_{k=0}^{N-1} v_{yyyy}(x_i, y_j, t_k)\bar{v}(x_i, y_j, t_k)\rho_i\rho_j\rho_k \\
&\quad - 2\sum_{i=1}^{N-1}\sum_{j=1}^{N-1}\sum_{k=0}^{N-1} v_{xxyy}(x_i, y_j, t_k)\bar{v}(x_i, y_j, t_k)\rho_i\rho_j\rho_k,
\end{aligned}$$

or

$$\begin{aligned}
&\lambda \sum_{i,j,k=0}^{N} |v(x_i, y_j, t_k)|^2 \rho_i\rho_j\rho_k \\
&= \sum_{i,j,k=0}^{N} v_{txx}(x_i, y_j, t_k)\bar{v}(x_i, y_j, t_k)\rho_i\rho_j\rho_k + \sum_{i,j,k=0}^{N} v_{tyy}(x_i, y_j, t_k)\bar{v}(x_i, y_j, t_k)\rho_i\rho_j\rho_k \\
&\quad - \sum_{i,j,k=0}^{N} v_{xxxx}(x_i, y_j, t_k)\bar{v}(x_i, y_j, t_k)\rho_i\rho_j\rho_k - \sum_{i,j,k=0}^{N} v_{yyyy}(x_i, y_j, t_k)\bar{v}(x_i, y_j, t_k)\rho_i\rho_j\rho_k \\
&\quad - 2\sum_{i,j,k=0}^{N} v_{xxyy}(x_i, y_j, t_k)\bar{v}(x_i, y_j, t_k)\rho_i\rho_j\rho_k,
\end{aligned}$$

or

$$\begin{aligned}
\lambda &= \sum_{i,j,k=0}^{N} v_{txx}(x_i, y_j, t_k)\bar{v}(x_i, y_j, t_k)\rho_i\rho_j\rho_k + \sum_{i,j,k=0}^{N} v_{tyy}(x_i, y_j, t_k)\bar{v}(x_i, y_j, t_k)\rho_i\rho_j\rho_k \\
&\quad - \sum_{j,k=0}^{N} \rho_j\rho_k \int_{-1}^{1} v_{xxxx}(x, y_j, t_k)\bar{v}(x, y_j, t_k)dx - \sum_{i,k=0}^{N} \rho_i\rho_k \int_{-1}^{1} v_{yyyy}(x_i, y, t_k)\bar{v}(x_i, y, t_k)dy \\
&\quad - 2\sum_{i,j,k=0}^{N} v_{xxyy}(x_i, y_j, t_k)\bar{v}(x_i, y_j, t_k)\rho_i\rho_j\rho_k \\
&= \int_{-1}^{1}\int_{-1}^{1}\int_{-1}^{1} v_{txx}(x, y, t)\bar{v}(x, y, t)dxdydt + \int_{-1}^{1}\int_{-1}^{1}\int_{-1}^{1} v_{tyy}(x, y, t)\bar{v}(x, y, t)dxdydt \\
&\quad - \sum_{j,k=0}^{N} \rho_j\rho_k \int_{-1}^{1} |v_{xx}(x, y_j, t_k)|^2 dx - \sum_{i,k=0}^{N} \rho_i\rho_k \int_{-1}^{1} |v_{yy}(x_i, y, t_k)|^2 dy
\end{aligned}$$

$$- 2\int_{-1}^{1}\int_{-1}^{1}\int_{-1}^{1} v_{xxyy}(x,y,t)\bar{v}(x,y,t)dxdydt. \tag{2.28}$$

The complex conjugate of the above equation is

$$\begin{aligned}\bar{\lambda} = &\int_{-1}^{1}\int_{-1}^{1}\int_{-1}^{1} \bar{v}_{txx}(x,y,t)v(x,y,t)dxdydt + \int_{-1}^{1}\int_{-1}^{1}\int_{-1}^{1} \bar{v}_{tyy}(x,y,t)v(x,y,t)dxdydt\\ &- \sum_{j,k=0}^{N} \rho_j\rho_k \int_{-1}^{1} |v_{xx}(x,y_j,t_k)|^2dx - \sum_{i,k=0}^{N} \rho_i\rho_k \int_{-1}^{1} |v_{yy}(x_i,y,t_k)|^2dy\\ &- 2\int_{-1}^{1}\int_{-1}^{1}\int_{-1}^{1} \bar{v}_{xxyy}(x,y,t)v(x,y,t)dxdydt. \end{aligned}\tag{2.29}$$

Add and subtract (2.28) and (2.29) equations to obtain

$$\begin{aligned}2\Re\lambda = &\int_{-1}^{1}\int_{-1}^{1}\int_{-1}^{1}(v_{txx}(x,y,t)\bar{v}(x,y,t) + \bar{v}_{txx}(x,y,t)v(x,y,t))dxdydt\\ &+ \int_{-1}^{1}\int_{-1}^{1}\int_{-1}^{1}(v_{tyy}(x,y,t)\bar{v}(x,y,t) + \bar{v}_{tyy}(x,y,t)v(x,y,t))dxdydt\\ &- 2\sum_{j,k=0}^{N} \rho_j\rho_k \int_{-1}^{1} |v_{xx}(x,y_j,t_k)|^2dx - 2\sum_{i,k=0}^{N} \rho_i\rho_k \int_{-1}^{1} |v_{yy}(x_i,y,t_k)|^2dy\\ &- 2\int_{-1}^{1}\int_{-1}^{1}\int_{-1}^{1}(v_{xxyy}(x,y,t)\bar{v}(x,y,t) + \bar{v}_{xxyy}(x,y,t)v(x,y,t))dxdydt, \end{aligned}\tag{2.30}$$

$$\begin{aligned}2i\Im\lambda = &\int_{-1}^{1}\int_{-1}^{1}\int_{-1}^{1}(v_{txx}(x,y,t)\bar{v}(x,y,t) - \bar{v}_{txx}(x,y,t)v(x,y,t))dxdydt\\ &+ \int_{-1}^{1}\int_{-1}^{1}\int_{-1}^{1}(v_{tyy}(x,y,t)\bar{v}(x,y,t) - \bar{v}_{tyy}(x,y,t)v(x,y,t))dxdydt\\ &- 2\int_{-1}^{1}\int_{-1}^{1}\int_{-1}^{1}(v_{xxyy}(x,y,t)\bar{v}(x,y,t) - \bar{v}_{xxyy}(x,y,t)v(x,y,t))dxdydt. \end{aligned}\tag{2.31}$$

By (2.30) we get,

$$\begin{aligned}2\,|\Re\lambda| = &\Big|\int_{-1}^{1}\int_{-1}^{1}\int_{-1}^{1}(v_{txx}(x,y,t)\bar{v}(x,y,t) + \bar{v}_{txx}(x,y,t)v(x,y,t))dxdydt\\ &+ \int_{-1}^{1}\int_{-1}^{1}\int_{-1}^{1}(v_{tyy}(x,y,t)\bar{v}(x,y,t) + \bar{v}_{tyy}(x,y,t)v(x,y,t))dxdydt\\ &- 2\sum_{j,k=0}^{N} \rho_j\rho_k \int_{-1}^{1} |v_{xx}(x,y_j,t_k)|^2dx - 2\sum_{i,k=0}^{N} \rho_i\rho_k \int_{-1}^{1} |v_{yy}(x_i,y,t_k)|^2dy\\ &- 2\int_{-1}^{1}\int_{-1}^{1}\int_{-1}^{1}(v_{xxyy}(x,y,t)\bar{v}(x,y,t) + \bar{v}_{xxyy}(x,y,t)v(x,y,t))dxdydt\Big| \end{aligned}$$

$$
\begin{aligned}
&\leq \left| \int_{-1}^{1}\int_{-1}^{1}\int_{-1}^{1} (v_{txx}(x,y,t)\bar{v}(x,y,t) + \bar{v}_{txx}(x,y,t)v(x,y,t))dxdydt \right| \\
&\quad + \left| \int_{-1}^{1}\int_{-1}^{1}\int_{-1}^{1} (v_{tyy}(x,y,t)\bar{v}(x,y,t) + \bar{v}_{tyy}(x,y,t)v(x,y,t))dxdydt \right| \\
&\quad + 2\left| \sum_{j,k=0}^{N} \rho_j\rho_k \int_{-1}^{1} |v_{xx}(x,y_j,t_k)|^2 dx \right| + 2\left| \sum_{i,k=0}^{N} \rho_i\rho_k \int_{-1}^{1} |v_{yy}(x_i,y,t_k)|^2 dy \right| \\
&\quad + 2\left| \int_{-1}^{1}\int_{-1}^{1}\int_{-1}^{1} (v_{xxyy}(x,y,t)\bar{v}(x,y,t) + \bar{v}_{xxyy}(x,y,t)v(x,y,t))dxdydt \right| \\
&\leq \int_{-1}^{1}\int_{-1}^{1}\int_{-1}^{1} |v_{txx}\bar{v} + \bar{v}_{txx}v| \, dxdydt + \int_{-1}^{1}\int_{-1}^{1}\int_{-1}^{1} |v_{tyy}\bar{v} + \bar{v}_{tyy}v| \, dxdydt \\
&\quad + 2\sum_{j,k=0}^{N} \rho_j\rho_k \int_{-1}^{1} |v_{xx}(x,y_j,t_k)|^2 dx + 2\sum_{i,k=0}^{N} \rho_i\rho_k \int_{-1}^{1} |v_{yy}(x_i,y,t_k)|^2 dy \\
&\quad + 2\int_{-1}^{1}\int_{-1}^{1}\int_{-1}^{1} |v_{xxyy}\bar{v} + \bar{v}_{xxyy}v| \, dxdydt \\
&\leq 2\int_{-1}^{1}\int_{-1}^{1}\int_{-1}^{1} |v_{txx}| \, |v| \, dxdydt + 2\int_{-1}^{1}\int_{-1}^{1}\int_{-1}^{1} |v_{tyy}| \, |v| \, dxdydt \\
&\quad + 2\sum_{j,k=0}^{N} \rho_j\rho_k \int_{-1}^{1} |v_{xx}(x,y_j,t_k)|^2 dx + 2\sum_{i,k=0}^{N} \rho_i\rho_k \int_{-1}^{1} |v_{yy}(x_i,y,t_k)|^2 dy \\
&\quad + 4\int_{-1}^{1}\int_{-1}^{1}\int_{-1}^{1} |v_{xxyy}| \, |v| \, dxdydt \\
&\leq 2\left(\int_{-1}^{1}\int_{-1}^{1}\int_{-1}^{1} |v_{txx}(x,y,t)|^2 \, dxdydt \right)^{1/2} \left(\int_{-1}^{1}\int_{-1}^{1}\int_{-1}^{1} |v(x,y,t)|^2 \, dxdydt \right)^{1/2} \\
&\quad + 2\left(\int_{-1}^{1}\int_{-1}^{1}\int_{-1}^{1} |v_{tyy}(x,y,t)|^2 \, dxdydt \right)^{1/2} \left(\int_{-1}^{1}\int_{-1}^{1}\int_{-1}^{1} |v(x,y,t)|^2 \, dxdydt \right)^{1/2} \\
&\quad + 2CN^4 \sum_{j,k=0}^{N} \rho_j\rho_k \int_{-1}^{1} |v_x(x,y_j,t_k)|^2 dx + 2CN^4 \sum_{i,k=0}^{N} \rho_i\rho_k \int_{-1}^{1} |v_y(x_i,y,t_k)|^2 dy \\
&\qquad\qquad\qquad\qquad\qquad\qquad\qquad\qquad\qquad\qquad \text{(By inverse estimate)} \\
&\quad + 4\left(\int_{-1}^{1}\int_{-1}^{1}\int_{-1}^{1} |v_{xxyy}(x,y,t)|^2 \, dxdydt \right)^{1/2} \left(\int_{-1}^{1}\int_{-1}^{1}\int_{-1}^{1} |v(x,y,t)|^2 \, dxdydt \right)^{1/2} \\
&\leq CN^4 \left(\int_{-1}^{1}\int_{-1}^{1}\int_{-1}^{1} |v_t(x,y,t)|^2 \, dxdydt \right)^{1/2} \left(\int_{-1}^{1}\int_{-1}^{1}\int_{-1}^{1} |v(x,y,t)|^2 \, dxdydt \right)^{1/2} \\
&\quad + CN^4 \left(\int_{-1}^{1}\int_{-1}^{1}\int_{-1}^{1} |v_t(x,y,t)|^2 \, dxdydt \right)^{1/2} \left(\int_{-1}^{1}\int_{-1}^{1}\int_{-1}^{1} |v(x,y,t)|^2 \, dxdydt \right)^{1/2} \\
&\quad + CN^8 \sum_{j,k=0}^{N} \rho_j\rho_k \int_{-1}^{1} |v(x,y_j,t_k)|^2 dx + CN^8 \sum_{i,k=0}^{N} \rho_i\rho_k \int_{-1}^{1} |v(x_i,y,t_k)|^2 dy \\
&\quad + CN^4 \left(\int_{-1}^{1}\int_{-1}^{1}\int_{-1}^{1} |v_{yy}(x,y,t)|^2 \, dxdydt \right)^{1/2} \left(\int_{-1}^{1}\int_{-1}^{1}\int_{-1}^{1} |v(x,y,t)|^2 \, dxdydt \right)^{1/2} \\
&\leq CN^6\|v\|_N^2 + CN^6\|v\|_N^2 + CN^8\|v\|_N^2 + CN^8\|v\|_N^2 + CN^8\|v\|_N^2.
\end{aligned}
$$

Therefore, $|\Re\lambda| \leq CN^8$.

By (2.31) we get,

$$
\begin{aligned}
2\,|\Im\lambda| &\leq 2\int_{-1}^{1}\int_{-1}^{1}\int_{-1}^{1} |v_{txx}(x,y,t)|\,|v(x,y,t)|\,dxdydt + 2\int_{-1}^{1}\int_{-1}^{1}\int_{-1}^{1} |v_{tyy}(x,y,t)|\,|v(x,y,t)|\,dxdydt \\
&\quad + 4\int_{-1}^{1}\int_{-1}^{1}\int_{-1}^{1} |v_{xxyy}(x,y,t)|\,|v(x,y,t)|\,dxdydt \\
&\leq 2\left(\int_{-1}^{1}\int_{-1}^{1}\int_{-1}^{1} |v_{txx}(x,y,t)|^2\,dxdydt\right)^{1/2}\left(\int_{-1}^{1}\int_{-1}^{1}\int_{-1}^{1} |v(x,y,t)|^2\,dxdydt\right)^{1/2} \\
&\quad + 2\left(\int_{-1}^{1}\int_{-1}^{1}\int_{-1}^{1} |v_{tyy}(x,y,t)|^2\,dxdydt\right)^{1/2}\left(\int_{-1}^{1}\int_{-1}^{1}\int_{-1}^{1} |v(x,y,t)|^2\,dxdydt\right)^{1/2} \\
&\quad + 4\left(\int_{-1}^{1}\int_{-1}^{1}\int_{-1}^{1} |v_{xxyy}(x,y,t)|^2\,dxdydt\right)^{1/2}\left(\int_{-1}^{1}\int_{-1}^{1}\int_{-1}^{1} |v(x,y,t)|^2\,dxdydt\right)^{1/2} \\
&\leq CN^4\left(\int_{-1}^{1}\int_{-1}^{1}\int_{-1}^{1} |v_t(x,y,t)|^2\,dxdydt\right)^{1/2}\left(\int_{-1}^{1}\int_{-1}^{1}\int_{-1}^{1} |v(x,y,t)|^2\,dxdydt\right)^{1/2} \\
&\quad + CN^4\left(\int_{-1}^{1}\int_{-1}^{1}\int_{-1}^{1} |v_t(x,y,t)|^2\,dxdydt\right)^{1/2}\left(\int_{-1}^{1}\int_{-1}^{1}\int_{-1}^{1} |v(x,y,t)|^2\,dxdydt\right)^{1/2} \\
&\quad + CN^4\left(\int_{-1}^{1}\int_{-1}^{1}\int_{-1}^{1} |v_{yy}(x,y,t)|^2\,dxdydt\right)^{1/2}\left(\int_{-1}^{1}\int_{-1}^{1}\int_{-1}^{1} |v(x,y,t)|^2\,dxdydt\right)^{1/2} \\
&\leq CN^6\|v\|_N^2 + CN^6\|v\|_N^2 + CN^8\|v\|_N^2.
\end{aligned}
$$

Therefore, $|\Im\lambda| \leq CN^8$.

Thus,

$$|\lambda|^2 = (\Re\lambda)^2 + (\Im\lambda)^2 \leq (CN^8)^2 + (CN^8)^2 \leq (CN^8)^2,$$

implying $|\lambda| \leq CN^8$.

To prove lower bound we want to show: $|\lambda|^2 = (\Re\lambda)^2 + (\Im\lambda)^2 \geq C$. By squaring (2.30) we get,

$$
\begin{aligned}
4(\Re\lambda)^2 = \Big(&\int_{-1}^{1}\int_{-1}^{1}\int_{-1}^{1} (v_{txx}\bar{v} + \bar{v}_{txx}v)dxdydt + \int_{-1}^{1}\int_{-1}^{1}\int_{-1}^{1} (v_{tyy}\bar{v} + \bar{v}_{tyy}v)dxdydt \\
&- 2\sum_{j,k=0}^{N} \rho_j\rho_k \int_{-1}^{1} |v_{xx}(x,y_j,t_k)|^2 dx - 2\sum_{i,k=0}^{N} \rho_i\rho_k \int_{-1}^{1} |v_{yy}(x_i,y,t_k)|^2 dy
\end{aligned}
$$

$$
\begin{aligned}
&\quad - 2\int_{-1}^{1}\int_{-1}^{1}\int_{-1}^{1}(v_{xxyy}\bar{v} + \bar{v}_{xxyy}v)dxdydt\Big)^2 \\
&= 4\Big((k_3 + k_4 + k_5 - k_1 - k_2)^2 + 2k_5(k_3 + k_4 - k_1 - k_2)\Big) \qquad (2.32)
\end{aligned}
$$

where

$$
\begin{aligned}
k_1 &= \Re\int_{-1}^{1}\int_{-1}^{1}\int_{-1}^{1}(v_{txx}\bar{v})dxdydt \\
&= -\Re\int_{-1}^{1}\int_{-1}^{1}\int_{-1}^{1}(v_{tx}\bar{v}_x)dxdydt \quad \text{(By integration by parts)} \\
&= -\frac{1}{2}\Re\left(\int_{-1}^{1}\int_{-1}^{1}\int_{-1}^{1}(v_{tx}\bar{v}_x)dxdydt + \int_{-1}^{1}\int_{-1}^{1}\int_{-1}^{1}(\bar{v}_{tx}v_x)dxdydt\right) \quad (\text{since} \quad \Re(z) = \Re(\bar{z})\,) \\
&= -\frac{1}{2}\Re\int_{-1}^{1}\int_{-1}^{1}\int_{-1}^{1}\frac{\partial}{\partial t}|v_x|^2 dtdxdy \\
&= -\frac{1}{2}\Re\int_{-1}^{1}\int_{-1}^{1}\left(|v_x(x,y,1)|^2 - |v_x(x,y,-1)|^2\right)dxdy \\
&= \frac{1}{2}\left(\int_{-1}^{1}\int_{-1}^{1}\left(|v_x(x,y,-1)|^2 - |v_x(x,y,1)|^2\right)dxdy\right).
\end{aligned}
$$

Since $v(x_p, y_l, -1) = 0$ for $0 \le p, l \le N$, implying $v(x, y, -1) \equiv 0$ for all x and y. Hence $v_x(x, y, -1) = 0$, resulting in $k_1 = -\frac{1}{2}\int_{-1}^{1}\int_{-1}^{1}|v_x(x, y, 1)|^2 dxdy \le 0$. Similarly, we can show that $k_2 = \Re\int_{-1}^{1}\int_{-1}^{1}\int_{-1}^{1}(v_{tyy}\bar{v})dxdydt \le 0$. Also

$$
\begin{aligned}
k_3 &= \sum_{j,k=0}^{N}\rho_j\rho_k\int_{-1}^{1}|v_{xx}(x, y_j, t_k)|^2 dx \\
&\ge \frac{\pi^2}{4}\sum_{j,k=0}^{N}\rho_j\rho_k\int_{-1}^{1}|v_x(x, y_j, t_k)|^2 dx \qquad \text{(By Poincare inequality)} \\
&\ge \frac{\pi^2}{4}\times\frac{\pi^2}{4}\sum_{j,k=0}^{N}\rho_j\rho_k\int_{-1}^{1}|v(x, y_j, t_k)|^2 dx \qquad \text{(By Poincare inequality)} \\
&\ge \frac{\pi^4}{16}\times\frac{1}{3}\|v\|_N^2 = \frac{\pi^4}{48} > 0.
\end{aligned}
$$

Similarly, $k_4 = \sum_{i,k=0}^{N}\rho_i\rho_k\int_{-1}^{1}|v_{yy}(x_i, y, t_k)|^2 dy \ge \frac{\pi^4}{48} > 0$.

In addition,

$$
k_5 = \Re\int_{-1}^{1}\int_{-1}^{1}\int_{-1}^{1}(v_{xxyy}\bar{v})dxdydt
$$

$$= -\Re \int_{-1}^{1}\int_{-1}^{1}\int_{-1}^{1}(v_{xyy}\bar{v}_x)dxdydt \quad \text{(By integration by parts)}$$
$$= \Re \int_{-1}^{1}\int_{-1}^{1}\int_{-1}^{1}(v_{xy}\bar{v}_{xy})dydxdt \quad \text{(By integration by parts)}$$
$$= \int_{-1}^{1}\int_{-1}^{1}\int_{-1}^{1}|v_{xy}|^2 dxdydt \geq 0.$$

By squaring (2.31) we get,

$$\begin{aligned} 4(\Im\lambda)^2 &= \Big(\frac{1}{i}\Big(\int_{-1}^{1}\int_{-1}^{1}\int_{-1}^{1}(v_{txx}\bar{v} - \bar{v}_{txx}v)dxdydt + \int_{-1}^{1}\int_{-1}^{1}\int_{-1}^{1}(v_{tyy}\bar{v} - \bar{v}_{tyy}v)dxdydt \\ &\quad - 2\int_{-1}^{1}\int_{-1}^{1}\int_{-1}^{1}(v_{xxyy}\bar{v} - \bar{v}_{xxyy}v)dxdydt\Big)\Big)^2 \\ &= 4\left(l_1^2 + l_2^2 + l_3^2 + 2l_1l_2 - 4l_1l_3 - 4l_2l_3\right) \\ &= 4\left(l_1 + l_2 - 2l_3\right)^2 \geq 0, \end{aligned} \tag{2.33}$$

where $l_1 = \int_{-1}^{1}\int_{-1}^{1}\int_{-1}^{1}\Im(v_{txx}\bar{v})dxdydt$, $l_2 = \int_{-1}^{1}\int_{-1}^{1}\int_{-1}^{1}\Im(v_{tyy}\bar{v})dxdydt$ and $l_3 = \int_{-1}^{1}\int_{-1}^{1}\int_{-1}^{1}\Im(v_{xxyy}\bar{v})dxdydt$.

By adding (2.32) and (2.33) we get,

$$4(\Re\lambda)^2 + 4(\Im\lambda)^2 = 4\left((k_3 + k_4 + k_5 - k_1 - k_2)^2 + 2k_5(k_3 + k_4 - k_1 - k_2)\right) + 4\left(l_1 + l_2 - 2l_3\right)^2$$
$$\begin{aligned} (\Re\lambda)^2 + (\Im\lambda)^2 &\geq (k_3 + k_4 + k_5 - k_1 - k_2)^2 \\ &\geq (k_3 + k_4)^2 \geq \left(\frac{\pi^4}{48} + \frac{\pi^4}{48}\right)^2 = \left(\frac{\pi^4}{24}\right)^2. \end{aligned}$$

Hence,

$$|\lambda| \geq \frac{\pi^4}{24}.$$

This completes the proof of the theorem.

□

Although the condition number is $\mathcal{O}(N^8)$, which is quite large, the scheme

remains well-behaved when N is not large, say $N \leq 25$. Beyond that, the ill-conditioning becomes apparent, with the error increasing rapidly, much more so than in the case of second-order PDEs.

Numerical observations show a similar spectral condition number for the Chebyshev discrete spectral operator A_h, though proving the lower bound is more complex due to the weight function. Now, we discuss space-time spectral convergence for the 2D unsteady Stokes equation.

Theorem 2.13. Let ψ be the solution of the 2D unsteady Stokes equation. Assume ψ is separately analytic in each variable. Let $N \geq 2$ and $\hat{\psi}_h$ be the solution of the space-time method with the Chebyshev spectral collocation matrix $A_h = \Big(B_2 \otimes I_{N-1} + I_{N-1} \otimes B_2\Big) \otimes [D] - \Big(B_4 \otimes I_{N-1} + I_{N-1} \otimes B_4 + 2B_2 \otimes B_2\Big) \otimes I_N$. Define the error vector E_h as the difference of ψ evaluated at the collocation points and $\hat{\psi}_h$. Then

$$\left|W^{1/2} E_h\right| \leq cN^{7.5} e^{-CN}.$$

Proof. Define

$$\psi_h(t) = \begin{bmatrix} \psi(x_1, y_1, t) \\ \psi(x_2, y_1, t) \\ \vdots \\ \psi(x_{N-1}, y_1, t) \\ \psi(x_1, y_2, t) \\ \vdots \\ \psi(x_{N-1}, y_{N-1}, t) \end{bmatrix} \in \mathbb{R}^{(N-1)^2}, \quad f_h(t) = \begin{bmatrix} f(x_1, y_1, t) \\ f(x_2, y_1, t) \\ \vdots \\ f(x_{N-1}, y_1, t) \\ f(x_1, y_2, t) \\ \vdots \\ f(x_{N-1}, y_{N-1}, t) \end{bmatrix} \in \mathbb{R}^{(N-1)^2}.$$

A semi-discrete approximation of the 2D unsteady Stokes equation is

$$(B_2 \otimes I_{N-1} + I_{N-1} \otimes B_2)\psi_h'(t) = (B_4 \otimes I_{N-1} + I_{N-1} \otimes B_4 + 2B_2 \otimes B_2)\psi_h(t) + f_h(t),$$
$$\psi_h(-1) = \psi_{0h},$$

where ψ_{0h} is the initial data evaluated at the vector of interior Chebyshev Gauss-Lobatto points (x_h, y_h); i.e., $\psi_{0h} = \psi_0(x_h, y_h)$.

Define the error function $e_h(t) = \psi_h(t) - \psi(x_h, y_h, t)$ with components $e_j(t) = (e_h(t))_j$. Thus

$$e_h(t) = \begin{bmatrix} \psi_h(x_1, y_1, t) - \psi(x_1, y_1, t) \\ \psi_h(x_2, y_1, t) - \psi(x_2, y_1, t) \\ \vdots \\ \psi_h(x_{N-1}, y_1, t) - \psi(x_{N-1}, y_1, t) \\ \psi_h(x_1, y_2, t) - \psi(x_1, y_2, t) \\ \vdots \\ \psi_h(x_{N-1}, y_{N-1}, t) - \psi(x_{N-1}, y_{N-1}, t) \end{bmatrix} \in \mathbb{R}^{(N-1)^2}.$$

Using the above equation, it is easy to see that the error satisfies, for $0 \le k \le N-1$,

$$\begin{aligned}
&(B_2 \otimes I_{N-1} + I_{N-1} \otimes B_2)e_h'(t_k) \\
&= (B_2 \otimes I_{N-1} + I_{N-1} \otimes B_2)\psi_h'(t_k) - (B_2 \otimes I_{N-1} + I_{N-1} \otimes B_2)\psi_t(x_h, y_h, t_k) \\
&= (B_4 \otimes I_{N-1} + I_{N-1} \otimes B_4 + 2B_2 \otimes B_2)\psi_h(t_k) + f_h(t_k) - (B_2 \otimes I_{N-1} + I_{N-1} \otimes B_2)\psi_t(x_h, y_h, t_k) \\
&= (B_4 \otimes I_{N-1} + I_{N-1} \otimes B_4 + 2B_2 \otimes B_2)e_h(t_k) + (B_4 \otimes I + I \otimes B_4 + 2B_2 \otimes B_2)\psi(x_h, y_h, t_k) \\
&\quad + f_h(t_k) - (B_2 \otimes I_{N-1} + I_{N-1} \otimes B_2)\psi_t(x_h, y_h, t_k) \\
&= (B_4 \otimes I_{N-1} + I_{N-1} \otimes B_4 + 2B_2 \otimes B_2)e_h(t_k) + (B_4 \otimes I_{N-1} + I_{N-1} \otimes B_4 + 2B_2 \otimes B_2)\psi(x_h, y_h, t_k) \\
&\quad - \psi_{xxxx}(x_h, y_h, t_k) - \psi_{yyyy}(x_h, y_h, t_k) - 2\psi_{xxyy}(x_h, y_h, t_k) + (\psi_t)_{xx}(x_h, y_h, t_k) + (\psi_t)_{yy}(x_h, y_h, t_k)
\end{aligned}$$

$$- (B_2 \otimes I_{N-1} + I_{N-1} \otimes B_2)\psi_t(x_h, y_h, t_k).$$

Therefore,

$$(B_2 \otimes I_{N-1} + I_{N-1} \otimes B_2)e_h'(t_k) = (B_4 \otimes I_{N-1} + I_{N-1} \otimes B_4 + 2B_2 \otimes B_2)e_h(t_k) + r(t_k), \tag{2.34}$$

where

$$\begin{aligned} r(t_k) = (B_4 \otimes I_{N-1} + I_{N-1} \otimes B_4 + 2B_2 \otimes B_2)\psi(x_h, y_h, t_k) - \psi_{xxxx}(x_h, y_h, t_k) - \psi_{yyyy}(x_h, y_h, t_k) \\ - 2\psi_{xxyy}(x_h, y_h, t_k) + \psi_{txx}(x_h, y_h, t_k) + \psi_{tyy}(x_h, y_h, t_k) \\ - (B_2 \otimes I_{N-1} + I_{N-1} \otimes B_2)\psi_t(x_h, y_h, t_k). \end{aligned}$$

For any analytic z such that $z(-1) = 0$, recall the definition of the interpolant

$$\mathcal{I}_N z(t) = \sum_{j=0}^{N-1} z(t_j)\ell_j(t), \tag{2.35}$$

where $\ell_j \in P_N$ is the Lagrange polynomials with respect to the Chebyshev nodes, $\ell_j(x_k) = \delta_{jk}$. For $0 \leq k \leq N-1$,

$$\begin{aligned} z'(t_k) &= (\mathcal{I}_N z)'(t_k) + \tilde{\epsilon}_k \\ &= ([D]z(t_h))_k + \tilde{\epsilon}_k, \end{aligned} \tag{2.36}$$

where $\tilde{\epsilon}_k = (z - \mathcal{I}_N z)'(t_k)$ satisfies

$$|\tilde{\epsilon}_k| \leq CN^2 e^{-CN} \tag{2.37}$$

according to [83].

Take $z(t) = e_j(t)$ in (2.36), observing that $e_j(-1) = 0$, then

$$(e_h'(t_k))_j = e_j'(t_k) = ([D]e_j(t_h))_k + \epsilon_{jk}, \tag{2.38}$$

where $|\epsilon_{jk}| \leq CN^2e^{-CN}$ for $1 \leq j \leq (N-1)^2$, $0 \leq k \leq N-1$.

Define

$$e_j(t_h) = \begin{bmatrix} e_j(t_0) \\ \vdots \\ e_j(t_{N-1}) \end{bmatrix}, \quad E_h = \begin{bmatrix} e_1(t_h) \\ \vdots \\ e_{(N-1)^2}(t_h) \end{bmatrix}, \quad \tilde{R}_h = \begin{bmatrix} r_1(t_h) \\ \vdots \\ r_{(N-1)^2}(t_h) \end{bmatrix},$$

where residual vectors are defined by

$$\begin{aligned} r_j(t_h) = {} & (B_4 \otimes I_{N-1} + I_{N-1} \otimes B_4 + 2B_2 \otimes B_2)\psi(x_j, y_j, t_h) - \psi_{xxxx}(x_j, y_j, t_h) - \psi_{yyyy}(x_j, y_j, t_h) \\ & - 2\psi_{xxyy}(x_j, y_j, t_h) + \psi_{txx}(x_j, y_j, t_h) + \psi_{tyy}(x_j, y_j, t_h) \\ & - (B_2 \otimes I_{N-1} + I_{N-1} \otimes B_2)\psi_t(x_j, y_j, t_h). \end{aligned} \tag{2.39}$$

In vector notation, the equation (2.38) is

$$E_h' = (I_{N-1} \otimes I_{N-1} \otimes [D])E_h + \epsilon,$$

where ϵ is a long vector formed by stacking together vectors $[\epsilon_{j0}, \ldots, \epsilon_{j,N-1}]^T$ for $1 \leq j \leq (N-1)^2$; and each component of E_h' has the form $e_j'(t_k)$. Then, from (2.34), we have

$$\Big((B_2 \otimes I_{N-1} + I_{N-1} \otimes B_2)e_h'(t_k)\Big)_j = \Big((B_4 \otimes I_{N-1} + I_{N-1} \otimes B_4 + 2B_2 \otimes B_2)e_h(t_k)\Big)_j + r_j(t_k),$$

or

$$\Big((B_2 \otimes I_{N-1} + I_{N-1} \otimes B_2) \otimes I_N\Big)E'_h = \Big((B_4 \otimes I_{N-1} + I_{N-1} \otimes B_4 + 2B_2 \otimes B_2) \otimes I_N\Big)E_h + \tilde{R}_h,$$

or

$$\Big((B_2 \otimes I_{N-1} + I_{N-1} \otimes B_2) \otimes I_N\Big)\Big((I_{N-1} \otimes I_{N-1} \otimes [D])E_h + \epsilon\Big) = \Big((B_4 \otimes I_{N-1} + I_{N-1} \otimes B_4 + 2B_2 \otimes B_2) \otimes I_N\Big)E_h + \tilde{R}_h,$$

or

$$\Big((B_2 \otimes I_{N-1} + I_{N-1} \otimes B_2) \otimes [D]\Big)E_h + \Big((B_2 \otimes I_{N-1} + I_{N-1} \otimes B_2) \otimes I_N\Big)\epsilon = \Big((B_4 \otimes I_{N-1} + I_{N-1} \otimes B_4 + 2B_2 \otimes B_2) \otimes I_N\Big)E_h + \tilde{R}_h,$$

leading to

$$\Big((B_2 \otimes I_{N-1} + I_{N-1} \otimes B_2) \otimes [D] - (B_4 \otimes I_{N-1} + I_{N-1} \otimes B_4 + 2B_2 \otimes B_2) \otimes I_N\Big)E_h = \tilde{R}_h - \Big((B_2 \otimes I_{N-1} + I_{N-1} \otimes B_2) \otimes I_N\Big)\epsilon.$$

or

$$A_h E_h = R_h := \tilde{R}_h - \Big((B_2 \otimes I_{N-1} + I_{N-1} \otimes B_2) \otimes I_N\Big)\epsilon.$$

From (2.39), we get

$$\begin{aligned} |r_j(t_h)|_\infty \leq\ & |(B_4 \otimes I_{N-1})\psi(x_j, y_j, t_h) - \psi_{xxxx}(x_j, y_j, t_h)|_\infty \\ & + |(I_{N-1} \otimes B_4)\psi(x_j, y_j, t_h) - \psi_{yyyy}(x_j, y_j, t_h)|_\infty \\ & + |2(B_2 \otimes B_2)\psi(x_j, y_j, t_h) - 2\psi_{xxyy}(x_j, y_j, t_h)|_\infty \end{aligned}$$

$$+ \left|\psi_{txx}(x_j, y_j, t_h) - (B_2 \otimes I_{N-1})\psi_t(x_j, y_j, t_h)\right|_\infty$$
$$+ \left|\psi_{tyy}(x_j, y_j, t_h) - (I_{N-1} \otimes B_2)\psi_t(x_j, y_j, t_h)\right|_\infty .$$

From the estimate shown in [83],

$$\left|(B_4 \otimes I_{N-1})\psi(x_j, y_j, t_h) - \psi_{xxxx}(x_j, y_j, t_h)\right|_\infty \le cN^7 e^{-CN},$$
$$\left|(I_{N-1} \otimes B_4)\psi(x_j, y_j, t_h) - \psi_{yyyy}(x_j, y_j, t_h)\right|_\infty \le cN^7 e^{-CN}.$$

Furthermore,

$$\begin{aligned}
&\left|(B_2 \otimes B_2)\psi(x_j, y_j, t_h) - \psi_{xxyy}(x_j, y_j, t_h)\right|_\infty \\
&= \left|(B_2 \otimes I_{N-1})(I_{N-1} \otimes B_2)\psi(x_j, y_j, t_h) - \psi_{xxyy}(x_j, y_j, t_h)\right|_\infty \\
&\le \left|(B_2 \otimes I_{N-1})[(I_{N-1} \otimes B_2)\psi(x_j, y_j, t_h) - \psi_{yy}(x_j, y_j, t_h)]\right|_\infty \\
&\quad + \left|(B_2 \otimes I_{N-1})\psi_{yy}(x_j, y_j, t_h) - \psi_{xxyy}(x_j, y_j, t_h)\right|_\infty \\
&\le \|B_2\| \left|(I_{N-1} \otimes B_2)\psi(x_j, y_j, t_h) - \psi_{yy}(x_j, y_j, t_h)\right|_\infty \\
&\quad + \left|(B_2 \otimes I_{N-1})\psi_{yy}(x_j, y_j, t_h) - \psi_{xxyy}(x_j, y_j, t_h)\right|_\infty \\
&\le cN^4 cN^3 e^{-CN} + cN^3 e^{-CN} \le cN^7 e^{-CN}.
\end{aligned}$$

Also, for each $t \in [-1, 1]$,

$$\left|\psi_{txx}(x_j, y_j, t_h) - (B_2 \otimes I_{N-1})\psi_t(x_j, y_j, t_h)\right|_\infty \le C(t)N^3 e^{-c(t)N},$$

where $c(t) \ge c > 0$ for $t \in [-1, 1]$. Thus,

$$\left|\psi_{txx}(x_j, y_j, t_h) - (B_2 \otimes I_{N-1})\psi_t(x_j, y_j, t_h)\right|_\infty \le c_1 N^3 e^{-c_2 N},$$

where $c_1 = \sup_{t\in[-1,1]} C(t)$ and $c_2 = \inf_{t\in[-1,1]} c(t)$. Similarly,

$$|\psi_{tyy}(x_j, y_j, t_h) - (I_{N-1} \otimes B_2)\psi_t(x_j, y_j, t_h)|_\infty \leq c_3 N^3 e^{-c_4 N}.$$

Therefore,

$$\left|\tilde{R}_h\right|_\infty \leq cN^7 e^{-CN}. \tag{2.40}$$

Furthermore, using Proposition 3.6 in [82] and the above estimates, it follows that $|R_h|_\infty \leq cN^7 e^{-CN}$.

Assume that A_h is diagonalizable so that there are diagonal G and invertible X so that $A_h = XGX^{-1}$. Let $W = [[W_h]] \otimes [[W_h]] \otimes [W_h]$. Re-scaling X if necessary, it can be assumed that

$$|W^{1/2}X^{-1}W^{-1/2}|_2 = 1. \tag{2.41}$$

For any vector x, define the norm $\nu(x) = |W^{1/2}X^{-1}x|_2$. The presence of the factor $W^{1/2}$ is so that ν scales approximately like the L^2 norm of a function in space and time whose values are $X^{-1}x$ at the collocation points.

Theorem 2.12 says that $|\lambda| \geq c$ for any eigenvalue λ of A_h. Hence $|G^{-1}|_2 \leq c$. Since $XGX^{-1}E_h = R_h$, it follows that

$$\begin{aligned} W^{1/2}X^{-1}E_h &= (W^{1/2}G^{-1}W^{-1/2})(W^{1/2}X^{-1}W^{-1/2})(W^{1/2}R_h) \\ &= G^{-1}(W^{1/2}X^{-1}W^{-1/2})(W^{1/2}R_h). \end{aligned}$$

Also we know that if ψ is analytic, then $|r(t_j)|_\infty \leq cN^7 e^{-cN}$ for every $0 \leq j < N$.

Further, let z_h be an unit N-vector so that $|B_2 z_h|_2 = |B_2|_2$. Then

$$|B_2 z_h|_2 \leq |W_h^{-1/2}|_2 |W_h^{1/2} B_2 z_h|_2$$

$$\leq cN^{1/2}\|z''\|_{L^2_\omega}$$
$$\leq cN^{9/2}\|z\|_{L^2_\omega}$$
$$\leq cN^{9/2}N^{-1/2}|z_h|_2 = cN^4|z_h|_2,$$

where $z \in P_n$ such that $z(x_h) = z_h$.

Therefore,

$$\begin{aligned}
\nu(E_h)^2 &\leq |G^{-1}|_2^2|W^{1/2}X^{-1}W^{-1/2}|_2^2|W^{1/2}|_2^2|R_h|_2^2 \\
&\leq \frac{2c}{N}\left(\left(\sum_{j=0}^{N-1}|r(t_j)|_2^2\right) + 2|B_2|_2^2\sum_{j=0}^{N-1}|\epsilon_j|_2^2\right) \\
&\leq \frac{2c}{N}\left(N\left(\sum_{j=0}^{N-1}c^2N^{14}e^{-2cN} + 2(cN^4)\sum_{j=0}^{N-1}c^2N^4e^{-2cN}\right)\right) \\
&\leq cN^{15}e^{-2cN}.
\end{aligned}$$

In the above, we used (2.37), (2.40), (2.41) and the fact that $|M_1 \otimes M_2|_2 = |M_1|_2|M_2|_2$ for any matrices M_1, M_2.

If A_h is not diagonalizable, then there is some sequence $(A_h)_n$ converging to A_h so that $(A_h)_n = X_nG_nX_n^{-1}$ for some diagonal G_n and invertible X_n so that $|W^{1/2}X_n^{-1}W^{-1/2}|_2 = 1$. Without loss of generality, take

$$X_1 = I \quad \text{and} \quad (A_h)_1 = G_1. \tag{2.42}$$

For any vector x, define

$$\nu(x) = \sup_{n\geq 1}|W^{1/2}X_n^{-1}x|_2.$$

Now proceed as before with G_n and X_n replacing G and X, respectively. Then

take $n \to \infty$ to obtain, again,

$$\nu(E_h) \leq cN^{7.5}e^{-cN}.$$

The result of the theorem now follows from

$$c|W^{1/2}x|_2 \leq \nu(x), \quad x \in \mathbb{R}^{N(N-1)^2}, \tag{2.43}$$

which follows from (2.42).

This completes the proof of the theorem. □

This chapter establishes the numerical stability and accuracy of the space-time spectral method by proving a condition number estimate for the unsteady Stokes operator and demonstrating spectral convergence using Chebyshev collocation. These results provide a theoretical foundation for the application of space-time spectral methods to time-dependent PDEs.

2.5 Nonlinear PDEs

2.5.1 Navier–Stokes Equations

The Navier–Stokes equations for an incompressible, homogeneous Newtonian fluid over a bounded domain with a Lipschitz boundary are described by a set of two equations. These involve basic physics concepts of momentum and mass conservation where equations (2.44) and (2.45) describe the former and latter, respectively. Let $\Omega = (-1, 1)^2$. The equation in non-dimensional form reads

$$u_t + (u \cdot \nabla)u + \nabla p - \frac{1}{Re}\Delta u = f \quad in \quad \Omega \times (-1, 1), \tag{2.44}$$

$$\nabla \cdot u = 0 \quad in \quad \Omega \times (-1, 1), \tag{2.45}$$

$$u = 0 \quad on \quad \partial\Omega \times (-1, 1), \tag{2.46}$$

$$u(x, y, -1) = u_0(x, y) \quad in \quad \Omega. \tag{2.47}$$

In the equations above, u represents the velocity vector, p is the pressure, and both are functions of space and time.

The non-dimensional quantity Reynolds number is denoted by the symbol Re. This non-dimensional number plays a pivotal role in fluid dynamics. The magnitude of Re is an indication to how significant inertial forces are compared to viscous forces. For $Re \ll 1$, it is possible to neglect the non-linearity (inertial effects) and the Navier-Stokes equations reduce to the Stokes equations. Fluid flow can be identified under two categories. At low Re, the flow is considered to be laminar. In this case, fluid particles flow in an orderly, predictable manner. However, as Re increases, the flow tends to be more complex. In many flows of interest, Re is substantially large. When $Re \gg 1$, the flow typically becomes turbulent.

Further, it can be shown that, taking the curl and using $u = \frac{\partial \psi}{\partial y}\underline{i} - \frac{\partial \psi}{\partial x}\underline{j}$, we can obtain the stream function form of the Navier–Stokes equations;

$$-\Delta\psi_t + \frac{1}{Re}\Delta^2\psi - \psi_y\psi_{xxx} + \psi_x\psi_{yyy} + \psi_x\psi_{yxx} - \psi_y\psi_{xyy} = f_{2x} - f_{1y} \quad in \quad \Omega \times (-1,1), \tag{2.48}$$

$$\psi = \frac{\partial\psi}{\partial\nu} = 0 \quad on \quad \partial\Omega \times (-1,1), \tag{2.49}$$

$$\psi(x,y,-1) = \psi_0(x,y) \quad in \quad \Omega. \tag{2.50}$$

Now, a spectral scheme based on the space-time collocation method can be derived for the unsteady Navier–Stokes equation:

$$-\Delta\psi_t + \frac{1}{Re}\Delta^2\psi - \psi_y\psi_{xxx} + \psi_x\psi_{yyy} + \psi_x\psi_{yxx} - \psi_y\psi_{xyy} = f.$$

A spectral scheme based on the space-time collocation method is

$$\begin{aligned}
&-\Big\{D \otimes \Big((D^2 \otimes I_{N+1}) + (I_{N+1} \otimes D^2)\Big)\Big\}\psi_h + \frac{1}{Re}\Big\{I_{N+1} \otimes \Big((D^4 \otimes I_{N+1}) + (I_{N+1} \otimes D^4)\\
&+ 2(D^2 \otimes D^2)\Big)\Big\}\psi_h - \mathrm{diag}\Big(I_{N+1} \otimes (I_{N+1} \otimes D)\psi_h\Big)(I_{N+1} \otimes (D^3 \otimes I_{N+1}))\psi_h\\
&+ \mathrm{diag}\Big(I_{N+1} \otimes (D \otimes I_{N+1})\psi_h\Big)(I_{N+1} \otimes (I_{N+1} \otimes D^3))\psi_h\\
&+ \mathrm{diag}\Big(I_{N+1} \otimes (D \otimes I_{N+1})\psi_h\Big)(I_{N+1} \otimes (D^2 \otimes D))\psi_h\\
&- \mathrm{diag}\Big(I_{N+1} \otimes (I_{N+1} \otimes D)\psi_h\Big)(I_{N+1} \otimes (D \otimes D^2))\psi_h = f_h,
\end{aligned}$$

where ψ_h and f_h are the vectors of ψ and f, respectively, evaluated at the collocation points. Let B_2 be the spectral second derivative (2.20), B_3 be the spectral third derivative (2.23) and B_4 be the spectral fourth derivative (2.24) defined above.

Finally we may write

$$-\Big\{[D] \otimes \Big((B_2 \otimes I_{N-1}) + (I_{N-1} \otimes B_2)\Big)\Big\}\hat{\psi}_h + \frac{1}{Re}\Big\{I_N \otimes \Big((B_4 \otimes I_{N-1}) + (I_{N-1} \otimes B_4)$$

$$+ 2(B_2 \otimes B_2)\Big)\Big\}\hat{\psi}_h - \mathrm{diag}\Big(I_N \otimes (I_{N-1} \otimes [[D]])\hat{\psi}_h\Big)(I_N \otimes (B_3 \otimes I_{N-1}))\hat{\psi}_h$$
$$+ \mathrm{diag}\Big(I_N \otimes ([[D]] \otimes I_{N-1})\hat{\psi}_h\Big)(I_N \otimes (I_{N-1} \otimes B_3))\hat{\psi}_h$$
$$+ \mathrm{diag}\Big(I_N \otimes ([[D]] \otimes I_{N-1})\hat{\psi}_h\Big)(I_N \otimes (B_2 \otimes [[D]]))\hat{\psi}_h$$
$$- \mathrm{diag}\Big(I_N \otimes (I_{N-1} \otimes [[D]])\hat{\psi}_h\Big)(I_N \otimes ([[D]] \otimes B_2))\hat{\psi}_h = \hat{f}_h - (d_h \otimes \psi_{0h}).$$

Here, the known boundary and initial values have been removed. This nonlinear system can be linearized by replacing one variable by an old iterate in nonlinear terms. Then a simple fixed-point iteration ($k \geq 0$) can be used to solve it for small Re.

$$A_k \psi_h^{k+1} = \tilde{f}_h,$$

where $\tilde{f}_h = \hat{f}_h - (d_h \otimes \psi_{0h})$ and

$$A_k = -[D] \otimes \Big((B_2 \otimes I_{N-1}) + (I_{N-1} \otimes B_2)\Big) + \frac{1}{Re} I_N \otimes \Big((B_4 \otimes I_{N-1}) + (I_{N-1} \otimes B_4)$$
$$+ 2(B_2 \otimes B_2)\Big) - \mathrm{diag}\Big(I_N \otimes (I_{N-1} \otimes [[D]])\hat{\psi}_h^k\Big)(I_N \otimes (B_3 \otimes I_{N-1}))$$
$$+ \mathrm{diag}\Big(I_N \otimes ([[D]] \otimes I_{N-1})\hat{\psi}_h^k\Big)(I_N \otimes (I_{N-1} \otimes B_3))$$
$$+ \mathrm{diag}\Big(I_N \otimes ([[D]] \otimes I_{N-1})\hat{\psi}_h^k\Big)(I_N \otimes (B_2 \otimes [[D]]))$$
$$- \mathrm{diag}\Big(I_N \otimes (I_{N-1} \otimes [[D]])\hat{\psi}_h^k\Big)(I_N \otimes ([[D]] \otimes B_2)).$$

A nonlinear preconditioning method, RASPEN ([32]), is effective for solving nonlinear system at high Reynolds numbers. Details of its implementation are provided in our previous work [82].

2.5.2 Allen–Cahn equation

Consider

$$u_t = \Delta u + au(1-u^2) + f(x,y,t) \quad \text{in} \quad \Omega \times (-1,1),$$

with initial condition $u(x,y,-1) = u_0(x,y)$ and homogeneous Dirichlet boundary conditions. Here a is a positive constant. A spectral scheme based on the space-time collocation method is

$$\Big\{D \otimes (I_{N+1} \otimes I_{N+1})\Big\}u_h = \Big\{I_{N+1} \otimes \Big((D^2 \otimes I_{N+1}) + (I_{N+1} \otimes D^2)\Big)\Big\}u_h + a(u_h - u_h^3) + f_h,$$

where f_h is f evaluated at collocation points.

Deleting the known boundary and initial values, the final scheme reads

$$\Big\{[D] \otimes (I_{N-1} \otimes I_{N-1}) - I_N \otimes \Big(([[D^2]] \otimes I_{N-1}) + (I_{N-1} \otimes [[D^2]])\Big) - aI\Big\}\hat{u}_h + a\hat{u}_h^3 = \hat{f}_h - (d_h \otimes u_{0h}).$$

This nonlinear system can be solved using the simple fixed-point iteration ($k \geq 0$)

$$\Big\{[D] \otimes (I_{N-1} \otimes I_{N-1}) - I_N \otimes \Big(([[D^2]] \otimes I_{N-1}) + (I_{N-1} \otimes [[D^2]])\Big) - aI + a\,\mathrm{diag}((\hat{u}_h^{(k)})^2)\Big\}\hat{u}_h^{(k+1)} = \hat{f}_h - (d_h \otimes u_{0h}).$$

2.5.3 Nonlinear Schrödinger equation

Consider

$$iu_t = -\Delta u + |u|^2 u + f(x,y,t) \quad \text{in} \quad \Omega \times (-1,1),$$

with initial condition $u(x, y, -1) = u_0(x, y)$ and homogeneous Dirichlet boundary conditions. Here a is a positive constant. The spectral scheme is

$$i\Big\{D \otimes (I_{N+1} \otimes I_{N+1})\Big\}u_h = -\Big\{I_{N+1} \otimes \Big((D^2 \otimes I_{N+1}) + (I_{N+1} \otimes D^2)\Big)\Big\}u_h + |u_h|^2 u_h + f_h,$$

where f_h is f evaluated at collocation points.

Deleting the known boundary and initial values, the final scheme reads

$$\Big\{i\Big([D] \otimes (I_{N-1} \otimes I_{N-1})\Big) + I_N \otimes \Big(([[D^2]] \otimes I_{N-1}) + (I_{N-1} \otimes [[D^2]])\Big)\Big\}\hat{u}_h - |\hat{u}_h|^2 \hat{u}_h = \hat{f}_h - (d_h \otimes u_{0h}).$$

This nonlinear system can be solved using the simple fixed-point iteration ($k \geq 0$)

$$\Big\{i\Big([D] \otimes (I_{N-1} \otimes I_{N-1})\Big) + I_N \otimes \Big(([[D^2]] \otimes I_{N-1}) + (I_{N-1} \otimes [[D^2]])\Big)\Big\}\tilde{u}_h^{(k+1)} - |\hat{u}_h^{(k)}|^2 \tilde{u}_h^{(k+1)} = \hat{f}_h - (d_h \otimes u_{0h}),$$

$$\hat{u}_h^{(k+1)} = \frac{\tilde{u}_h^{(k+1)} + \hat{u}_h^{(k)}}{2}.$$

3

Space-Time Spectral Methods for PDEs in Irregular Geometry

3.1 Literature Review

Spectral methods are among the most dominant methods with high-order accuracy that are used to solve PDEs in various fields such as fluid dynamics, quantum mechanics, heat conduction, and weather prediction. However, in contrast to finite-difference and finite-element methods, there are some drawbacks of spectral methods. One drawback is that using spectral methods to discretize PDEs results in the solution of systems of linear or nonlinear equations involving full matrices. On the other hand, traditional methods lead to systems with much larger but sparse matrices that can be handled by appropriate methods to significantly reduce the complexity of the calculations. Another major drawback of basic spectral methods is their inability to handle irregularly shaped domains. However, there have been attempts to address this shortcoming.

The numerical solution of PDEs in complex geometries presents significant challenges due to irregular domain shapes arising from physical constraints and phe-

nomena. Various strategies have been developed to address these challenges, such as spectral element methods, coordinate transformation, and domain embedding. S. Orszag [81] presented a technique that permits the efficient application of spectral methods for solving problems in (nearly) arbitrary geometries. He introduced a new iterative procedure to solve efficiently the full matrix equations resulting from spectral approximations to non-constant coefficient boundary-value problems in complex geometries. Also, K. Korczak and A. Patera [63] presented an isoparametric spectral element technique to solve the two-dimensional Navier–Stokes equations in arbitrary (curvy) geometries. Both these approaches usually involve finite-element preconditioning or use of spectral elements which are similar to finite elements. Other works include [61, 31] and the references therein. Spectral element methods require careful mesh generation and refinement, which can be computationally expensive, and also there is a potential loss of spectral accuracy near element interfaces, particularly for non-smooth solutions.

Coordinate transformation techniques, on the other hand, map irregular domains onto regular ones (e.g., a rectangle or disk) by defining a transformation between the physical and computational domains [64]. This allows standard numerical methods to be applied in the transformed coordinate system. These methods are limited by the fact that analytical transformations are often unavailable for irregular geometries, and poorly constructed transformations can result in a loss of spectral accuracy. Domain embedding simplifies the handling of complex geometries by embedding the irregular domain into a larger, regular domain and extending the problem data to the larger regular domain. Unlike spectral element methods, it avoids the need for mesh generation, and unlike coordinate transformation techniques, it does not rely on the availability of an analytical transformation.

Domain Embedding

Domain embedding methods, also known as 'fictitious domain methods' or 'embedded boundary methods' are numerical techniques used to solve PDEs by embedding a complex or irregular physical domain within a larger, fictitious, and regular domain [6, 7, 13, 21, 24, 25, 36, 72, 48, 49, 94, 95]. With domain embedding, the original PDE defined on an irregular domain is transferred to a regular domain. Doing so simplifies the numerical computation significantly since numercial methods such as finite element and spectral methods perform optimally on regular domains. When formulating the problem, the governing PDEs for the problem are expressed in terms of the variables defined over the larger domain and the boundary conditions of the original domain are then imposed as constraints of the PDE on the fictitious domain.

Spectral Domain Embedding Methods: An approach that combines domain embedding techniques with spectral methods is illustrated by Bueno-Orovio [22, 23], who introduced the 'Spectral Smoothed Boundary Method' which was implemented via Fast Fourier Transform routines. This method approximates the solution of PDEs in irregular domains with no-flux boundary conditions by employing a smoothing term to integrate the boundary conditions into a modified equation suitable for standard spectral methods. Despite its innovative framework, this method has two main drawbacks: It generally achieves lower accuracy compared to traditional spectral methods applied to rectangular domains and also it necessitates a large number of discretization points when using uniform grids.

Another notable contribution in this area is from Stein [55], who proposed the 'Immersed Boundary Smooth Extension Method', designed to solve two-dimensional elliptic and parabolic PDEs on general smooth domains using Fourier spectral methods. Similar to Bueno-Orovio's method, this approach employs domain embedding and approximates both the unknown solution and its smooth extension by solving

a coupled, dense system of equations simultaneously. However, a critical limitation arises from the inversion method used, which relies on an expensive precomputation dependent on both the physical domain and the discretization.

Moreover, there have been several other attempts to use spectral domain embedding methods to solve PDEs in irregular domains, [18, 20, 22, 34, 35, 72] and the references therein. The reference [18] introduced the spectral smoothed boundary method for PDEs in irregular domains. Also, the reference [20] introduced a novel two-dimensional Fourier continuation (2D-FC) method for the biperiodic extension of functions defined on arbitrary smooth two-dimensional domains. A fictitious domain method is introduced in the references [24, 25] that maintains spectral accuracy for elliptic PDE solutions. This approach showcases how complex geometries can be handled effectively using fictitious domains.

Further, in the reference [40], a Lagrange multiplier approach is implemented to solve Dirichlet problems using a fictitious domain method. In [41] the authors extended this methodology to include direct numerical simulations of incompressible viscous flow past moving rigid bodies, thereby illustrating the versatility of fictitious domain methods in fluid dynamics applications. Also, they explored the application of fictitious domain methods for second-order elliptic problems, addressing the derivation of formulations and the iterative solutions using preconditioned conjugate gradient methods [42]. In the reference [41] the authors demonstrated the application of their fictitious domain approach in simulating particulate flow and flow past rigid bodies. Their methodology included operator splitting techniques to manage the complexities of fluid-solid interactions, showcasing the efficacy of fictitious domain methods in practical scenarios.

Moreover, the paper [72] proposed an interesting domain embedding method based on pseudospectral collocation, determining the unknown boundary function on the fictitious domain's boundary while ensuring that the solution satisfies the

boundary conditions along the original irregular domain's boundary. The main disadvantage of this new method is the assumption that the source term is known in the extended regular domain. Often in real applications, this does not hold. Also, this implementation is not optimal since in Legendre collocation, the nodes cluster near the boundary of the rectangle which is outside the domain of interest.

Smooth Extension Embedding Method: Agress and Guidotti [1, 2] proposed a 'Smooth Extension Embedding Method', which reformulates boundary value problems as constrained optimization problems. The focus of this method is to minimize the residual error while still satisfying boundary conditions without the need for an explicit extension. The problem is reformulated as a constrained optimization problem where some error function is minimized, subject to boundary constraints. This strategy derives a computationally efficient and accurate solution within the embedded domain directly. Further, the reference [29] explores how complex boundary conditions can be effectively and accurately handled by applying a smooth extension methods to inhomogeneous elliptic PDEs.

Penalty Methods

Penalty methods are numerical techniques used to weakly enforce boundary conditions in the solution of PDEs. By introducing penalty terms into the governing equations, these methods allow for greater flexibility in how boundary conditions are applied [1, 34, 35, 46, 86]. This is particularly useful in complex geometries where traditional methods may struggle to enforce conditions strictly. The underlying concept of penalty methods is based on modifying the governing equations of the PDE to include additional terms that penalize deviations from specified boundary conditions. This approach transforms the original problem into one that can accommodate some degree of violation of the boundary conditions, thus facilitating the use

of various numerical methods without requiring exact adherence to those conditions. Penalty methods enable flexible handling of complex geometries by weakly enforcing boundary conditions. However, the challenge is to choose appropriate penalty parameters to ensure stability and accuracy.

Elghaoui and Pasquetti [34] presented a mixed spectral-boundary element embedding algorithm that effectively combines penalty methods with spectral techniques to solve fluid dynamics problems. Their findings demonstrate the benefits of penalty methods in achieving stable and accurate solutions in complex geometries. The reference [46] introduced the Smooth Forcing Extension Method, which employs penalty approaches to manage boundary conditions effectively. Their method shows promising results in terms of accuracy and efficiency when solving elliptic PDEs.

Active Penalty Methods are an advanced version of traditional penalty methods used to solve PDEs [86]. Unlike standard penalty methods that apply a fixed penalty term to enforce boundary conditions, active penalty methods adaptively modify the penalty parameters based on the local behavior of the solution. This dynamic approach aims to enhance the accuracy and stability of the numerical solution, particularly in fluid dynamics and other applications where interfaces and boundaries play critical roles. The theoretical concept behind Active Penalty Methods is to further the weak enforcement of boundary conditions by incorporating mechanisms that are adaptive and responsive to the characteristics of the solution. The goal is to minimize the errors associated with enforcing boundary conditions while maintaining the physical accuracy of the solution. Active penalty methods can achieve greater accuracy in satisfying boundary conditions, especially in complex flows where traditional methods may struggle. The dynamic adjustment of penalty parameters improves the stability of the numerical solution but these adjustments can lead to increased computational costs compared to traditional penalty methods.

Shirokoff and Nave [86] presented an active penalty method for solving incom-

pressible Navier-Stokes equations, showcasing improved accuracy over conventional methods. Their work highlights the effectiveness of adapting penalty terms in fluid dynamics applications. The reference [2] introduced a smooth extension method and discussed the advantages of implementing adaptive techniques that agree with the principles of active penalty methods.

Cut-off Techniques

Cut-off techniques are numerical methods employed to manage boundary conditions and address irregular geometries when solving PDEs. These techniques involve creating smooth approximations or modifying the characteristic functions of the domains to enhance numerical stability and convergence [21, 29]. Cut-off functions are typically used to define the regions where the PDE is valid and to enforce boundary conditions effectively. The theoretical foundation of these techniques is based on the principle of modifying the characteristic function of a domain to create a smooth transition between the solution domain and the exterior or background region. This approach enables us to apply standard numerical methods that are known to perform well in regular domains while minimizing numerical oscillations near the boundaries. Since sharp transitions lead to numerical instabilities, a cut-off function is used to apply boundary conditions in a smooth and continuous manner. These techniques can be combined with finite element methods, finite difference methods, or spectral methods to ensure that the numerical scheme effectively handles irregular geometries. By employing smooth approximations of characteristic functions, cut-off techniques improve stability and facilitate the application of numerical methods, although the introduction of smoothing can lead to approximation errors, especially if the cut-off function is not chosen appropriately.

Alfonso [21] discusses the application of cut-off techniques in spectral methods for fluid dynamics problems, highlighting their role in managing boundary conditions

effectively. Also, the reference [29] explores the role of cut-off techniques in maintaining spectral accuracy while solving inhomogeneous elliptic PDEs, emphasizing their effectiveness in complex geometries.

Hybrid Methods

Multiple numerical techniques are combined to create hybrid methods that improve flexibility and performance. These are well suited for capturing local behavior while maintaining global accuracy. Such hybrid methods are superior to single-method approaches that may struggle to deliver the desired accuracy or efficiency when used to solve PDEs in complex geometries. By integrating techniques such as finite element, finite difference, and spectral methods, hybrid methods provide a versatile framework for tackling a wide range of problems in computational mathematics and engineering. The core idea behind hybrid methods is to divide the computational domain into subdomains where different numerical techniques can be optimally applied based on the characteristics of each region [5, 18, 76]. For example, smooth regions may employ spectral methods due to their high accuracy, while complex or irregular regions may utilize finite element methods. Special care is taken at the interfaces between different methods to ensure that the solutions remain consistent and that discontinuities are avoided. In some cases, iterative methods are employed to update the solutions in adjacent subdomains until convergence is achieved, ensuring consistency across the computational domain. By intelligently combining these approaches, hybrid methods aim to exploit the respective advantages of each technique. Often, implementing hybrid methods proves more challenging than a single numerical technique as the interfaces and coupling conditions need to be managed very carefully. If not handled properly, the interfaces between different methods can introduce numerical instabilities, especially if the methods yield significantly divergent solutions.

Bruno and Lyon [18] highlighted the advantages of combining spectral accuracy with finite element flexibility by studying how hybrid spectral methods can be used to solve PDEs in complex domains. Further, Lyon [76] explained the effectiveness of coupling spectral and finite element techniques in capturing complex flow dynamics, particularly in fluid dynamics applications.

3.2 Domain Embedding and Fourier Continuation

This section provides a more detailed explanation of domain embedding, as the proposed technique in this thesis is based on this concept. There are only a limited number of studies on spectral collocation methods for time-dependent PDEs in complex geometries. Thus, in this thesis, we propose a numerical method to approximate solutions of PDEs in irregular domains using space-time spectral collocation methods. By an irregular domain, we mean a domain that is neither a square nor a disk, so that standard spectral methods cannot be applied directly. The main idea of our method is to embed the irregular domain in a regular one and apply periodic or non-periodic extensions [13, 58]. There are several ways available to extend a function to a larger domain.

Strategies for smooth extension of inhomogeneous term: Methodologies for extending inhomogeneous terms in PDEs have made significant progress over the years. In 1996, Elghaoui and Pasquetti [35] introduced a domain embedding method applicable to unsteady advection-diffusion and the unsteady incompressible Navier–Stokes equations. This method was implemented by converting the PDE into a semi-discrete elliptic linear problem using a finite difference semi-implicit scheme in time. The reduced problem is then solved using a combination of Fourier approximations and a boundary element approach, which facilitates the imposition of

boundary conditions. A key feature of this approach is the 'periodic extension' produced using Fourier approximation, which enables a smooth extension of the body force from an irregular domain into a fictitious, regular domain.

Following this work, Boyd [13] presented a closely related methodology for solving PDEs in non-rectangular domains. Boyd's strategy involves extending the inhomogeneous term $f(x, y)$ to the fictitious rectangular domain through a 'window' function. This ensures that the extended function $g(x, y)$ is periodic, infinitely differentiable, and retains the value of $f(x, y)$ throughout the physical domain. Boyd's extension technique relies on defining a suitable form for $g(x, y)$ when $f(x, y)$ and the boundary of the irregular domain are described by a C^∞ function. Under these conditions, the solution to the PDE can be expressed as a two-dimensional Fourier series. After that, Bueno-Orovio [21] developed a convolution-based extension method for cases where the boundary of the irregular domain cannot be defined as the zero isoline of a C^∞ function. However, both Boyd's [13] and Bueno-Orovio's [21] methods primarily focus on PDEs with constant coefficients, such as the Poisson equation.

Fourier-Continuation (FC) Methods: In 2010, the concept of periodic extensions for solving the Heat and Laplace equations in smooth boundaries re-emerged in a paper by Bruno and Lyon [18]. They introduced a numerical scheme that discretizes the PDE in time, subsequently splitting it into sets of uncoupled spatial ODEs using an alternating direction method. To complete the time-stepping algorithm, each spatial ODE is solved with high-order accuracy on the corresponding Cartesian line through the FC-Gram method. This method is based on Gram Polynomials and generates a Fourier series with period $b > 0$ for a smooth periodic extension of a given function. It effectively resolves the Gibbs phenomenon and can be computed at Fast Fourier Transform (FFT) speed [14].

The FC-Gram approach provides a highly accurate approximation with computa-

tional costs equivalent to a single FFT, although it offers only fixed-order accuracy. Influenced by this work, Lyon [69] developed a super-algebraically convergent algorithm specifically for computing Fourier continuations of nonperiodic functions. However, this algorithm is slower than the FC-Gram method and is designed to produce a Fourier extension with a unique period $b = 2$.

To address the limitations of fixed periodicity, Huybrechs [58, 59] proposed new algorithms aimed at computing Fourier extensions without the restrictions imposed by previous methods. These advancements reflect the ongoing efforts to refine techniques for handling complex geometries and inhomogeneous terms in the context of PDEs, ensuring greater flexibility and accuracy in numerical simulations. One of the main advantages of the Fourier continuation method is that high-order accuracy can be achieved with a small number of grid points. Additionally, it can handle complex geometries with arbitrary shapes and can be used to solve a wide range of PDEs, including elliptic, parabolic, and hyperbolic PDEs.

3.3 Extension Techniques and Novel Contributions for Solving PDEs on Irregular Domains

In this thesis, we consider three cases. In the first case, the non-homogeneous term is assumed to be known in the extended domain. In the second case, the non-homogeneous term is only known within the physical domain, and a periodic extension is performed to extend it to the larger domain. Similarly, in the third case, a non-periodic extension is applied to the extended domain.

In general, the function is unknown outside the physical domain. However, in the first case, we assume that the non-homogeneous term is analytic and periodic in the extended domain. This was a first attempt to extend the method introduced in [72] to time-dependent PDEs. Then we use spectral domain embedding methods to solve

PDEs in the complex geometries. That is, first we embed the complex geometry in a larger, regular (rectangular) domain using a domain embedding method and then extend the solution of the PDE outside the complex geometry using a periodic function. The solution of the PDE on this regular domain can be approximated using the Fourier spectral method. Finally, the extended solution can be interpolated back to the complex geometry which provides an accurate approximation of the solution.

Consider a bounded domain Ω in $\mathbb{R}^2$ with a complex boundary. Suppose f is a smooth function. Define the PDE

$$-\Delta u = f \quad in \;\; \Omega, \tag{3.1}$$

$$u = g \quad on \;\; \partial\Omega. \tag{3.2}$$

The basic idea is to embed Ω in a larger rectangle and then apply the FC method. Here, we consider the domain Ω to be a strict subset of the square $R = (-\pi, \pi)^2$ and we adjust the values on the boundary of the square so that $u = g$ on $\partial\Omega$. Here we use the Fourier spectral method to solve the PDE on R.

Let x_j be evenly spaced points in $[-\pi, \pi)$, $j = 0, \ldots, N-1$ with N odd and D_h be an $N \times N$ matrix, called the Fourier pseudospectral derivative matrix, which is given by

$$(D_h)_{kk} = 0, \qquad (D_h)_{kj} = \frac{(-1)^{k-j}}{2\sin((k-j)\pi/N)}, \quad j \neq k. \tag{3.3}$$

Let M be the number of constraints to be imposed on the boundary $\partial\Omega$. That is, let $(p_i, q_i), i = 1, ..., M$ (we take $M = 2N + 1$) be equally-spaced points along $\partial\Omega$ such that $u(p_i, q_i) = g(p_i, q_i)$. We generate M equally spaced points along the boundary $\partial\Omega$ by uniformly discretizing the parameter $s \in [0, 2\pi)$ with step size $\Delta s = \frac{2\pi}{M}$. These points are then mapped to the boundary using a parametric representation $z(s) = (x(s), y(s))$, depending on the geometry of Ω.

For different domains, we define the boundary points (x_i, y_i) as follows:

- Circle: $z(s) = r\,[\cos(s), \sin(s)]$ for some fixed $r > 0$.
- Ellipse: $z(s) = [r_1 \cos(s),\ r_2 \sin(s)]$ where $r_1, r_2 > 0$ define the semi-axes.
- Butterfly-shaped domain: $z(s) = r\,[\cos(s),\ \sin(2s)]$.

In each case, we define a vector of M angles:

$$s_i = \frac{2\pi(i-1)}{M}, \quad i = 1, 2, \ldots, M$$

and use the above parametric forms to compute the boundary nodes $(x_i, y_i) \in \partial\Omega$. This procedure produces points that are equally spaced in the parameter s, which corresponds to equally spaced angles for the circle and smooth parametric spacing for more general shapes.

Therefore the global system is

$$\begin{bmatrix} A & W \\ V_1 & V_2 \end{bmatrix} \begin{bmatrix} u_1 \\ u_2 \end{bmatrix} = \begin{bmatrix} f_h \\ g \end{bmatrix}, \tag{3.4}$$

where $A = [A_0;\ A_x;\ A_y]$, $W = [W_0;\ W_x;\ W_y]$ and $f_h = [f_0;\ f_x;\ f_y]$. The unknowns in the interior of R are denoted by u_1, while u_2 denotes unknowns along ∂R. Here, $A_0 \in \mathbb{R}^{N^2 \times N^2}$ is the discrete Laplacian Fourier spectral differential operator on R corresponding to unknowns in its interior and $W_0 \in \mathbb{R}^{N^2 \times (N-1)^2}$ is the boundary differential operator involving terms along the boundary of the rectangle.

The matrices A_x and $A_y \in \mathbb{R}^{(N-1)^2 \times N^2}$ are the discrete differential operators involving periodic Neumann boundary conditions on ∂R corresponding to interior unknowns on R, while W_x and $W_y \in \mathbb{R}^{(N-1)^2 \times (N-1)^2}$ correspond to the differential operators involving terms along the boundary of the rectangle. The components of the $M \times (N+1)^2$ matrix $V = [V_1, V_2]$ are the coefficients of the constraint equations.

Further, interpolation is required to relate values along $\partial\Omega$ and values in R. See Figure 4.2 in Chapter 4.

This concept can be extended to solve time-dependent PDEs in irregular geometries as well. Here we use Fourier spectral method for space variables and the Legendre collocation method for the time variable. The temporal domain is considered as $(-1, 1)$.

Now let's consider the stream function formulation of the unsteady Stokes equation defined in a complex domain Ω.

$$-\Delta\psi_t + \Delta^2\psi = f \quad in \quad \Omega \times (-1, 1), \tag{3.5}$$

$$\psi = g \quad on \quad \partial\Omega \times (-1, 1), \tag{3.6}$$

$$\psi_x = h_1, \;\; \psi_y = h_2 \quad on \quad \partial\Omega \times (-1, 1), \tag{3.7}$$

$$\psi(x, y, -1) = \psi_0(x, y) \quad in \quad \Omega. \tag{3.8}$$

Thus, the corresponding global system is

$$\begin{bmatrix} A & W \\ V & U \\ V_x & U_x \\ V_y & U_y \end{bmatrix} \begin{bmatrix} u_1 \\ u_2 \end{bmatrix} = \begin{bmatrix} f_h \\ g \\ h_1 \\ h_2 \end{bmatrix}, \tag{3.9}$$

where $A = [A_0;\;\; A_x;\;\; A_y]$, $W = [W_0;\;\; W_x;\;\; W_y]$ and $f_h = [f_0 - (\psi_{0h} \otimes d_h);\;\; f_x;\;\; f_y]$. Here $d_h = D(0 : N - 1, N)$, where D is the Legendre pseudospectral derivative matrix. The unknowns in the interior of R are denoted by u_1 while u_2 denotes unknowns along ∂R. Here, $A_0 \in \mathbb{R}^{N^3 \times N^3}$ is the discrete Fourier spectral differential operator on R corresponding to unknowns in its interior and $W_0 \in \mathbb{R}^{N^3 \times N(N-1)^2}$ is the differential operator involving terms along the boundary of the rectangle.

The matrices A_x and $A_y \in \mathbb{R}^{N(N-1)^2 \times N^3}$ are the differential operators involving

periodic Neumann boundary conditions on ∂R corresponding to interior unknowns on R, while W_x and $W_y \in \mathbb{R}^{N(N-1)^2 \times N(N-1)^2}$ correspond to the differential operators involving terms along the boundary of the rectangle. The components of the $NM \times N(N+1)^2$ matrix $[V, U]$ are the coefficients of the constraint equations corresponding to Dirichlet boundary conditions on $\partial\Omega$. Similarly, the components of the matrices $[V_x, U_x]$ and $[V_y, U_y]$ are the coefficients of the constraint equations corresponding to Neumann boundary conditions on $\partial\Omega$. Interpolation is required to implement all these constraint equations. See Figure 4.3 in Chapter 4. Moreover, with a fixed point iteration, for instance, the above space-time Fourier continuation domain embedding method can also be used to solve nonlinear PDEs. See Figure 4.4 in Chapter 4.

In the second case, we assume that the non-homogeneous term is only known in the physical domain and perform a periodic extensions to the extended domain. Initially, we implemented Boyd's technique [13] for this Fourier extension and observed super-algebraic convergence only. Then we applied the method introduced by Huybrechs' [58] to extend the non-homogeneous term of the PDE from the physical domain to the regular domain with exponential accuracy for special domains. Subsequently, in the third case, we modified Huybrechs' method to perform a non-periodic extension with exponential accuracy for general domains.

We now review Boyd's periodic extension method and Huybrechs' method based on half-range Chebyshev polynomials, which provide the theoretical foundation for our work.

3.3.1 Fourier Extension - Boyd's Method

Define $\partial\Omega$ as the zero-isoline (level set) of a C^∞ function $\Phi(x, y)$. Rescale $\Phi(x, y)$ as $\tilde{\Phi}(x, y) \equiv C\Phi(x, y)$ where C is a constant chosen so that the level surface $\tilde{\Phi}(x, y) = 1$ is a curve ∂A which is

i) contained within the extended domain and

ii) is exterior to $\partial\Omega$.

The basic idea for extending $f(x, y)$ is to multiply it by a 'window' function $\rho(x, y)$ with the following properties:

1. $\rho(x, y) \equiv 1$ everywhere in Ω,

2. ρ is 'infinitely flat' everywhere on ∂A and its exterior,

3. $\rho(x, y)$ is C^∞.

Definition 3.1 (Infinitely flat)**.** A C^∞ function $g(x, y)$ is said to be 'infinitely flat' at a point if g and all its derivatives are zero at that point.

Such a window function is $\rho(x, y) \equiv \mathcal{H}(1 - 2\tilde{\Phi}(x, y))$, where $\mathcal{H}$ is a smoothed approximation to the step function:

$$\mathcal{H}(x; L) \equiv \frac{1}{2}\{1 + \mathcal{E}(x; L)\},$$

where $\mathcal{E}$ is an error-function-like function such as

$$\mathcal{E}(x; L) = \begin{cases} -1, & x < -1, \\ \operatorname{erf}\left(\frac{Lx}{\sqrt{1-x^2}}\right), & x \in [-1, 1], \\ 1, & x > 1, \end{cases}$$

and L is an experimentally chosen scaling factor that specifies how rapidly the erf-like, ramp, and window functions tend to their limits.

The extended function is then the product of f with the window function ρ:

$$g(x, y) \equiv \rho(x, y) f(x, y).$$

By construction, $g(x, y) \equiv f(x, y)$ everywhere in Ω. Similarly, $g(x, y)$ is identically zero everywhere outside the curve ∂A.

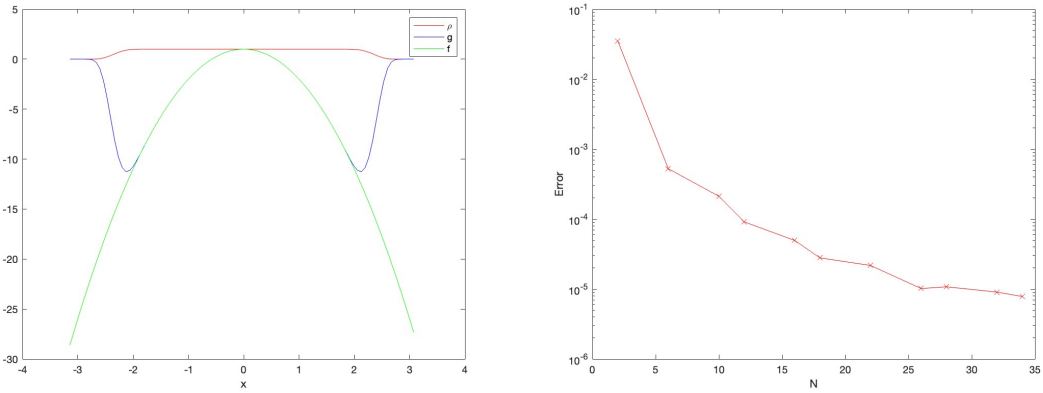

Figure 3.1: Fourier extension and error convergence for the 1D Poisson equation.

Figure 3.1 shows Fourier extension of $f(x) = 1 - 3x^2$ using Boyd's method and the error convergence of 1-D Poisson equation having the non-homogeneous term f. The convergence rate is super-algebraic and not spectral.

3.3.2 Half-Range Chebyshev Polynomials

Orthogonal polynomials play a crucial role in numerical analysis and various other fields. Classical families, such as Jacobi, Hermite, and Laguerre polynomials, have been extensively studied and applied across a wide range of mathematical methods and disciplines. Here we focus on two families of non-classical orthogonal polynomials introduced by Huybrechs in [58]: the half-range Chebyshev polynomials of the first and second kinds.

These polynomials derive their name from the fact that they share the same weight functions as the classical Chebyshev polynomials, yet they are orthogonal on a smaller interval. Similar to their classical counterparts, the half-range Chebyshev polynomials can be utilized in various applications, including approximation techniques and solving differential equations through spectral methods. To effectively employ these polynomials, it is essential to have a robust algorithm for their computation. To address this need, Orel and Perne [80] describe an efficient method to

construct these polynomials using modified Chebyshev algorithm.

3.3.2.1 Chebyshev polynomials:

Chebyshev polynomials $T_k(y)$ of the first kind are classical polynomials. They are orthogonal with respect to the weight function $1/\sqrt{1-y^2}$ on the interval $[-1,1]$, and normalized such that $T_k(1) = 1$. These polynomials are derived as solutions to the Chebyshev differential equation and are characterized by the following relationship:

$$\cos(k\theta) = T_k(\cos\theta), \quad k \in \mathbb{N}, \tag{3.10}$$

This equation indicates that $\cos(k\theta)$ can be expressed as a polynomial in $\cos\theta$. Chebyshev polynomials $U_k(y)$ of the second kind are orthogonal with respect to the weight function $\sqrt{1-y^2}$ on the interval $[-1,1]$, and normalized such that $U_k(1) = k+1$. The corresponding property to (3.10) is given by:

$$\frac{\sin((k+1)\theta)}{\sin\theta} = U_k(\cos\theta), \quad k \in \mathbb{N}, \tag{3.11}$$

which expresses the fact that $\sin((k+1)\theta)$ is also a polynomial in $\cos\theta$, up to a factor $\sin\theta$.

3.3.2.2 Three-term recurrence relation and modified Chebyshev algorithm:

For the stable construction of a family of orthogonal polynomials, the recursion coefficients α_k and β_k are required for each k in the three-term recurrence relation $(\pi_1(x) = 0, \pi_2(x) = \text{const})$:

$$\tilde{\pi}_{k+1}(x) = (x - \alpha_k)\pi_k(x) - \beta_k\pi_{k-1}(x), \quad k = 2, 3, \ldots \tag{3.12}$$

where

$$\alpha_k = \int_0^1 x(\pi_k(x))^2 w(x)\,dx, \tag{3.13}$$

$$\beta_k = \int_0^1 x\pi_k(x)\pi_{k-1}(x)w(x)\,dx \tag{3.14}$$

and

$$\pi_{k+1}(x) = \frac{\tilde{\pi}_{k+1}(x)}{\|\tilde{\pi}_{k+1}(x)\|}. \tag{3.15}$$

Here, the polynomials π_k are orthogonal polynomials with an integrable non-negative weight function $w(x)$. Unfortunately, the calculation of the recursive coefficients α_k and β_k using formulas (3.13) and (3.14) can be numerically unstable. With standard finite-precision arithmetic, we begin to lose accuracy starting from a small value of k (for example, $k = 12$). To address this issue, we can apply a stable modified Chebyshev algorithm for the computation of recursion coefficients, which is effective with standard finite-precision arithmetic.

The modified Chebyshev algorithm:

The objective is to calculate the first N recursion coefficients α_j and β_j that define the three-term recurrence relation given by:

$$\pi_1(x) = 0, \quad \pi_2(x) = 1,$$

$$\pi_{j+1}(x) = (x - \alpha_j)\pi_j(x) - \beta_j\pi_{j-1}(x), \quad j = 2, 3, 4, \ldots$$

for a family of monic orthogonal polynomials π_j defined over the interval (a, b), ensuring that the orthogonality conditions are satisfied:

$$\int_a^b \pi_k(x)\pi_\ell(x)w(x)\,dx = 0, \quad k \neq \ell. \tag{3.16}$$

The main concept behind constructing the first N orthogonal polynomials is to use the first $2N$ modified moments:

$$\nu_j = \int_a^b p_j(x)w(x)\,dx, \quad j = 1, 2, \ldots, 2N, \tag{3.17}$$

instead of the initial $2N$ power moments:

$$\mu_j = \int_a^b x^{j-1}w(x)\,dx, \quad j = 1, 2, \ldots, 2N. \tag{3.18}$$

Here, $w(x)$ is the weight function associated with the orthogonal family from which we seek the coefficients. The polynomials p_j are orthogonal polynomials defined over the same interval (a, b) as the family of π_j being constructed, but with a different weight function. They satisfy a recurrence relation:

$$p_1(x) = 0, \quad p_2(x) = 1, \tag{3.19}$$

$$p_{j+1}(x) = (x - a_j)p_j(x) - b_j p_{j-1}(x), \quad j = 2, 3, 4, \ldots \tag{3.20}$$

where the coefficients a_j and b_j are known explicitly.

Now, we present the algorithm proposed by Wheeler in [93].

$$\sigma_{k,\ell} = \int_a^b \pi_k(x)\pi_\ell(x)w(x)\,dx, \quad k, \ell \geq 1. \tag{3.21}$$

The orthogonality conditions imply that $\sigma_{k,\ell} = 0$ for $\ell < k$. The input data for the algorithm consist of the known recursive coefficients a_j and b_j, along with the modified moments v_j, which must be computed accurately. The output data are the recursive coefficients α_j and β_j.

Algorithm 1. Initialize:

$$\begin{aligned}
\alpha_1 &= a_1 + \frac{v_2}{v_1}, & \beta_1 &= v_1; \\
\sigma_{1,\ell} &= 0, & \ell &= 2, \ldots, 2N-1; \\
\sigma_{2,\ell} &= v_\ell, & \ell &= 1, \ldots, 2N.
\end{aligned}$$

For $k = 3, 4, \ldots, N+1$ compute:

$$\begin{aligned}
\sigma_{k,\ell} &= \sigma_{k-1,\ell+1} - (\alpha_{k-2} - a_\ell)\sigma_{k-1,\ell} \\
&\quad - \beta_{k-2}\sigma_{k-2,\ell} + b_{\ell-1}\sigma_{k-1,\ell-1}, \quad \ell = 2, \ldots, 2N-(k-1)+1; \\
\alpha_{k-1} &= a_{k-1} + \frac{\sigma_{k,k}}{\sigma_{k,k-1}} - \frac{\sigma_{k-1,k-1}}{\sigma_{k-1,k-2}}; \\
\beta_{k-1} &= \frac{\sigma_{k,k-1}}{\sigma_{k-1,k-2}}.
\end{aligned}$$

The normalization factors can be calculated as:

$$\|\pi_1\|^2 = v_1,$$

$$\|\pi_j\|^2 = \beta_j \|\pi_{j-1}\|^2, \quad j = 2, 3, \ldots, N.$$

Since the two families of orthogonal polynomials are not monic, we compute the recursive coefficients for the normalized polynomials as:

$$\alpha_j^* = \alpha_j, \quad j = 1, 2, \ldots \tag{3.22}$$

$$\beta_j^* = \beta_j \frac{\|\pi_{j-1}\|}{\|\pi_j\|}, \quad j = 2, 3, \ldots \tag{3.23}$$

The formulas (3.22) and (3.23) are derived easily by comparing the three-term re-

currence relations for both monic and normalized polynomials.

3.3.2.3 Half-range Chebyshev polynomials of the first kind

Half-range Chebyshev polynomials have the same weight functions as the classical Chebyshev polynomials of the first and second kinds, but are orthogonal on the interval $[0,1]$ rather than on the interval $[-1,1]$. Therefore, half-range Chebyshev polynomials of the first kind are orthogonal on the interval $[0,1]$ with the weight function $w(x) = \frac{1}{\sqrt{1-x^2}}$.

Definition 3.2. Let $T_k^h(x)$ be the unique normalized sequence of orthogonal polynomials satisfying

$$\int_0^1 T_k^h(x) x^\ell \frac{1}{\sqrt{1-x^2}}\, dx = 0, \quad \ell = 0, \ldots, k-1, \tag{3.24}$$

$$\frac{4}{\pi}\int_0^1 (T_k^h(x))^2 \frac{1}{\sqrt{1-x^2}}\, dx = 1. \tag{3.25}$$

Then the set $\{T_k^h(x)\}_{k=0}^\infty$ is called *half-range Chebyshev polynomials of the first kind.*

Lemma 3.3. [80] The power moments for the the half-range Chebyshev polynomials of the first kind are

$$\mu_{2k} = \frac{\binom{2k}{k}\pi}{2^{2k+1}}, \quad k = 0, 1, \ldots \tag{3.26}$$

$$\mu_{2k+1} = \frac{(2k)!!}{(2k+1)!!}, \quad k = 0, 1, \ldots \tag{3.27}$$

For the construction of the recursion coefficients with the modified Chebyshev algorithm, we use the shifted Legendre polynomials on the interval $[0,1]$ as a known family of orthogonal polynomials $p_k(x)$. Since the polynomials for the modified Chebyshev algorithm should be monic, the set of p_k's is given by

$$p_k(x) = \frac{(k!)^2}{(2k)!} P_k(2x-1), \tag{3.28}$$

where $P_k(2x-1)$ represents the shifted Legendre polynomials. The recursion coefficients in the recurrence relation for the shifted monic Legendre polynomials are

$$a_k = \frac{1}{2}, \quad k = 1, 2, \ldots, \tag{3.29}$$

$$b_k = \frac{1}{4(4-k^{-2})}, \quad k = 1, 2, \ldots \tag{3.30}$$

The modified moments ν_k defined by (3.17) are computed using a symbolic computation package from the power moments μ_k, given in (3.26) and (3.27), and are plotted in Figure 3.2. Let $p_j(x) = \sum_{j=1}^{2N} c_j x^{j-1}$. Thus, by (3.17),

$$\begin{aligned}
\nu_j &= \int_a^b \sum_{j=1}^{2N} c_j x^{j-1} w(x) dx \\
&= \sum_{j=1}^{2N} c_j \int_a^b x^{j-1} w(x) dx \\
&= \sum_{j=1}^{2N} c_j \mu_j \quad \text{by} \quad (3.18),
\end{aligned}$$

where c_j are the coefficients of orthogonal polynomials defined in 3.28. To calculate the shifted Legendre polynomials and c_j, we use the MATLAB commands 'legendreP$(n, 2x-1)$' and 'coeffs()' respectively. Then $\nu_j = \text{sum}(c_j \cdot * \mu_j)$.

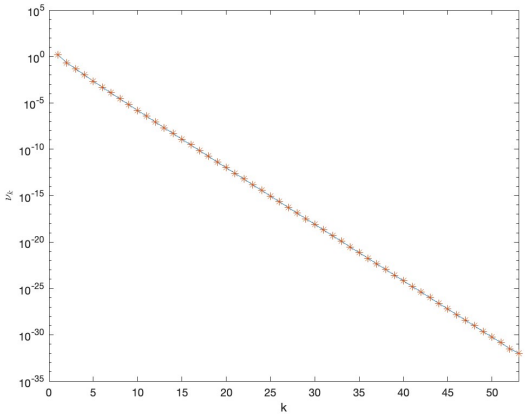

Figure 3.2: Modified moments ν_k for the half-range Chebyshev polynomials of the first kind.

The modified Chebyshev algorithm returns the recursion coefficients α_k and β_k for the monic half-range Chebyshev polynomials $\pi_k(x)$ of the first kind and the norms of these polynomials. We are now able to compute the recursion coefficients α_k^* and β_k^* of the half-range Chebyshev polynomials $T_k^h(x)$ of the first kind defined above via the formulas (3.22) and (3.23).

Monic polynomials:

$$\pi_1(x) = 0, \quad \pi_2(x) = 1,$$

$$\pi_{j+1}(x) = (x - \alpha_j)\pi_j(x) - \beta_j \pi_{j-1}(x), \quad j = 2, 3, 4, \ldots.$$

Non-monic polynomials:

$$\pi_1^*(x) = 0, \quad \pi_2^*(x) = \frac{1}{\sqrt{2}},$$

$$\pi_{j+1}^*(x) = \frac{\|\pi_{j-1}\|}{\|\pi_j\|}((x - \alpha_j^*)\pi_j^*(x) - \beta_j^* \pi_{j-1}^*(x)), \quad j = 2, 3, 4, \ldots.$$

The first five half-range Chebyshev polynomials of the first kind are shown in Figure 3.3:

$$T_0^h(x) = 0.7071,$$

$$T_1^h(x) = 2.298x - 1.463,$$

$$T_2^h(x) = 9.024x^2 - 10.11x + 1.924,$$

$$T_3^h(x) = 35.818x^3 - 57.827x^2 + 25.144x - 2.296,$$

$$T_4^h(x) = 142.663x^4 - 301.254x^3 + 205.607x^2 - 48.791x + 2.615.$$

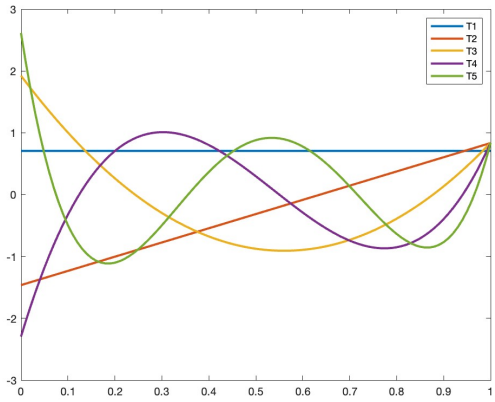

Figure 3.3: First five half-range Chebyshev polynomials of the first kind.

3.3.2.4 Half-range Chebyshev polynomials of the second kind

Half-range Chebyshev polynomials of the second kind are orthogonal on the interval $[0, 1]$ with the weight function $\sqrt{1-x^2}$.

Definition 3.4. Let $U_k^h(x)$ be the unique normalized sequence of orthogonal polynomials satisfying

$$\int_0^1 U_k^h(x) x^\ell \sqrt{1-x^2}\, dx = 0, \quad \ell = 0, \ldots, k-1, \tag{3.31}$$

$$\frac{4}{\pi} \int_0^1 (U_k^h(x))^2 \sqrt{1-x^2}\, dx = 1. \tag{3.32}$$

Then the set $\{U_k^h(x)\}_{k=0}^\infty$ is called *half-range Chebyshev polynomials of the second kind.*

Lemma 3.5. [80] The power moments for the the half-range Chebyshev polynomials of the second kind are

$$\mu_{2k} = \frac{\binom{2k}{k}\pi}{2^{2k+2}(k+1)}, \quad k = 0, 1, \ldots \tag{3.33}$$

$$\mu_{2k+1} = \frac{(2k)!!}{(2k+3)!!}, \quad k = 0, 1, \ldots \tag{3.34}$$

For the construction of the recursion coefficients using the modified Chebyshev algorithm, we again use the monic shifted Legendre polynomials defined in (3.28) over the interval $[0, 1]$ with coefficients given in (3.29) and (3.30) as a known family of orthogonal polynomials p_k. The modified moments ν_k, defined by (3.17), are computed using a symbolic computation package from the power moments μ_k provided in (3.33) and (3.34), and these are plotted in Figure 3.4.

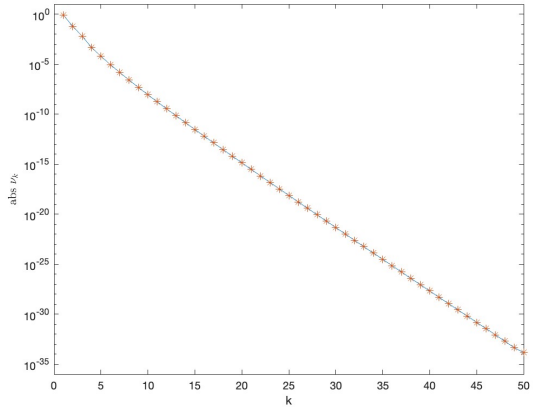

Figure 3.4: Absolute value of modified moments ν_k for the half-range Chebyshev polynomials of the second kind.

The modified Chebyshev algorithm yields the recursion coefficients α_k and β_k for the monic half-range Chebyshev polynomials $\pi_k(x)$ of the second kind, along with the norms of these polynomials. We are now able to compute the recursion coefficients α_k^* and β_k^* of the half-range Chebyshev polynomials $U_k^h(x)$ of the second kind defined above via the formulas (3.22) and (3.23).

Monic polynomials:

$$\pi_1(x) = 0, \quad \pi_2(x) = 1,$$

$$\pi_{j+1}(x) = (x - \alpha_j)\pi_j(x) - \beta_j\pi_{j-1}(x), \quad j = 2, 3, 4, \ldots.$$

Non-monic polynomials:

$$\pi_1^*(x) = 0, \quad \pi_2^*(x) = 1,$$

$$\pi^*_{j+1}(x) = \frac{\|\pi_{j-1}\|}{\|\pi_j\|}((x-\alpha^*_j)\pi^*_j(x) - \beta^*_j\pi^*_{j-1}(x)), \quad j = 2, 3, 4, \ldots.$$

The first five half-range Chebyshev polynomials of the second kind are shown in Figure 3.5:

$$U^h_0(x) = 1,$$
$$U^h_1(x) = 3.783x - 1.606,$$
$$U^h_2(x) = 14.912x^2 - 13.586x + 2.038,$$
$$U^h_3(x) = 59.259x^3 - 83.342x^2 + 31.027x - 2.393,$$
$$U^h_4(x) = 236.162x^4 - 449.649x^3 + 273.965x^2 - 57.44x + 2.701.$$

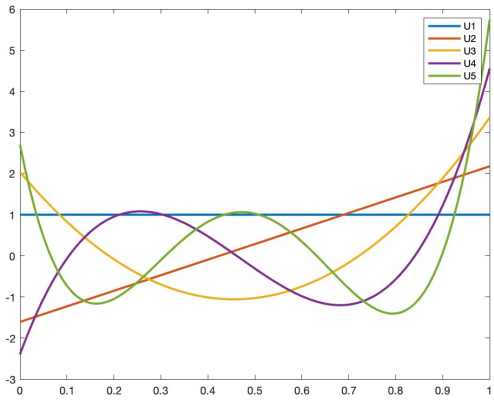

Figure 3.5: First five half-range Chebyshev polynomials of the second kind.

3.3.3 Fourier Extension - Huybrechs' Method

The representation of non-periodic functions through periodic Fourier series presents significant challenges, particularly due to convergence issues and artifacts such as the Gibbs phenomenon, which occurs near discontinuities or boundaries. These challenges can limit the effectiveness of Fourier analysis in various applications, including signal processing, numerical simulations, and data approximation. To address

these limitations, Huybrechs [58] introduced a robust method for constructing periodic extensions of non-periodic functions. The fundamental idea is to achieve a spectrally accurate Fourier series by extending a non-periodic function f, defined on the interval $[-1, 1]$, into a periodic function over a larger interval, typically $[-T, T]$ for some $T > 1$.

3.3.3.1 Optimization Problem

Consider a function $f \in L^2_{[-1,1]}$ that is not necessarily periodic. The problem of finding a suitable extended function g of f that is periodic on a larger interval has been explored by Boyd [14], as well as by Bruno [16] and Bruno, Han, and Pohlman [17]. These authors proposed solving the following optimization problem.

Problem 1. For $T > 1$ and positive integer n, let G_n be the space of $2T$-periodic functions of the form

$$G_n = \left\{ \frac{a_0}{2} + \sum_{k=1}^{n} a_k \cos \frac{\pi k x}{T} + b_k \sin \frac{\pi k x}{T}, a_k, b_k \in \mathbb{R} \right\}.$$

The Fourier extension of f, defined on the interval $[-1, 1]$, to the interval $[-T, T]$ is the solution to the optimization problem

$$g_n := \arg\min_{g \in G_n} \|f - g\|_{L^2_{[-1,1]}}.$$

This problem is called Fourier continuation by Bruno and coworkers [16, 17] and Fourier extension of the third kind by Boyd in [14]. Fourier extension of the first kind is a problem where f is known explicitly outside the interval $[-1, 1]$. Fourier extension of the second kind is a problem where f is also known outside $[-1, 1]$ but has singularities there.

Huybrechs also analyzed above Problem 1 and used half-range Chebyshev poly-

nomials of the first and second kinds to solve the problem for $T = 2$. Define

$$D_n := C_n \cup S_n,$$

where

$$C_n := \left\{ \frac{1}{\sqrt{2}} \right\} \cup \left\{ \cos \frac{k\pi x}{2} \right\}_{k=1}^{n}, \quad S_n := \left\{ \sin \frac{k\pi x}{2} \right\}_{k=1}^{n}.$$

Note that the set C_n consists of even functions and the set S_n of odd functions. The function space is the span of D_n, which for any finite n, forms a basis for a finite-dimensional subspace of $L^2([-1,1])$; that is, all functions in D_n are linearly independent and belong to $L^2([-1,1])$. It was proved by Huybrechs in [58] that the set

$$\left\{ T_k^h \left(\cos \frac{\pi x}{2} \right) \right\}_{k=0}^{n}$$

is an orthonormal basis for $\mathcal{C}_n := \operatorname{span}(C_n)$ on $[-1,1]$ and the set

$$\left\{ U_k^h \left(\cos \frac{\pi x}{2} \right) \sin \frac{\pi x}{2} \right\}_{k=0}^{n-1}$$

is an orthonormal basis for $\mathcal{S}_n := \operatorname{span}(S_n)$ on $[-1,1]$. Here the functions T_k^h and U_k^h are the half-range Chebyshev polynomials introduced in Section 3.2.2.

The sets $\mathcal{C}_n$ and $\mathcal{S}_n$ consist of even and odd functions, respectively. According to this, we can expand an arbitrary function $f \in L^2_{[-1,1]}$ into a so-called half-range Chebyshev–Fourier series:

$$f(x) = \sum_{k=0}^{\infty} a_k T_k^h \left(\cos \frac{\pi x}{2} \right) + \sum_{k=0}^{\infty} b_k U_k^h \left(\cos \frac{\pi x}{2} \right) \sin \frac{\pi x}{2}. \tag{3.35}$$

Huybrechs in [58] proved that the solution to Problem 1 is a truncated half-range Chebyshev–Fourier series.

Theorem 3.6. [58] For a given $f \in L^2_{[-1,1]}$, the solution to the Problem 1 is

$$g_n(x) = \sum_{k=0}^{n} a_k T_k^h \left(\cos\frac{\pi x}{2}\right) + \sum_{k=0}^{n-1} b_k U_k^h \left(\cos\frac{\pi x}{2}\right) \sin\frac{\pi x}{2} \tag{3.36}$$

where

$$a_k = \int_{-1}^{1} f(x) T_k^h \left(\cos\frac{\pi x}{2}\right) dx, \tag{3.37}$$

$$b_k = \int_{-1}^{1} f(x) U_k^h \left(\cos\frac{\pi x}{2}\right) \sin\frac{\pi x}{2} dx. \tag{3.38}$$

Here T_k^h and U_k^h are half-range Chebyshev polynomials of the first and second kinds.

3.3.3.2 Computing the coefficients

In this section, we follow the approach presented in [58] to calculate the coefficients a_k, b_k using Gaussian quadrature. Both families of orthogonal polynomials T_m^h and U_m^h have associated families of Gaussian quadrature. Denote by $\{y_j^{FK}\}_{j=1}^m$ the roots of the half-range Chebyshev polynomials of the first kind $T_m^h(y)$. Note that all roots lie in the interval $(0, 1)$ and that the associated weights are positive. The weights satisfy

$$\sum_{j=1}^{m} w_j^{FK} \left(y_j^{FK}\right)^j = \frac{4}{\pi} \int_0^1 y^j T_j^h(y) \frac{1}{\sqrt{1-y^2}}\, dy, \quad k = 0, \ldots, 2m-1;$$

i.e., the quadrature rule is exact for polynomials up to degree $2m-1$. Similarly, denote by $\{y_j^{SK}\}_{j=1}^m$ the roots of the half-range Chebyshev polynomials of the second kind $U_m^h(y)$. The associated weights satisfy

$$\sum_{j=1}^{m} w_j^{SK} \left(y_j^{SK}\right)^j = \frac{4}{\pi} \int_0^1 y^j U_j^h(y) \sqrt{1-y^2}\, dy, \quad k = 0, \ldots, 2m-1.$$

The weights can be computed efficiently in a numerically stable manner based on the recurrence coefficients of the orthogonal polynomials [44]. Any set of orthogonal

polynomials $\{p_j(x)\}_{j=1}^N$ satisfies a three-term recurrence relationship:

$$p_j(x) = (a_j x + b_j)p_{j-1}(x) - c_j p_{j-2}(x), \quad j = 1, 2, \ldots, N; \quad p_{-1}(x) \equiv 0, \quad p_0(x) \equiv 1, \tag{3.39}$$

with $a_j > 0, c_j > 0$. In our case, $a_j = \frac{\|\pi_{j-1}\|}{\|\pi_j\|}, b_j = \left(\frac{\|\pi_{j-1}\|}{\|\pi_j\|}\right)\alpha_j^*$ and $c_j = \left(\frac{\|\pi_{j-1}\|}{\|\pi_j\|}\right)\beta_j^*$ with the corresponding $p_{-1}(x)$ and $p_0(x)$. We may identify 3.39 with the matrix equation:

$$x\begin{bmatrix} p_0(x) \\ p_1(x) \\ p_2(x) \\ \vdots \\ p_{N-2}(x) \\ p_{N-1}(x) \end{bmatrix} = \begin{bmatrix} -\frac{b_1}{a_1} & \frac{1}{a_1} & 0 & 0 & \cdots & 0 \\ \frac{c_2}{a_2} & -\frac{b_2}{a_2} & \frac{1}{a_2} & 0 & \cdots & 0 \\ 0 & \frac{c_3}{a_3} & -\frac{b_3}{a_3} & \frac{1}{a_3} & \cdots & 0 \\ \vdots & & \ddots & \ddots & \ddots & \vdots \\ 0 & & & \ddots & \ddots & \frac{1}{a_{N-1}} \\ 0 & 0 & 0 & \cdots & \frac{c_N}{a_N} & -\frac{b_N}{a_N} \end{bmatrix} \begin{bmatrix} p_0(x) \\ p_1(x) \\ p_2(x) \\ \vdots \\ p_{N-2}(x) \\ p_{N-1}(x) \end{bmatrix} + \begin{bmatrix} 0 \\ 0 \\ 0 \\ \vdots \\ \vdots \\ \frac{p_N(x)}{a_N} \end{bmatrix}$$

or, equivalently in matrix notation

$$xp(x) = Tp(x) + \left(\frac{1}{a_N}\right) p_N(x) e_N$$

where T is the tridiagonal matrix and $e_N = (0, 0, \ldots, 0, 1)^T$. Thus $p_N(t_j) = 0$ if and only if $t_j p(t_j) = Tp(t_j)$ where t_j is an eigenvalue of the tridiagonal matrix T. We can show that T is symmetric if the polynomials are orthonormal. If T is not symmetric, then we may perform a diagonal similarity transformation D which will yield a symmetric tridiagonal matrix J. Thus,

$$DTD^{-1} = J = \begin{bmatrix} \alpha_1 & \beta_1 & 0 & 0 & \cdots & 0 \\ \beta_1 & \alpha_2 & \beta_2 & 0 & \cdots & 0 \\ 0 & \beta_2 & \alpha_3 & \beta_3 & \cdots & 0 \\ \vdots & & \ddots & \ddots & \ddots & \vdots \\ 0 & & & \ddots & \ddots & \beta_{N-1} \\ 0 & 0 & 0 & \cdots & \beta_{N-1} & \alpha_N \end{bmatrix}$$

where

$$\alpha_i = -\frac{b_i}{a_i}, \quad \beta_i = \left(\frac{c_{i+1}}{a_i \cdot a_{i+1}} \right)^{1/2}. \tag{3.40}$$

As a consequence of the Christoffel-Darboux identity

$$w_j [p(t_j)]^T [p(t_j)] = 1, \quad j = 1, 2, \ldots, N, \tag{3.41}$$

where $p(t_j)$ corresponds to the eigenvector associated with the eigenvalue t_j. Suppose that the eigenvectors of T are calculated so that

$$Jq_j = t_j q_j, \quad j = 1, 2, \ldots, N \tag{3.42}$$

with $q_j^T q_j = 1$. If $q_j^T = (q_{1,j}, q_{2,j}, \ldots, q_{N,j})$, then

$$q_{1,j}^2 = w_j (p_0(t_j))^2 \text{ by (3.41).} \tag{3.43}$$

Thus,

$$w_j = \frac{q_{1,j}^2}{(p_0(t_j))^2} = \frac{q_{1,j}^2}{k_0^2} = q_{1,j}^2 \int_a^b \omega(x)\, dx \equiv q_{1,j}^2 \mu_0. \tag{3.44}$$

It is interesting to point out that the first kind of quadrature rule can also be applied to develop a quadrature rule on the interval $[-1, 1]$, which is exact for all trigonometric functions in G_{2m-1}. We define $2m$ quadrature points and weights as

follows:

$$\begin{aligned} x_j^{TR} &= \frac{2}{\pi}\cos^{-1} y_j^{FK}, \\ x_{j+m}^{TR} &= -\frac{2}{\pi}\cos^{-1} y_j^{FK}, \\ w_j^{TR} &= \frac{1}{2} w_j^{FK}, \\ w_{j+m}^{TR} &= \frac{1}{2} w_j^{FK}, \end{aligned} \tag{3.45}$$

for $j = 1, \ldots, m$.

The transformation $x = \frac{2}{\pi}\cos^{-1} y$ is applied to the points y_j^{FK}. This transformation maps the interval $[0, 1]$ to itself. However, the resulting rule may be applied only to even functions. The quadrature points are therefore mirrored to $[-1, 0]$, with halved weights, to select the even part of any given function f. As a result, the rule is exact for all odd functions on $[-1, 1]$.

Now we can compute the coefficients a_k and b_k as follows.

$$a_k \approx \sum_{j=1}^{m} w_j^{FK} f_e\left(\frac{2}{\pi}\cos^{-1} y_j^{FK}\right) T_k^h(y_j^{FK}), \tag{3.46}$$

$$b_k \approx \sum_{j=1}^{m} w_j^{SK} \frac{f_o\left(\frac{2}{\pi}\cos^{-1} y_j^{SK}\right)}{\sqrt{1-(y_j^{SK})^2}} U_k^h(y_j^{SK}), \tag{3.47}$$

where f_e and f_o are even and odd parts of f. Therefore, equivalent expressions are

$$a_k \approx \sum_{j=1}^{m} \frac{1}{2} w_j^{FK} \left[f\left(\frac{2}{\pi}\cos^{-1} y_j^{FK}\right) + f\left(\frac{-2}{\pi}\cos^{-1} y_j^{FK}\right)\right] T_k^h(y_j^{FK}), \tag{3.48}$$

$$b_k \approx \sum_{j=1}^{m} \frac{1}{2} w_j^{SK} \left[\frac{f\left(\frac{2}{\pi}\cos^{-1} y_j^{SK}\right)}{\sqrt{1-(y_j^{SK})^2}} - \frac{f\left(\frac{-2}{\pi}\cos^{-1} y_j^{SK}\right)}{\sqrt{1-(y_j^{SK})^2}} \right] U_k^h(y_j^{SK}). \tag{3.49}$$

Figure 3.6 shows the size of the a_k and b_k coefficients of g_n in the form (3.36) for two functions f. The first function (left panel) is entire but not periodic. The second function (right panel) is entire and periodic. The convergence rate for this example is faster than exponential. The computations were performed in MATLAB

in double precision using the algorithm outlined in section 3.3.3.2.

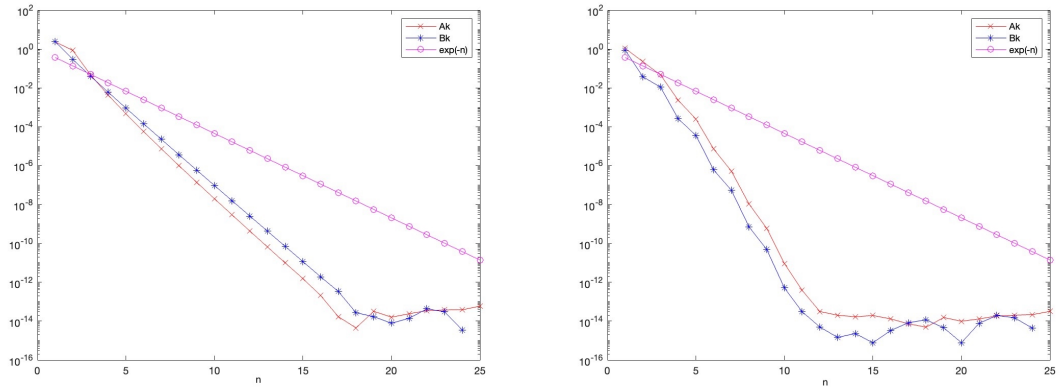

(a) $f(x) = 2x^2 + 3x + 1$ (b) $f(x) = \cos\cos\frac{\pi x}{2} + \sin\sin\frac{\pi x}{2}$

Figure 3.6: Logarithmic plots of the a_k coefficients and b_k coefficients of g_n in the form (3.36).

Huybrechs' method is defined to obtain a Fourier extension of a function from the domain $[-1, 1]$ to $[-2, 2]$. Figure (3.7) shows periodic extensions of two non-periodic functions from $[-1, 1]$ to $[-2, 2]$. By applying a simple scaling, Huybrechs' method can be modified to obtain a Fourier extension from any arbitrary domain $[-a, b]$ to $[-T, T]$. Figure (3.8) shows periodic extensions from two arbitrary physical domains $[-a, b]$ to $[-2, 2]$, where $a = 1, b = 0.75$ and $a = 1.5, b = 1.5$.

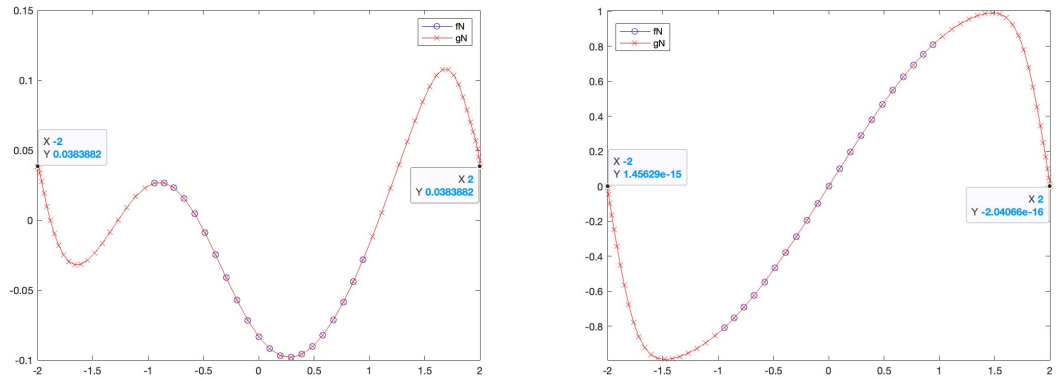

Figure 3.7: Periodic extensions from $[-1, 1]$ to $[-2, 2]$ for two different functions.

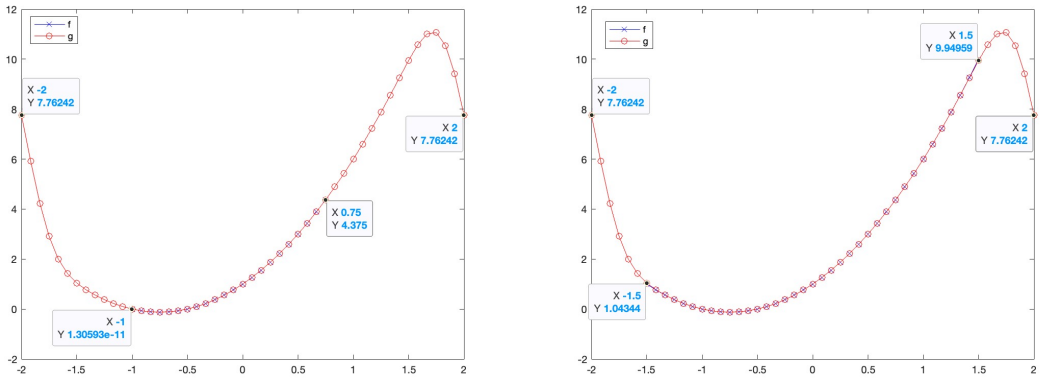

Figure 3.8: Periodic extensions from arbitrary physical domain $[-a, b]$ to $[-2, 2]$.

The following Figure (3.9) shows the approximation error within the physical domain between $f(x)$ and $g(x)$, where $f(x) = 2x^2 + 3x + 1$. Here, $f(x)$ is defined on the domain $[-1, 0.75]$ and $g(x)$ is the extended function on the domain $[-2, 2]$.

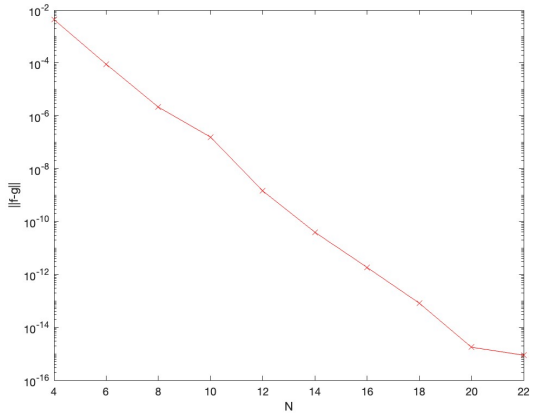

Figure 3.9: Approximation error $\|f - g\|_\infty$ where $f(x) = 2x^2 + 3x + 1$.

By utilizing the concept of one-dimensional Fourier extension, we introduced a new algorithm that can be used for two-dimensional Fourier extension.

3.3.3.3 Alternating Fourier Extension Algorithm

In the literature, Huybrech's technique is usually applied to 1D problems and tensor product 2D domains. We now introduce a new algorithm for two-dimensional Fourier extension by combining both techniques; 1D Fourier extension and domain embedding. The basic idea of this algorithm is to embed the complex geometry in a larger, regular (rectangular) domain and then apply Fourier extension in both x and y directions alternatingly until the periodicity error in both direction is very small. The algorithm is outlined below. Suppose our rectangular domain is $(-2, 2)^2$.

Two dimensional Fourier Extension - Algorithm

- Identify each set of endpoints $[x_{i,1}, x_{i,n+1}]$ corresponding to equally-spaced nodes y_i, with y_1, y_{n+1} being the minimum and maximum y coordinates of the physical domain, respectively.

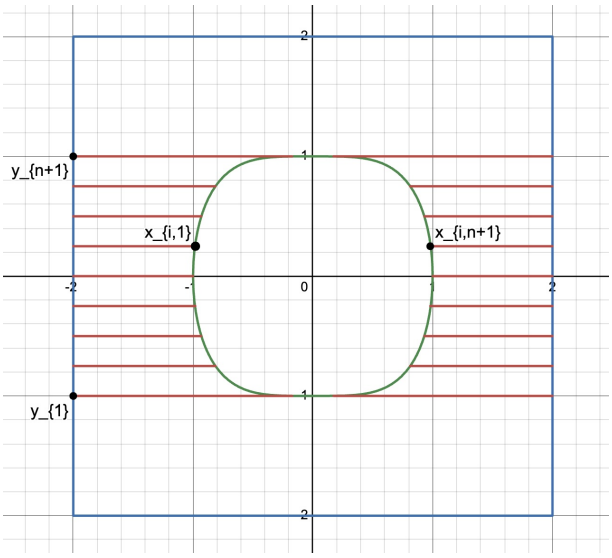

Figure 3.10: Periodic extension in the x-direction.

- At each y_i, extend $[x_{i,1}, x_{i,n+1}]$ in the $x-$direction to $[-2, 2]$ using a one-dimensional periodic extension. Say that extension is g_x^i :

$$(g_x)_{[-2,2]\times[y_1,y_{n+1}]} = \begin{pmatrix} g_x^1 \\ g_x^2 \\ \vdots \\ g_x^i \\ \vdots \\ g_x^{n+1} \end{pmatrix}.$$

- Then do the extension in $y-$direction using g_x.
- At each x_i extend $[y_1, y_{n+1}]$ in the $y-$direction to $[-2, 2]$ using a one-dimensional periodic extension. Say that extension is g_y^i :

  $(g_y)_{[-2,2]\times[-2,2]} = \begin{pmatrix} g_y^1 & g_y^2 & \dots & g_y^i & \dots & g_y^{n+1} \end{pmatrix}.$

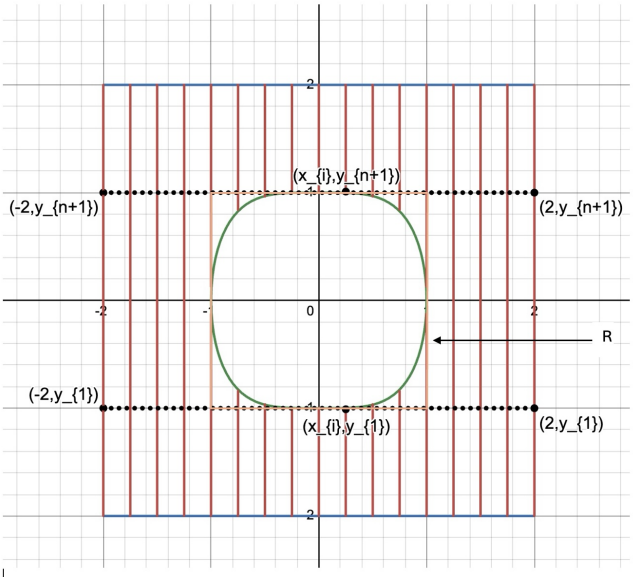

Figure 3.11: Periodic extension in the y-direction.

- Proceed with the second subsequent x-extension from the smallest rectangular domain R enclosing Ω to $(-2, 2)^2$, and so on.
- Repeat this process until the periodicity error in both directions is smaller than some tolerance $\epsilon > 0$.

This two-dimensional Alternating Fourier Extension algorithm allows us to solve PDEs defined on special irregular geometries using the Fourier spectral method, as explained in (3.4). Numerical experiments are given in Chapter 4.

However, we observed an issue when applying the Alternating Fourier Extension method for non-rectangular physical domains. Consider the complex domain $x^4 + y^2 = 1$ and say y_1 and y_{n+1} are the minimum and maximum y coordinates of the domain. Using the Alternating Fourier Extension, we first extend the domain in the x-direction for each y_i where $y_1 \leq y_i \leq y_{n+1}$. The issue arises when extending y_i's closer to the edge points y_1 and y_{n+1}, where the extension results in spikes at the corners of the extended domain $[-T, T]$. We were able to overcome this issue by implementing a non-periodic extension.

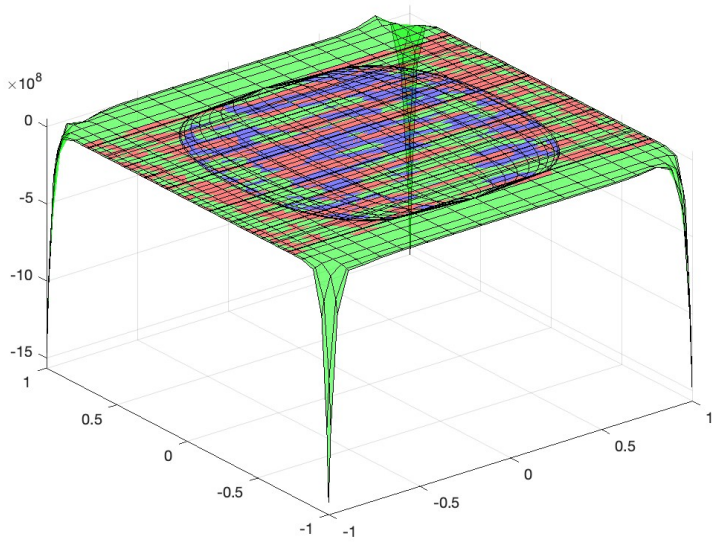

Figure 3.12: Spikes at the boundary of the extended domain.

3.3.4 Non-Periodic Extension

We now present a novel non-periodic extension strategy designed for general two-dimensional irregular domains. This development constitutes a central contribution of this thesis.

3.3.4.1 One-dimensional non-periodic extension

Suppose $f(x)$ is defined on the domain $(-a, b)$ where $a, b \in (0, 1)$, and we are trying to extend f, not necessarily periodically, to the domain $(-1, 1)$. See Figure (3.13).

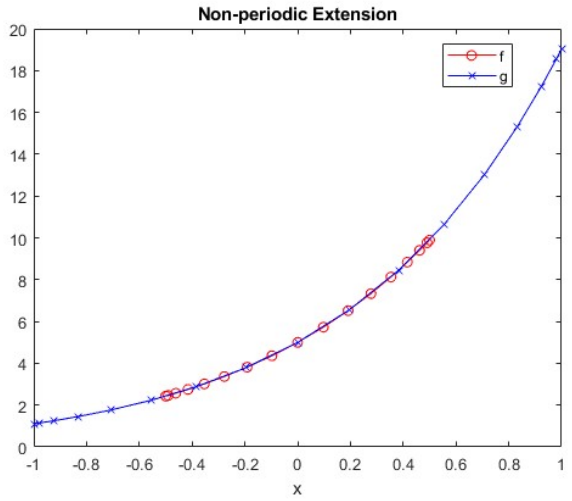

Figure 3.13: Non-periodic extension of function $f(x) = e^x(5 + 2x)$ from $[-0.5, 0.5]$ to $[-1, 1]$.

3.3.4.2 Alternating Non-Periodic Extension Algorithm

We introduce this algorithm for a two-dimensional non-periodic extension. The concept is very similar to Alternating Fourier Extension algorithm we introduced in the previous section. Here, we combined both techniques; 1D non-periodic extension and domain embedding. The basic idea of this algorithm is to embed the complex geometry in a larger, regular (rectangular) domain $(-1, 1)^2$ and then apply non-periodic extension in both x and y directions. For the non-periodic extension, the y_i's are the

Chebyshev Gauss-Lobatto points. The algorithm is outlined below.

Two dimensional Non-Periodic Extension - Algorithm

- Identify each set of endpoints $[x_{i,1}, x_{i,n+1}]$ corresponding to y_i, with y_1, y_{n+1}; the minimum and maximum y coordinates of the physical domain, respectively.
- If the domain is non simply connected, identify each set of x endpoints corresponding to y values.
- Take the number of points in each set to be proportional to the length of each line segment.

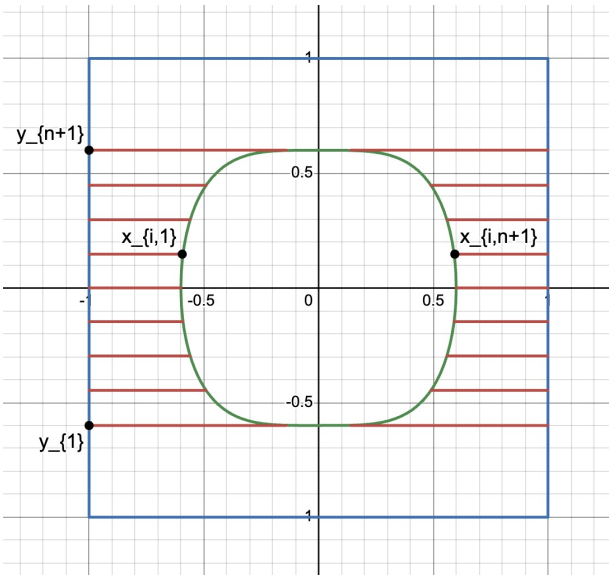

Figure 3.14: Non-periodic extension in the x-direction.

- At each y_i extend $[x_{i,1}, x_{i,n+1}]$ in the $x-$direction to $[-1, 1]$ using a one dimensional non-periodic extension. If there is more than one set of x endpoints for a given y, combine all intervals of x when implementing the extension in the $x-$ direction. Say that extension is g_x^i :

$$(g_x)_{[-1,1]\times[y_1,y_{n+1}]} = \begin{pmatrix} g_x^1 \\ g_x^2 \\ \vdots \\ g_x^i \\ \vdots \\ g_x^{n+1} \end{pmatrix}.$$

- Then do the extension for $y-$direction using g_x.
- At each x_i extend $[y_1, y_{n+1}]$ in the $y-$direction to $[-1, 1]$ using a one dimensional non-periodic extension. Say that extension is g_y^i :

  $(g_y)_{[-1,1]\times[-1,1]} = \begin{pmatrix} g_y^1 & g_y^2 & \dots & g_y^i & \dots & g_y^{n+1} \end{pmatrix}.$

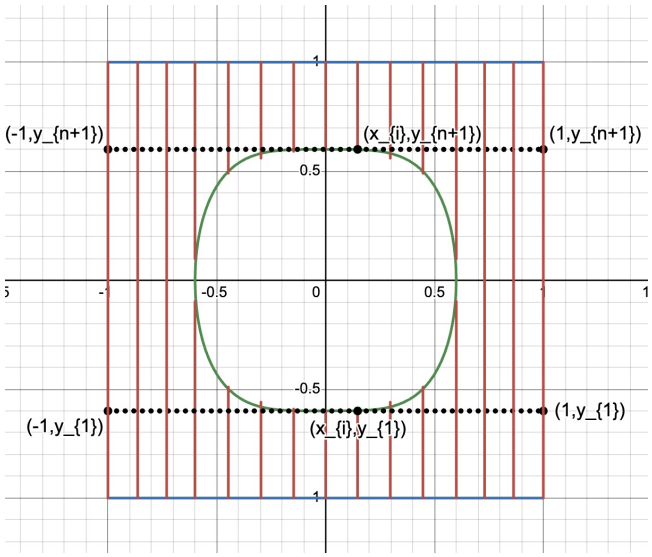

Figure 3.15: Non-periodic extension in the y-direction.

This two-dimensional Alternating Non-Periodic Extension allows us to solve PDEs defined on irregular geometries while at the same time, resolve the issue where the Alternating Periodic Extension resulted in spikes at the corners of the extended do-

main. This algorithm is also more efficient than the Alternating Periodic Extension since only one $x-$extension and one $y-$extension is required.

Consider a bounded domain Ω in $\mathbb{R}^2$ with a complex boundary. Define the PDE

$$-\Delta u = f \quad in \;\; \Omega, \tag{3.50}$$

$$u = r \quad on \;\; \partial\Omega. \tag{3.51}$$

The basic idea is to embed Ω in a larger rectangular domain and then apply the two-dimensional Alternating Non-Periodic Extension algorithm. Here, we assume the domain Ω is a strict subset of the rectangle $\tilde{\Omega} = (-1,1)^2$ and we adjust the values on the boundary of the rectangle so that $u = r$ on $\partial\Omega$. Here we use the Chebyshev spectral method to solve the PDE on $\tilde{\Omega}$. Let $x_j = \cos(\frac{\pi j}{n})$ be Chebyshev Gauss-Lobatto nodes in $[-1,1]$, $j = 0, \ldots, n$ and D_h be an $(n+1)\times(n+1)$ matrix, called the Chebyshev pseudospectral derivative matrix, which is given by

$$(D_h)_{kj} = \begin{cases} \frac{(-1)^{k+j}}{x_k - x_j}\frac{d_k}{d_j}, & k \neq j; \\ -\frac{x_k}{2(1-x_k^2)}, & 1 \leq k = j \leq n-1; \\ \frac{2n^2+1}{6}, & k = j = 0; \\ -\frac{2n^2+1}{6}, & k = j = n. \end{cases}$$

Here $d_j = \begin{cases} 2, & \text{if } j = 0,\, n; \\ 1, & \text{if } 1 \leq j \leq n-1. \end{cases}$

Let M be the number of constraints to be imposed on the boundary $\partial\Omega$. That is, let $(p_i, q_i), i = 1, ..., M$ (we take $M = 4n$) be points along $\partial\Omega$ such that $u(p_i, q_i) = r(p_i, q_i)$. Therefore the global system is

$$\begin{bmatrix} A \\ W \end{bmatrix} \begin{bmatrix} U_h \end{bmatrix} = \begin{bmatrix} [[g]] \\ r \end{bmatrix}. \tag{3.52}$$

Here, $A \in \mathbb{R}^{(n-1)^2 \times (n+1)^2}$ is the Chebyshev spectral differential operator $-\Delta$ on $\tilde{\Omega}$ and $W \in \mathbb{R}^{4n \times (n+1)^2}$ corresponds to the constraint equations such that $u(p_i, q_i) = r(p_i, q_i)$. Further, interpolation is required to relate values along $\partial\Omega$ and values in $\tilde{\Omega}$. The unknowns in $\tilde{\Omega}$ are denoted by U_h and g is the non-periodic extension obtained from the Alternating Non-Periodic extension algorithm.

Furthermore, this algorithm works well for various types of complex geometries, including circular, star-shaped, and other non-convex domains. When we have a non simply connected domain, we need to identify each set of x endpoints corresponding to y values. If there are more than one set of x endpoints for a given y, we need to consider all intervals of x when implementing the extension in $x-$direction. For example, consider a doughnut-shaped domain. Since it contains a hole, at some y values we must consider two separate $x-$intervals, while at other $y-$values we can proceed as before, using only one set of x endpoints when implementing the extension in the $x-$direction. Also, to improve accuracy, we can take the number of points in each set to be proportional to the length of each line segment. Numerical experiments are given in Chapter 4, and the results verify that this method accurately handles complex geometries, demonstrating its effectiveness across diverse domain shapes.

Huybrech's one-dimensional periodic extension has a complexity of $O(n^2)$. Hence, our non-periodic extension of two-dimensional domains has a complexity of $O(n^3)$. For time-dependent PDEs on two-dimensional spatial domains, the non-periodic extension of the source term over all times takes $O(n^4)$ operations. The solution of the linear system takes a complexity of $O(n^3 \log n)$, assuming that the FFT can be used. Hence the overall complexity is $O(n^4)$ with $O(n^3)$ unknowns.

Recent work ([50, 52, 79]) demonstrates how to accelerate half-range expansions using fast transforms, reducing the cost to quasi-optimal complexity $O(n \log^2 n)$. This is achieved by decomposing the process into structured steps involving conversion to shifted Jacobi polynomials, conversion to shifted Chebyshev polynomials, and the application of fast cosine/sine transforms (DCT/DST). Incorporating such fast algorithms into our non-periodic extension framework could further reduce the computational cost of the extension and solution stages in future implementations.

After performing the non-periodic extension, direct solvers can be applied to solve both linear and nonlinear time dependent PDEs defined on the extended regular domain. Since Gaussian elimination is computationally expensive, the Bartels-Stewart [10] or Hessenberg-Schur algorithm [45] can be used instead to solve the linear systems arising from the space-time spectral scheme. These methods are considerably faster than Gaussian elimination and can be used to solve matrix equations of the form $AX + XB = C; \quad A \in \mathbf{R}^{m\times m}$ and $B \in \mathbf{R}^{n\times n}$. Decompositions for the Hessenberg-Schur algorithm are defined as,

$$H = U^T A U, \qquad\qquad S = V^T B^T V, \tag{3.53}$$

where H is an upper-Hessenberg matrix and S is an upper quasi-triangular matrix. Forward or backward substitution can now be used to solve the simplified system.

$$HY + YS^T = F \qquad\qquad (F = U^T C V, \quad Y = U^T X V).$$

Assuming $S_{k,k-1}$ is zero, then it follows that

$$(H + S_{kk} I) y_k = f_k - \sum_{j=k+1}^{n} S_{kj} y_j,$$

where y_k is the kth column of Y. Now the solution can be found using $X = UYV^T$.

Therefore, the time complexity of the Hessenberg-Schur algorithm can be summarized as follows. Firstly, we shall assume that $\frac{5}{3}m^3$ and $10n^3$ operations [45] are required for the Schur decompositions mentioned in (3.53).

- Reduce A to upper Hessenberg and B^T to upper triangular matrices

  $H = U^T AU$ $\qquad\qquad$ $\frac{5}{3}m^3$.

  $S = V^T B^T V$ $\qquad\qquad$ $10n^3$.

- Update the right hand side

  $F = U^T CV$ $\qquad\qquad$ $m^2n + mn^2$.

- Back substitute for Y

  $HY + YS^T = F$ $\qquad\qquad$ $3m^2n + \frac{1}{2}mn^2$.

- Obtain solution

  $X = UYV^T$ $\qquad\qquad$ $m^2n + mn^2$.

Thus, overall time complexity for the Hessenberg-Schur algorithm is given by

$$\frac{5}{3}m^3 + 10n^3 + 5m^2n + \frac{5}{2}mn^2.$$

Thus, the time complexity of solving a two-dimensional, linear, time-dependent equation using the Hessenberg-Schur algorithm is $O(\frac{5}{3}N^6)$, where $n = N$ and $m = O(N^2)$.

For example, consider the system (2.26). Take $A_1 = (B_2 \otimes I_{N-1}) + (I_{N-1} \otimes B_2)$ and $A_2 = -\Big((B_4 \otimes I_{N-1}) + (I_{N-1} \otimes B_4) + 2(B_2 \otimes B_2)\Big)$. Now we have

$$\Big(I_{N-1} \otimes A_2 A_1^{-1} + [D] \otimes I_{N-1}\Big)\hat{\psi}_h = (I_N \otimes A_1^{-1})(\hat{f}_h - (d_h \otimes \psi_{0h})).$$

Then the system is equivalent to the Sylvester equation $A_2 A_1^{-1}\hat{\psi}_h + \hat{\psi}_h[D]^T = F_h$, where $vec(F_h) = (I_N \otimes A_1^{-1})(\hat{f}_h - (d_h \otimes \psi_{0h}))$. Thus, the time complexity of solving the above system using the Hessenberg-Schur algorithm is $O(\frac{5}{3}N^6)$, where $n = N$ and $m = O(N^2)$.

3.3.5 Analysis

We now analyze the proposed method for the Poisson, Heat, Wave and Stokes equations, with the objectives of establishing the uniqueness of the solution on the extended domain and proving spectral convergence.

3.3.5.1 Unique Continuation Property (UCP)

The PDE on the extended domain is non-standard. For example, for the Poisson equation, $-\Delta u = g_n$, where g_n is f extended to $\tilde{\Omega}$, the boundary condition is imposed on $\partial\Omega$ instead of $\partial\tilde{\Omega}$. We use UCP to show that the PDE is well-defined.

The unique continuation property is a fundamental concept in the theory of partial differential equations. It asserts that, if a solution to a PDE vanishes within a certain part of its domain, then, under appropriate conditions, it must vanish everywhere. This property reflects the rigidity of solutions and has important implications in areas such as inverse problems, control theory, and the qualitative analysis of PDEs.

UCP appears in several formulations, such as:

- Strong UCP: If a solution vanishes to infinite order at a point, then the solution must vanish identically.
- Weak UCP: If a solution vanishes in an open (nontrivial) subset of the domain, then it must vanish everywhere in the connected component.

The proof of UCP is typically established via Carleman estimates, which are weighted integral inequalities tailored to the structure of the PDE. These estimates vary depending on whether the operator is elliptic, parabolic, or hyperbolic.

The above two forms are explained for the elliptic Schrödinger operator $-\Delta + q$ where $q \in L^\infty(\Omega)$ by Mikko Salo in [84].

Theorem 3.7. [84] (Weak UCP) Let $\Omega \subset \mathbb{R}^n$ be a bounded connected open set, and let $q \in L^\infty(\Omega)$. If $u \in H^2(\Omega)$ satisfies

$$\begin{aligned}(-\Delta + q)u = 0 \quad &\text{in} \quad \Omega, \\ u = 0 \quad &\text{in a ball} \quad B \subset \Omega,\end{aligned}$$

then $u = 0$ in Ω.

Theorem 3.8. [84] (Strong UCP) If $u \in H^2(\Omega)$ satisfies

$$(-\Delta + q)u = 0 \quad \text{in } \Omega$$

and if u vanishes to infinite order at $x_0 \in \Omega$ in the sense that

$$\lim_{r \to 0} \frac{1}{r^N} \int_{B(x_0, r)} |u|^2 \, dx = 0 \quad \text{for all } N \geq 0,$$

then $u = 0$ in Ω.

Furthermore, the following theorem illustrates the weak UCP for harmonic functions. See Corollary 4.2 in [12] and Theorem 2.5 in [28].

Theorem 3.9. Let $\tilde{\Omega}$ be a bounded connected domain in $\mathbb{R}^2$ and u be harmonic on $\tilde{\Omega}$. Suppose there exists a nonempty open set Ω such that $\bar{\Omega} \subset \tilde{\Omega}$ and $u \equiv 0$ in $\bar{\Omega}$. Then $u \equiv 0$ in $\tilde{\Omega}$.

Proof. Define $\phi = u_x - iu_y$. Let $p(x, y) = u_x$ and $q(x, y) = -u_y$. Then

$$\begin{aligned}p_x - q_y &= u_{xx} - (-u_{yy}) = 0 \\ p_y + q_x &= u_{xy} - u_{yx} = 0.\end{aligned}$$

Therefore, ϕ satisfies the Cauchy-Riemann equations.

Since u is smooth, ϕ is also smooth, and therefore analytic on $\tilde{\Omega}$ by the Cauchy-Riemann theorem. Moreover, since $\phi \equiv 0$ in $\bar{\Omega}$, and in particular on the open set $\Omega \subset \tilde{\Omega}$, the identity theorem from complex analysis implies that $\phi \equiv 0$ in $\tilde{\Omega}$.

Since $\phi = u_x - iu_y = 0$, it follows that both partial derivatives vanish: $u_x = 0$, $u_y = 0$ in $\tilde{\Omega}$. Hence, u is constant in $\tilde{\Omega}$ since $\tilde{\Omega}$ is connected. But $u = 0$ on $\partial\Omega$, so the constant must be zero. Therefore, $u \equiv 0$ in $\tilde{\Omega}$. □

In addition, references [56, 65, 92] also address the unique continuation property for elliptic PDEs. For parabolic PDEs, such as the heat equation, key references include [8, 65, 92]. Moreover, the unique continuation property for hyperbolic PDEs, such as the wave equation, is discussed in [90].

Theorem 3.10. Consider the 1-D Heat equation defined in the physical space-time domain $\Omega \times (-1, 1)$ where $\Omega = (-a, b)$ with $0 < a < b < 1$ and the extended domain $\widetilde{\Omega} \times (-1, 1)$ where $\widetilde{\Omega} = (-1, 1)$.

$$
\begin{aligned}
u_t = u_{xx} + f(x,t) \quad \text{in } \Omega \times (-1,1), \qquad & \tilde{u}_t = \tilde{u}_{xx} + \tilde{f}(x,t) \quad \text{in } \tilde{\Omega} \times (-1,1), \\
u(-a,t) = 0 = u(b,t), \qquad & \tilde{u}(-a,t) = 0 = \tilde{u}(b,t), \quad \text{(constraint)}\ , \\
u(x,-1) = 0, \qquad & \tilde{u}(x,-1) = 0,
\end{aligned}
$$

where $\tilde{f}(x,t) = f(x,t)$ on $\bar{\Omega}$ for each $t \in [-1,1]$. Assume f is smooth. Then $\tilde{u}$ is uniquely determined on $\bar{\tilde{\Omega}} \times [-1,1]$, assuming it is uniformly continuous on the space-time domain.

Proof. To show that $\tilde{u}$ is uniquely determined on $\tilde{\Omega} \times (-1,1)$, consider solving the following problem:

$$
\begin{aligned}
\tilde{u}_t = \tilde{u}_{xx} + \tilde{f}(x,t) \quad \text{in} \quad \tilde{\Omega} \times (-1,1), \\
\tilde{u}(-a,t) = 0 = \tilde{u}(-b,t), \\
\tilde{u}(x,-1) = 0 \quad \text{on} \quad \tilde{\Omega},
\end{aligned}
$$

where $\bar{\Omega} \subset \tilde{\Omega}$. Suppose there exists $\tilde{v}(x,t)$ such that

$$\begin{aligned} \tilde{v}_t &= \tilde{v}_{xx} + \tilde{f}(x,t) \quad \text{in} \quad \tilde{\Omega} \times (-1,1), \\ \tilde{v}(-a,t) &= 0 = \tilde{v}(-b,t), \\ \tilde{v}(x,-1) &= 0 \quad \text{on} \quad \tilde{\Omega}. \end{aligned}$$

Define $\tilde{w}(x,t) = \tilde{u}(x,t) - \tilde{v}(x,t)$. Then

$$\begin{aligned} \tilde{w}_t &= \tilde{w}_{xx} \quad \text{in} \quad \tilde{\Omega} \times (-1,1), \\ \tilde{w}(-a,t) &= 0 = \tilde{w}(b,t), \\ \tilde{w}(x,-1) &= 0 \quad \text{on} \quad \tilde{\Omega}. \end{aligned}$$

Therefore, $\tilde{w} = 0$ on $(-a,b) \times (-1,1)$. By using UCP for parabolic PDEs, we can conclude that $\tilde{w} \equiv 0$ on $\tilde{\Omega} \times (-1,1)$. Furthermore, $\tilde{w}$ can be uniquely extended to $\hat{w} : \bar{\tilde{\Omega}} \times (-1,1) \to \mathbb{R} \times (-1,1)$ such that $\hat{w}$ is uniformly continuous on $\bar{\tilde{\Omega}} \times [-1,1]$. In fact $\hat{w} \equiv 0$ on $\bar{\tilde{\Omega}} \times [-1,1]$. To see this, define $\hat{w}(-1,t) = 0 = \hat{w}(1,t)$. Then $\hat{w}$ is clearly uniformly continuous on $\bar{\tilde{\Omega}} \times [-1,1]$. Suppose w is another uniformly continuous extension of $\tilde{w}$ to $\bar{\tilde{\Omega}} \times [-1,1]$. Let $x \in \partial\tilde{\Omega}$ and $x_n \in \tilde{\Omega}$ such that $x_n \to x$. Then $w(x_n,t) = 0$ for $t \in [-1,1]$ and w is continuous on $\bar{\tilde{\Omega}} \times [-1,1]$. This implies that $w(x,t) = 0$. Hence $w = \hat{w}$ on $\bar{\tilde{\Omega}} \times [-1,1]$.

□

Theorem 3.11. Consider the 2-D Poisson equation defined in the irregular domain Ω and the extended domain $\widetilde{\Omega}$ which is assumed to be connected:

$$\begin{aligned} -\Delta u &= f \quad \text{in } \Omega, & -\Delta \tilde{u} &= \tilde{f} \quad \text{in } \tilde{\Omega} = (-1,1)^2, \\ u &= 0 \quad \text{on } \partial\Omega. & \tilde{u} &= 0 \quad \text{on } \partial\Omega, \quad \text{(constraint)}, \end{aligned}$$

where $\tilde{f} = f$ on $\bar{\Omega}$. Assume f is smooth. Then $\tilde{u}$ is uniquely determined on $\bar{\tilde{\Omega}}$,

assuming it is uniformly continuous on $\bar{\tilde{\Omega}}$.

Proof. To show that $\tilde{u}$ is uniquely determined on $\tilde{\Omega}$, consider solving the following problem.

$$\begin{aligned} -\Delta\tilde{u} &= \tilde{f} \quad \text{in} \quad \tilde{\Omega}, \\ \tilde{u} &= 0 \quad \text{on} \quad \partial\Omega, \end{aligned}$$

where $\bar{\Omega} \subset \tilde{\Omega}$. Suppose there exists $\tilde{v}$ and $\tilde{h}$ such that

$$\begin{aligned} -\Delta\tilde{v} &= \tilde{f} \quad \text{in} \quad \tilde{\Omega}, \\ \tilde{v} &= 0 \quad \text{on} \quad \partial\Omega. \end{aligned}$$

Define $\tilde{w} = \tilde{u} - \tilde{v}$. Then $\tilde{w}$ satisfies

$$\begin{aligned} -\Delta\tilde{w} &= 0 \quad \text{in} \quad \tilde{\Omega}, \\ \tilde{w} &= 0 \quad \text{on} \quad \partial\Omega. \end{aligned}$$

Thus, $\tilde{w} = 0$ on Ω. By using UCP for harmonic functions, it follows that $\tilde{w} \equiv 0$ on $\tilde{\Omega}$. Furthermore, $\tilde{w}$ can be uniquely extended to $\hat{w} : \bar{\tilde{\Omega}} \to \mathbb{R}$ such that $\hat{w}$ is uniformly continuous on $\bar{\tilde{\Omega}}$. In fact $\hat{w} \equiv 0$ on $\bar{\tilde{\Omega}}$. To see this, define $\hat{w} = 0$ on $\partial\tilde{\Omega}$. Then $\hat{w}$ is clearly uniformly continuous on $\bar{\tilde{\Omega}}$. Suppose w is another uniformly continuous extension of $\tilde{w}$ to $\bar{\tilde{\Omega}}$. Let $x \in \partial\tilde{\Omega}$ and $x_n \in \tilde{\Omega}$ such that $x_n \to x$. Then $w(x_n) = 0$ and w is continuous on $\bar{\tilde{\Omega}}$. This implies that $w(x) = 0$. Hence $w = \hat{w}$ on $\bar{\tilde{\Omega}}$.

□

Theorem 3.12. Consider the 2-D Heat equation defined in the irregular spatial

domain Ω and the extended domain $\widetilde{\Omega}$ where temporal domain is $(-1,1)$.

$$\begin{aligned} u_t &= \Delta u + f(x,y,t) \quad \text{in } \Omega \times (-1,1), & \tilde{u}_t &= \Delta \tilde{u} + \tilde{f}(x,y,t) \quad \text{in } \tilde{\Omega} \times (-1,1), \\ u(x,y,t) &= g(x,y,t) \quad \text{on } \partial\Omega \times (-1,1), & \tilde{u}(x,y,t) &= g(x,y,t) \quad \text{on } \partial\Omega \times (-1,1), \\ u(x,y,-1) &= 0 \quad \text{in } \Omega. & \tilde{u}(x,y,-1) &= 0 \quad \text{in } \tilde{\Omega}, \end{aligned}$$

where $\tilde{f}(x,y,t) = f(x,y,t)$ on $\bar{\Omega}$ for each fixed $t \in [-1,1]$. Assume f is smooth. Then $\tilde{u}$ is uniquely determined on $\bar{\tilde{\Omega}} \times [-1,1]$, assuming it is uniformly continuous on the space-time domain.

Proof. By applying the unique continuation property for the parabolic equations and following the same procedure as before, we can show that $\tilde{u}$ is uniquely determined on $\bar{\tilde{\Omega}} \times [-1,1]$. □

Theorem 3.13. Consider the 2-D Wave equation defined in the irregular spatial domain Ω and the extended domain $\widetilde{\Omega}$ where temporal domain is $(-1,1)$.

$$\begin{aligned} u_{tt} &= \Delta u + f(x,y,t) \quad \text{in } \Omega \times (-1,1), & \tilde{u}_{tt} &= \Delta \tilde{u} + \tilde{f}(x,y,t) \quad \text{in } \tilde{\Omega} \times (-1,1), \\ u(x,y,t) &= g(x,y,t) \quad \text{on } \partial\Omega \times (-1,1), & \tilde{u}(x,y,t) &= g(x,y,t) \quad \text{on } \partial\Omega \times (-1,1), \\ u(x,y,-1) &= 0 \quad \text{in } \Omega. & \tilde{u}(x,y,-1) &= 0 \quad \text{in } \tilde{\Omega}, \\ u_t(x,y,-1) &= 0 \quad \text{in } \Omega. & \tilde{u}_t(x,y,-1) &= 0 \quad \text{in } \tilde{\Omega}, \end{aligned}$$

where $\tilde{f}(x,y,t) = f(x,y,t)$ on $\bar{\Omega}$ for each fixed $t \in [-1,1]$. Assume f is smooth. Then $\tilde{u}$ is uniquely determined on $\bar{\tilde{\Omega}} \times [-1,1]$, assuming it is uniformly continuous on the space-time domain.

Proof. By applying the unique continuation property for hyperbolic PDEs and following the same procedure as before, we can show that $\tilde{u}$ is uniquely determined on $\bar{\tilde{\Omega}} \times [-1,1]$. □

Now we can prove that UCP holds for unsteady Stokes equation as well. Suppose

$$\Delta\psi_t = \Delta^2\psi \quad \text{on} \quad \tilde{\Omega} \times (-1, 1),$$

and $\psi = 0$ on an open ball D in $\tilde{\Omega} \times (-1, 1)$. Define $\phi = \Delta\psi$. Then $\phi = 0$ on D and $\phi_t = \Delta\phi$ on $\tilde{\Omega} \times (-1, 1)$. So ϕ satisfies the heat equation. By the UCP for the heat equation, this implies $\Delta\psi = \phi = 0$ on $\tilde{\Omega} \times (-1, 1)$. Since $D \subset \tilde{\Omega}$ is open, there exists a space-time cylinder $B \times S \subset D$, where $B \subset \tilde{\Omega}$ is an open ball and $S \subset (-1, 1)$ is an open time interval. Fix $t \in S$. By the unique continuation property for the Laplace equation for ψ implies that $\psi(\tilde{\Omega}, t) = 0$. Since $\phi = \Delta\psi$ satisfies the heat equation, it is analytic in t and x, which implies ψ also analytic in t. Hence $\psi = 0$ on $\tilde{\Omega} \times (-1, 1)$.

Theorem 3.14. Consider the streamline formulation of the 2D Stokes equation defined in the irregular spatial domain Ω and the extended domain $\widetilde{\Omega}$ where temporal domain is $(-1, 1)$.

$$\begin{aligned}
\Delta\psi_t &= \Delta^2\psi + f(x, y, t) \quad \text{in } \Omega \times (-1, 1), & \Delta\tilde{\psi}_t &= \Delta^2\tilde{\psi} + \tilde{f}(x, y, t) \quad \text{in } \tilde{\Omega} \times (-1, 1), \\
\psi(x, y, t) = 0 = \frac{\partial\psi}{\partial\nu} &\quad \text{on } \partial\Omega \times (-1, 1), & \tilde{\psi}(x, y, t) = 0 = \frac{\partial\tilde{\psi}}{\partial\nu} &\quad \text{on } \partial\Omega \times (-1, 1), \\
\psi(x, y, -1) = 0 &\quad \text{in } \Omega. & \tilde{\psi}(x, y, -1) = 0 &\quad \text{in } \tilde{\Omega},
\end{aligned}$$

where $\tilde{f}(x, y, t) = f(x, y, t)$ on $\bar{\Omega}$ for each fixed $t \in [-1, 1]$. Assume f is smooth. Then $\tilde{\psi}$ is uniquely determined on $\bar{\tilde{\Omega}} \times [-1, 1]$, assuming $\tilde{\psi}$ is uniformly continuous on the space-time domain.

Proof. To show that $\tilde{\psi}$ is uniquely determined on $\tilde{\Omega} \times (-1, 1)$, consider solving the following problem:

$$\Delta\tilde{\psi}_t = \Delta^2\tilde{\psi} + \tilde{f}(x, y, t) \quad \text{in } \tilde{\Omega} \times (-1, 1),$$

$$\tilde{\psi}(x,y,t) = 0 = \frac{\partial \tilde{\psi}}{\partial \nu} \quad \text{on } \partial\Omega \times (-1,1)$$
$$\tilde{\psi}(x,y,-1) = 0 \quad \text{on} \quad \tilde{\Omega},$$

where $\bar{\Omega} \subset \tilde{\Omega}$. Suppose there exists $\tilde{\varphi}$ such that

$$\Delta\tilde{\varphi}_t = \Delta^2\tilde{\varphi} + \tilde{f}(x,y,t) \quad \text{in } \tilde{\Omega} \times (-1,1),$$
$$\tilde{\varphi}(x,y,t) = 0 = \frac{\partial \tilde{\varphi}}{\partial \nu} \quad \text{on } \partial\Omega \times (-1,1)$$
$$\tilde{\varphi}(x,y,-1) = 0 \quad \text{on} \quad \tilde{\Omega}.$$

Define $\tilde{\eta}(x,t) = \tilde{\psi}(x,t) - \tilde{\varphi}(x,t)$. Then for each fixed t, we have

$$\Delta\tilde{\eta}_t = \Delta^2\tilde{\eta} \quad \text{in } \tilde{\Omega} \times (-1,1),$$
$$\tilde{\eta}(x,y,t) = 0 = \frac{\partial \tilde{\eta}}{\partial \nu} \quad \text{on } \partial\Omega \times (-1,1)$$
$$\tilde{\eta}(x,y,-1) = 0 \quad \text{on} \quad \tilde{\Omega}.$$

Thus, $\tilde{\eta} = 0$ on $\Omega \times (-1,1)$. By using UCP for Stokes equation, we can conclude that $\tilde{\eta} \equiv 0$ on $\tilde{\Omega} \times (-1,1)$. Furthermore, $\tilde{\eta}$ can be uniquely extended to $\hat{\eta} : \bar{\tilde{\Omega}} \times (-1,1) \to \mathbb{R} \times (-1,1)$ such that $\hat{\eta}$ is uniformly continuous on $\bar{\tilde{\Omega}} \times [-1,1]$. In fact $\hat{\eta} \equiv 0$ on $\bar{\tilde{\Omega}} \times [-1,1]$. To see this, define $\hat{\eta} = 0$ on $\partial\tilde{\Omega} \times (-1,1)$. Then $\hat{\eta}$ is clearly uniformly continuous on $\bar{\tilde{\Omega}} \times [-1,1]$. Suppose η is another uniformly continuous extension of $\tilde{\eta}$ to $\bar{\tilde{\Omega}} \times [-1,1]$. Let $x \in \partial\tilde{\Omega}$ and $x_n \in \tilde{\Omega}$ such that $x_n \to x$. Then $\eta(x_n,t) = 0$ for $t \in [-1,1]$ and η is continuous on $\bar{\tilde{\Omega}} \times [-1,1]$. This implies that $\eta(x,t) = 0$. Hence $\eta = \hat{\eta}$ on $\bar{\tilde{\Omega}} \times [-1,1]$.

□

3.3.5.2 Convergence

In this section, we discuss spectral convergence of our method for the one-dimensional and two-dimensional Poisson, Heat, Wave and Stokes equations. Throughout this analysis, the notation $\|\cdot\|$ will be used to represent the $L^2(\Omega)$ norm, where Ω is the spatial domain unless stated otherwise.

Theorem 3.15. Let $u(x)$ and $f(x)$ be the solution and analytic non-homogeneous term of the 1-D Poisson equation in the physical domain $\Omega = (-a, b)$ with homogeneous Dirichlet boundary conditions. Assume $a, b \in (0, 1)$. Suppose that $v(x)$ and $g(x)$ are the extended solution and the extended non-homogeneous term in $\widetilde{\Omega} = (-1, 1)$. For any positive integer n, define v_n be the solution of $-v_n'' = g_n$ on $\widetilde{\Omega}$ where g_n is the non-periodic extension of f to $\widetilde{\Omega}$. The error between $u(x)$ and $v_n(x)$ on the physical domain Ω can be defined as $e_n(x) = u(x) - v_n(x)|_\Omega$. Then $\|e_n\| + \|e_n'\| + \|e_n''\| \leq Ce^{-cn}$.

Proof. Consider the 1-D Poisson equation in the physical domain Ω and the extended domain $\widetilde{\Omega}$ as follows.

$$\begin{aligned} -u'' &= f(x) \quad \text{in } \Omega, & -v_n'' &= g_n(x) \quad \text{in } \tilde{\Omega}, \\ u(-a) &= 0 = u(b). & v_n(-a) &= 0 = v_n(b), \quad \text{(constraint)}. \end{aligned}$$

Let $e_n(x)$ be the error between $u(x)$ and $v_n(x)$ on the physical domain Ω.

$$\begin{aligned} e_n(x) &= u(x) - v_n(x)|_\Omega. \\ -e_n''(x) &= f(x) - g_n(x)|_\Omega \\ &= \sum_{k=n+1}^{\infty} a_k T_k^h\left(\cos\frac{\pi x}{2}\right) + \sum_{k=n}^{\infty} b_k U_k^h\left(\cos\frac{\pi x}{2}\right)\sin\frac{\pi x}{2}. \\ \|e_n''\| &= \left\| \sum_{k=n+1}^{\infty} a_k T_k^h\left(\cos\frac{\pi x}{2}\right) + \sum_{k=n}^{\infty} b_k U_k^h\left(\cos\frac{\pi x}{2}\right)\sin\frac{\pi x}{2} \right\| \end{aligned} \tag{3.54}$$

$$\leq \left\| \sum_{k=n+1}^{\infty} a_k T_k^h \left(\cos \frac{\pi x}{2} \right) \right\| + \left\| \sum_{k=n}^{\infty} b_k U_k^h \left(\cos \frac{\pi x}{2} \right) \sin \frac{\pi x}{2} \right\|$$
$$\leq \sum_{k=n+1}^{\infty} |a_k| \left\| T_k^h \left(\cos \frac{\pi x}{2} \right) \right\| + \sum_{k=n}^{\infty} |b_k| \left\| U_k^h \left(\cos \frac{\pi x}{2} \right) \sin \frac{\pi x}{2} \right\|.$$

Since $\Omega = (-a, b)$, the norm of both families of Half-range Chebyshev polynomials satisfies $\left\| T_k^h(y) \right\|^2 \leq 1$ and $\left\| U_k^h(y) \sin \frac{\pi x}{2} \right\|^2 \leq 1$ for every k, where $y = \cos \frac{\pi x}{2}$. Thus

$$\|e_n''\| \leq \sum_{k=n+1}^{\infty} |a_k| + \sum_{k=n}^{\infty} |b_k|.$$

According to Corollary 3.15. in [58], the coefficients a_k and b_k of g_n in the form of (3.37) and (3.38), satisfy $a_k, b_k \sim \rho^{-k}$, where $\rho > 1$. This is verified numerically by the logarithmic plots of a_k and b_k coefficients in Figure 3.6. Let $|a_k| \leq \widetilde{C} e^{-ck}$ and $|b_k| \leq \widetilde{C} e^{-ck}$ where $c = \log(\rho)$, $k \geq n$. Therefore,

$$\begin{aligned} \|e_n''\| &\leq \widetilde{C} \left(\sum_{k=n+1}^{\infty} e^{-kc} + \sum_{k=n}^{\infty} e^{-kc} \right) \\ &= \widetilde{C} \left(\frac{e^{-c(n+1)}}{1 - e^{-c}} + \frac{e^{-cn}}{1 - e^{-c}} \right) \\ &= \widetilde{C} \left(\frac{1 + e^c}{e^c - 1} \right) e^{-cn} \\ &= C e^{-cn}. \end{aligned}$$

Thus, $\|e_n''\| \leq C e^{-cn}$, where $C = \widetilde{C} \left(\frac{1+e^c}{e^c - 1} \right) > 1$ and $c = \log(\rho)$. This result says $e_n''(x) \to 0$. Next, we show that $\|e_n\|, \|e_n'\| \leq C e^{-cn}$.

Multiply both sides of the equation (3.54) by $e_n(x) \in H_0^1(-a, b)$ (a Sobolev space consisting of functions v such that $v' \in L^2$ and $v(-a) = 0 = v(b)$), and integrate over $(-a, b)$:

$$\int_{-a}^{b} e_n(x)(-e_n''(x))dx = \int_{-a}^{b} e_n(x)(f(x) - g_n(x))dx$$
$$\int_{-a}^{b} e_n'(x)e_n'(x)dx - [e_n'(x)e_n(x)]_a^b = \int_{-a}^{b} e_n(x)(f(x) - g_n(x))dx \quad \text{(By integration by parts).}$$

Since the boundary term vanishes, the weak form of (3.54) becomes:

$$\int_{-a}^{b} e_n'(x)e_n'(x)dx = \int_{-a}^{b} e_n(x)(f(x) - g_n(x))dx.$$

Then we get

$$\int_{-a}^{b} |e_n'(x)|^2 dx = \int_{-a}^{b} e_n(x)(f(x) - g_n(x))dx. \tag{3.55}$$

By Cauchy-Schwarz inequality,

$$\left| \int_{-a}^{b} e_n(x)(f(x) - g_n(x))dx \right| \leq \|e_n\| \, \|f - g_n\| \, . \tag{3.56}$$

Using the Poincaré inequality (since $e_n(a) = 0 = e_n(b)$),

$$\|e_n\| \leq c \, \|e_n'\| \, . \tag{3.57}$$

By (3.56) and (3.57) we get,

$$\left| \int_{-a}^{b} e_n(x)(f(x) - g_n(x))dx \right| \leq c \, \|e_n'\| \, \|f - g_n\| \, .$$

Thus, by (3.55),

$$\begin{aligned} \|e_n'\|^2 &\leq c \, \|e_n'\| \, \|f - g_n\| \\ \|e_n'\| &\leq c \, \|f - g_n\| \\ \|e_n'\| &\leq Ce^{-cn} \quad (\text{Since } \|e_n''\| = \|f - g_n\| \leq Ce^{-cn}). \end{aligned} \tag{3.58}$$

Now by (3.57) and (3.58), we get $\|e_n\| \leq Ce^{-cn}$. Hence e_n'', e_n', e_n all decay exponentially. □

Let Ω be a bounded domain in $\mathbb{R}^2$ and $F \in C(\bar{\Omega})$. For a given y, define

$$\|F(.,y)\| = \left(\int_{-1}^{1} F^2(x,y)dx\right)^{1/2}$$

and similarly $\|F(x,.)\| = \left(\int_{-1}^{1} F^2(x,y)dy\right)^{1/2}$ for a given x.

Theorem 3.16. Let $u(x,t)$ and $f(x,t)$ be the solution and analytic non-homogeneous term of the 1-D Heat equation in the physical space-time domain $\Omega \times (-1,1)$, where $\Omega = (-a,b)$ with $0 < a < b < 1$, with homogeneous Dirichlet boundary conditions and zero initial condition. Let n be a positive integer, and g_n be the non-periodic extension of f to $\widetilde{\Omega} \times (-1,1)$, where $\widetilde{\Omega} = (-1,1)$. Let $v_n(x,t)$ be solution of $(v_n)_t = (v_n)_{xx} + g_n$ on $\widetilde{\Omega}$, where

$$\begin{aligned}
g_n(x,t) &= \sum_{k=0}^{n} a_k(t) T_k^h\left(\cos\frac{\pi x}{2}\right) + \sum_{k=0}^{n-1} b_k(t) U_k^h\left(\cos\frac{\pi x}{2}\right)\sin\frac{\pi x}{2}, \\
a_k(t) &= \int_{-a}^{b} f(x,t) T_k^h\left(\cos\frac{\pi x}{2}\right) dx, \\
b_k(t) &= \int_{-a}^{b} f(x,t) U_k^h\left(\cos\frac{\pi x}{2}\right)\sin\frac{\pi x}{2} dx.
\end{aligned}$$

At a fixed time $t \in [-1,1]$, the error between $u(x,t)$ and $v_n(x,t)$ on the physical spatial domain can be defined as $e_n(x,t) = u(x,t) - v_n(x,t)$. Then $\|e_n(\cdot,t)\| \leq Ce^{-cn}$, $t \in [-1,1]$.

Proof. Consider the 1-D Heat equation in $\Omega \times [-1,1]$ and the extended domain $\widetilde{\Omega} \times [-1,1]$ as follows.

$$\begin{aligned}
u_t &= u_{xx} + f \quad \text{in } \Omega \times [-1,1], & (v_n)_t &= (v_n)_{xx} + g_n \quad \text{in } \tilde{\Omega} \times [-1,1], \\
u(-a,t) &= 0 = u(b,t), & v_n(-a,t) &= 0 = v_n(b,t), \quad \text{(constraint)} \\
u(x,-1) &= 0. & v_n(x,-1) &= 0.
\end{aligned}$$

For fixed t, let $e_n(x,t)$ be the error between $u(x,t)$ and $v_n(x,t)$ on the physical spatial domain: $e_n(x,t) = u(x,t) - v_n(x,t)|_{(-a,b)}$. Then

$$\begin{aligned}(e_n)_t - (e_n)_{xx} &= f(x,t) - g_n(x,t)|_{(-a,b)} \\ &= \sum_{k=n+1}^{\infty} a_k(t) T_k^h\left(\cos\frac{\pi x}{2}\right) + \sum_{k=n}^{\infty} b_k(t) U_k^h\left(\cos\frac{\pi x}{2}\right)\sin\frac{\pi x}{2}.\end{aligned} \tag{3.59}$$

Thus

$$\begin{aligned}\|(e_n)_t - (e_n)_{xx}\| &= \left\| \sum_{k=n+1}^{\infty} a_k(t) T_k^h\left(\cos\frac{\pi x}{2}\right) + \sum_{k=n}^{\infty} b_k(t) U_k^h\left(\cos\frac{\pi x}{2}\right)\sin\frac{\pi x}{2} \right\| \\ &\le \left\| \sum_{k=n+1}^{\infty} a_k(t) T_k^h\left(\cos\frac{\pi x}{2}\right) \right\| + \left\| \sum_{k=n}^{\infty} b_k(t) U_k^h\left(\cos\frac{\pi x}{2}\right)\sin\frac{\pi x}{2} \right\| \\ &\le \sum_{k=n+1}^{\infty} |a_k(t)| \left\| T_k^h\left(\cos\frac{\pi x}{2}\right) \right\| + \sum_{k=n}^{\infty} |b_k(t)| \left\| U_k^h\left(\cos\frac{\pi x}{2}\right)\sin\frac{\pi x}{2} \right\| \\ &\le \left(\sum_{k=n+1}^{\infty} |a_k(t)| + \sum_{k=n}^{\infty} |b_k(t)| \right).\end{aligned} \tag{3.60}$$

For each $t \in [-1,1]$, since f, g_n are analytic, there exist continuous c_1 and C_1 such that $a_k(x,t) \le C_1(t)e^{-c_1(t)k}$ with both c_1 and C_1 positive and bounded away from zero. Similarly, we have $b_k(x,t) \le C_2(t)e^{-c_2(t)k}$.

Therefore, by 3.60, we get

$$\begin{aligned}\|(e_n)_t - (e_n)_{xx}\| &\le \left(\sum_{k=n+1}^{\infty} C_1(t)e^{-c_1(t)k} + \sum_{k=n}^{\infty} C_2(t)e^{-c_2(t)k} \right) \\ &= \left(C_1(t)\left(\frac{e^{-c_1(t)(n+1)}}{1-e^{-c_1(t)}}\right) + C_2(t)\left(\frac{e^{-c_2(t)n}}{1-e^{-c_2(t)}}\right)\right) \\ &=: \tilde{C}_1(t)\left(\frac{e^{-c_1(t)(n+1)}}{1-e^{-c_1(t)}}\right) + \tilde{C}_2(t)\left(\frac{e^{-c_2(t)n}}{1-e^{-c_2(t)}}\right) \\ &=: C(t)e^{-c(t)n}.\end{aligned} \tag{3.61}$$

Thus, $\|(e_n)_t - (e_n)_{xx}\| \le Ce^{-cn}$ for some positive constants c and C where, $C = \sup_{t\in[-1,1]} C(t)$ and $c = \inf_{t\in[-1,1]} c(t)$. Now we need to show that $\|e_n(\cdot,t)\|$ also

decay exponentially for all $t \in [-1, 1]$.

Multiply the error equation (3.59) by $e_n(x,t)$ and integrate over the spatial domain $(-a, b)$ to obtain

$$\int_{-a}^{b} ((e_n)_t - (e_n)_{xx}) e_n(x,t) dx = \int_{-a}^{b} (f(x,t) - g_n(x,t)) e_n(x,t) dx. \tag{3.62}$$

$$\begin{aligned}
\int_{-a}^{b} ((e_n)_t - (e_n)_{xx}) e_n(x,t) dx &= \int_{-a}^{b} (e_n(x,t))_t e_n(x,t) dx - \int_{-a}^{b} (e_n(x,t))_{xx} e_n(x,t) dx \\
&= \frac{1}{2}\frac{d}{dt} \|e_n(\cdot,t)\|^2 - [(e_n(x,t))_x e_n(x,t)]_{x=-a}^{b} + \int_{-a}^{b} |(e_n(x,t))_x|^2 dx \\
&= \frac{1}{2}\frac{d}{dt} \|e_n(\cdot,t)\|^2 + \|(e_n(\cdot,t))_x\|^2 . \qquad (3.63)
\end{aligned}$$

The last equality holds since $e_n(-a,t) = 0 = e_n(b,t)$.

Further, by Cauchy-Schwarz inequality,

$$\begin{aligned}
\left| \int_{-a}^{b} (f(x,t) - g_n(x,t)) e_n(x,t) dx \right| &\leq \|f(\cdot,t) - g_n(\cdot,t)\| \, \|e_n(\cdot,t)\| \\
&\leq C(t) e^{-c(t)n} \|e_n(\cdot,t)\| \quad \text{(By (3.61))} \\
&\leq C e^{-cn} \|e_n(\cdot,t)\| , \qquad (3.64)
\end{aligned}$$

where, $C = \sup_{t\in[-1,1]} C(t)$ and $c = \inf_{t\in[-1,1]} c(t)$.

By substituting (3.63) and (3.64) to (3.62) we get,

$$\frac{1}{2}\frac{d}{dt} \|e_n(\cdot,t)\|^2 + \|(e_n(\cdot,t))_x\|^2 \leq C e^{-cn} \|e_n(\cdot,t)\| . \tag{3.65}$$

Let $E(t) = \int_{-a}^{b} |e_n(x,t)|^2 dx$, so

$$\begin{aligned}
\frac{d}{dt} E(t) + 2 \|(e_n(\cdot,t))_x\|^2 &\leq 2C e^{-cn} \sqrt{E(t)} \\
E'(t) &\leq 2C e^{-cn} \sqrt{E(t)}
\end{aligned}$$

$$y'(t) \le Ce^{-cn} \quad \text{where} \quad y(t) = \sqrt{E(t)}$$
$$y(t) \le y(-1) + Ce^{-cn}t.$$

Since $y(-1) = 0$, $y(t) \le Ce^{-cn}$ for each $t \in [-1, 1]$,

$$\|e_n(\cdot, t)\| \le Ce^{-cn}. \tag{3.66}$$

□

Theorem 3.17. Let $\psi(x,t)$ and $f(x,t)$ be the solution and analytic non-homogeneous term of the 1-D Stokes equations in the physical space-time domain $\Omega \times (-1,1)$, where $\Omega = (-a,b)$ with $0 < a < b < 1$, with homogeneous boundary conditions and zero initial condition. Let n be a positive integer, and g_n be the non-periodic extension of f to $\widetilde{\Omega} \times (-1,1)$, where $\widetilde{\Omega} = (-1,1)$. Let $\phi_n(x,t)$ be solution of $(\phi_n)_{txx} = (\phi_n)_{xxxx} + g_n$ on $\widetilde{\Omega}$. At a fixed time $t \in [-1,1]$, the error between $\psi(x,t)$ and $\phi_n(x,t)$ on the physical spatial domain can be defined as $e_n(x,t) = \psi(x,t) - \phi_n(x,t)$. Then $\|e_n(\cdot,t)\| \le Ce^{-cn}$ and $\|e_{n,x}(\cdot,t)\| \le Ce^{-cn}$, $t \in [-1,1]$.

Proof. Consider the stream function formulation for the 1-D unsteady Stokes equations in $\Omega \times [-1,1]$ and the extended domain $\widetilde{\Omega} \times [-1,1]$ as follows.

$$\psi_{txx} = \psi_{xxxx} + f \quad \text{in } \Omega \times [-1,1], \qquad \phi_{n,txx} = \phi_{n,xxxx} + g_n \quad \text{in } \tilde{\Omega} \times [-1,1],$$
$$\psi(-a,t) = 0 = \psi(b,t), \qquad \phi_n(-a,t) = 0 = \phi_n(b,t), \quad \text{(constraint)}$$
$$\psi_x(-a,t) = 0 = \psi_x(b,t), \qquad \phi_{n,x}(-a,t) = 0 = \phi_{n,x}(b,t), \quad \text{(constraint)}$$
$$\psi(x,-1) = 0. \qquad \phi_n(x,-1) = 0.$$

For fixed t, let $e_n(x,t)$ be the error between $\psi(x,t)$ and $\phi_n(x,t)$ on the physical spatial domain: $e_n(x,t) = \psi(x,t) - \phi_n(x,t)|_{(-a,b)}$. Then

$$e_{n,txx} - e_{n,xxxx} = f(x,t) - g_n(x,t)|_{(-a,b)} \tag{3.67}$$

$$= \sum_{k=n+1}^{\infty} a_k(t) T_k^h\left(\cos\frac{\pi x}{2}\right) + \sum_{k=n}^{\infty} b_k(t) U_k^h\left(\cos\frac{\pi x}{2}\right)\sin\frac{\pi x}{2}.$$

Following the same approach explained for the 1-D Heat equation, we can obtain

$$\|e_{n,txx} - e_{n,xxxx}\| \leq C(t)e^{-c(t)n}, \tag{3.68}$$

where $C(t)$ and $c(t)$ are continuous with the latter bounded away from zero.

Thus, $\|e_{n,txx} - e_{n,xxxx}\| \leq Ce^{-cn}$ for some positive constants c and C where, $C = \sup_{t\in[-1,1]} C(t)$ and $c = \inf_{t\in[-1,1]} c(t)$. Now we need to show that $\|e_{n,x}(\cdot,t)\|$ and $\|e_n(\cdot,t)\|$ also decay exponentially for all $t \in [-1,1]$.

Multiply the error equation (3.67) by $e_n(x,t)$ and integrate over the spatial domain $(-a,b)$ to obtain

$$\int_{-a}^{b}(e_{n,txx} - e_{n,xxxx})e_n(x,t)dx = \int_{-a}^{b}(f(x,t) - g_n(x,t))e_n(x,t)dx. \tag{3.69}$$

$$\begin{aligned}
\int_{-a}^{b}(e_{n,txx} - e_{n,xxxx})e_n(x,t)dx &= \int_{-a}^{b} e_{n,txx}e_n dx - \int_{-a}^{b} e_{n,xxxx}e_n dx \\
&= -\int_{-a}^{b} e_{n,tx}e_{n,x}dx + \int_{-a}^{b} e_{n,xxx}e_{n,x}dx \\
&= -\frac{1}{2}\frac{d}{dt}\|e_{n,x}(\cdot,t)\|^2 - \int_{-a}^{b} e_{n,xx}e_{n,xx}dx \\
&= -\frac{1}{2}\frac{d}{dt}\|e_{n,x}(\cdot,t)\|^2 - \|e_{n,xx}(\cdot,t)\|^2 .
\end{aligned} \tag{3.70}$$

Further, by Cauchy-Schwarz inequality,

$$\begin{aligned}
\left|\int_{-a}^{b}(f(x,t) - g_n(x,t))e_n(x,t)dx\right| &\leq \|f(\cdot,t) - g_n(\cdot,t)\|\,\|e_n(\cdot,t)\| \\
&\leq C(t)e^{-c(t)n}\|e_n(\cdot,t)\| \quad \text{(By (3.68))} \\
&\leq Ce^{-cn}\|e_n(\cdot,t)\| .
\end{aligned} \tag{3.71}$$

By substituting (3.70) and (3.71) to (3.69) we get,

$$\begin{aligned}\frac{1}{2}\frac{d}{dt}\left\|e_{n,x}(\cdot,t)\right\|^2+\left\|e_{n,xx}(\cdot,t)\right\|^2 &\leq Ce^{-cn}\left\|e_n(\cdot,t)\right\| \\ &\leq Ce^{-cn}\left\|e_{n,x}(\cdot,t)\right\| \quad \text{(By Poincaré inequality).}\end{aligned} \tag{3.72}$$

Let $E(t)=\int_{-a}^{b}|e_{n,x}(x,t)|^2dx$, so

$$\begin{aligned}\frac{d}{dt}E(t)+2\left\|e_{n,xx}(\cdot,t)\right\|^2 &\leq 2Ce^{-cn}\sqrt{E(t)} \\ E'(t) &\leq 2Ce^{-cn}\sqrt{E(t)} \\ y'(t) &\leq Ce^{-cn} \quad \text{where} \quad y(t)=\sqrt{E(t)} \\ y(t) &\leq y(-1)+Ce^{-cn}t.\end{aligned}$$

Since $y(-1)=0$, $y(t)\leq Ce^{-cn}$ for each $t\in[-1,1]$,

$$\left\|e_{n,x}(\cdot,t)\right\|\leq Ce^{-cn}. \tag{3.73}$$

Using the Poincaré inequality (since $e_n(-a,t)=0=e_n(b,t)$),

$$\left\|e_n(\cdot,t)\right\|\leq c\left\|e_{n,x}(\cdot,t)\right\|\leq Ce^{-cn}. \tag{3.74}$$

□

Theorem 3.18. Let $u(x,y)$ and $f(x,y)$ be the solution and analytic non-homogeneous term of the 2-D Poisson equation in the irregular domain Ω with homogeneous Dirichlet boundary conditions. For any positive integer n, let $v_n(x,y)$ be solution of $-\Delta v_n=g_n$ on the extended domain $\widetilde{\Omega}$, where g_n is the Alternating non-periodic extension of f to $\widetilde{\Omega}$. The error between $u(x,y)$ and $v_n(x,y)$ on the irregular domain Ω can be defined as $e_n(x,y)=u(x,y)-v_n(x,y)|_\Omega$. Then $\|e_n\|+\|\nabla e_n\|\leq Ce^{-cn}$.

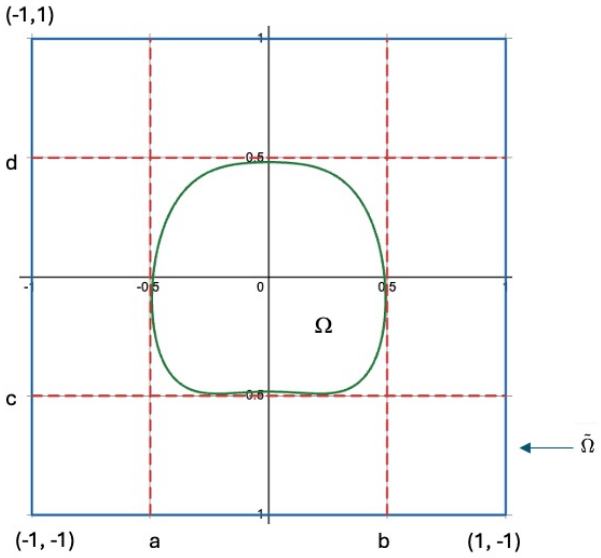

Figure 3.16: Irregular and the extended domain

Proof. Consider the 2-D Poisson equation defined in the irregular domain Ω and the extended domain $\widetilde{\Omega}$. See Figure (3.16).

$$-\Delta u = f \quad \text{in } \Omega, \qquad -\Delta v_n = g_n \quad \text{in } \tilde{\Omega} = (-1,1)^2,$$
$$u = 0 \quad \text{on } \partial\Omega. \qquad v_n = 0 \quad \text{on } \partial\Omega.$$

By UCP (Theorem 3.11), v_n is well defined on $\tilde{\Omega}$. Define the error function:

$$e_n(x,y) = u(x,y) - v_n(x,y)\Big|_{\Omega}.$$

Then

$$-\Delta e_n = f(x,y) - g_n(x,y)\Big|_{\Omega} \tag{3.75}$$
$$\|\Delta e_n\| = \|f - g_n\|.$$

In the Alternating Non-Periodic Extension, we perform one non-periodic extension

in the $x-$direction, followed by one in the $y-$direction. Therefore, for fixed y,

$$\begin{aligned} e_{n,xx}(x_i, y) &= \sum_{k=n+1}^{\infty} \tilde{a}_k(y) T_k^h\left(\cos\frac{\pi x_i}{2}\right) + \sum_{k=n}^{\infty} \tilde{b}_k(y) U_k^h\left(\cos\frac{\pi x_i}{2}\right)\sin\frac{\pi x_i}{2} \\ \|e_{n,xx}(x_i,\cdot)\| &= \left\| \sum_{k=n+1}^{\infty} \tilde{a}_k(\cdot) T_k^h\left(\cos\frac{\pi x_i}{2}\right) + \sum_{k=n}^{\infty} \tilde{b}_k(\cdot) U_k^h\left(\cos\frac{\pi x_i}{2}\right)\sin\frac{\pi x_i}{2} \right\| \\ &\leq C_1(x_i) e^{-cn}, \end{aligned}$$

by Theorem 3.15 and for some bounded C_1.

Similarly, for fixed x,

$$\begin{aligned} e_{n,yy}(x, y_j) &= \sum_{k=n+1}^{\infty} a_k(x) T_k^h\left(\cos\frac{\pi y_j}{2}\right) + \sum_{k=n}^{\infty} b_k(x) U_k^h\left(\cos\frac{\pi y_j}{2}\right)\sin\frac{\pi y_j}{2} \\ \|e_{n,yy}(\cdot,y_j)\| &= \left\| \sum_{k=n+1}^{\infty} a_k(\cdot) T_k^h\left(\cos\frac{\pi y_j}{2}\right) + \sum_{k=n}^{\infty} b_k(\cdot) U_k^h\left(\cos\frac{\pi y_j}{2}\right)\sin\frac{\pi y_j}{2} \right\| \\ &\leq C_2(y_j) e^{-cn}, \quad \text{for some bounded} \quad C_2. \end{aligned}$$

Define $\hat{C}_1 = \sup_{x\in[-1,1]} C_1(x) < \infty$, $\hat{C}_2 = \sup_{y\in[-1,1]} C_2(y) < \infty$. Let $x_i, 1 \leq i \leq n-1$ be interior Gauss-Lobatto nodes. Therefore,

$$\sum_{i=1}^{n-1} \|e_{n,xx}(x_i,\cdot)\|^2 \rho_i \leq \sum_{i=1}^{n-1} \hat{C}_1^2 e^{-2cn} \rho_i = 2\hat{C}_1^2 e^{-2cn} \tag{3.76}$$

$$\sum_{j=1}^{n-1} \|e_{n,yy}(\cdot,y_j)\|^2 \rho_j \leq \sum_{j=1}^{n-1} \hat{C}_2^2 e^{-2cn} \rho_j = 2\hat{C}_2^2 e^{-2cn}. \tag{3.77}$$

We know that

$$\|\Delta e_n\|^2 = \iint_{\Omega} (e_{n,xx}^2 + e_{n,yy}^2 + 2e_{n,xx}e_{n,yy})\, dx\, dy. \tag{3.78}$$

By Cauchy-Schwarz inequality, we get

$$\left| \iint\limits_{\Omega} 2e_{n,xx}e_{n,yy}\,dx\,dy \right| \leq 2\left(\iint\limits_{\Omega} e_{n,xx}^2\,dx\,dy \right)^{\frac{1}{2}} \left(\iint\limits_{\Omega} e_{n,yy}^2\,dx\,dy \right)^{\frac{1}{2}}.$$

Since $2\alpha\beta \leq \alpha^2 + \beta^2$ for any real numbers α and β, let $\alpha = \left(\iint\limits_{\Omega} e_{n,xx}^2\,dx\,dy \right)^{\frac{1}{2}}$ and $\beta = \left(\iint\limits_{\Omega} e_{n,yy}^2\,dx\,dy \right)^{\frac{1}{2}}$, we get

$$2\left(\iint\limits_{\Omega} e_{n,xx}^2\,dx\,dy \right)^{\frac{1}{2}} \left(\iint\limits_{\Omega} e_{n,yy}^2\,dx\,dy \right)^{\frac{1}{2}} \leq \iint\limits_{\Omega} e_{n,xx}^2\,dx\,dy + \iint\limits_{\Omega} e_{n,yy}^2\,dx\,dy.$$

Given y, define $X(y) \subset [-1,1]$ such that $(X(y), y) = \Omega \cap \{(x,y), x \in \mathbb{R}\}$. Given x, define $Y(x) \subset [-1,1]$ such that $(x, Y(x)) = \Omega \cap \{(x,y), y \in \mathbb{R}\}$. Extend the definition of e_n to $[-1,1]^2$ by extension by zero. Thus, by (3.78), we get

$$\begin{aligned} \|\Delta e_n\|^2 &\leq 2 \iint\limits_{\Omega} (e_{n,xx}^2 + e_{n,yy}^2)\,dx\,dy \\ &= 2\left(\int_{-1}^{1} \int_{X(y)} e_{n,xx}^2(x,y)\,dx\,dy + \int_{-1}^{1} \int_{Y(x)} e_{n,yy}^2(x,y)\,dy\,dx \right). \end{aligned} \tag{3.79}$$

Let $E_1(y) = \int_{X(y)} e_{n,xx}^2(x,y)\,dx$ and $E_2(x) = \int_{Y(x)} e_{n,yy}^2(x,y)\,dy$. Suppose $[a,b] = X(y)$ and $[c,d] = Y(x)$. Take $\tilde{x}_i = \left(\frac{b-a}{2}\right) x_i + \left(\frac{a+b}{2}\right)$ and $\tilde{y}_j = \left(\frac{d-c}{2}\right) y_j + \left(\frac{c+d}{2}\right)$. Thus

$$\begin{aligned} E_1(y) &= \int_{X(y)} e_{n,xx}^2(x,y)\,dx \\ &= \frac{b-a}{2} \int_{-1}^{1} e_{n,\tilde{x}\tilde{x}}^2(\tilde{x},y)\,d\tilde{x} \\ &= \frac{b-a}{2} \sum_{i=1}^{n-1} e_{n,\tilde{x}\tilde{x}}^2(\tilde{x}_i,y)\rho_i + \epsilon_1(y), \end{aligned}$$

where $|\epsilon_1(y)| \leq ce^{-\gamma_1 n}$ for some positive γ_1 and ρ_i are Legendre weights. This implies

that

$$\begin{aligned}\int_{-1}^{1}\int_{X(y)} e_{n,xx}^2(x,y)\,dx\,dy &= \int_{-1}^{1} E_1(y)\,dy \\ &\le \frac{b-a}{2}\sum_{i=1}^{n-1}\left\|e_{n,\tilde{x}\tilde{x}}(\tilde{x}_i,\cdot)\right\|^2\rho_i + ce^{-\gamma_1 n} \\ &\le \int_{-1}^{1} K_1 e^{-2cn}\,dy \\ &\le 2K_1 e^{-2cn}, \end{aligned} \tag{3.80}$$

by (3.76). Similarly,

$$\begin{aligned}E_2(x) &= \int_{Y(x)} e_{n,yy}^2(x,y)\,dy \\ &= \frac{d-c}{2}\sum_{j=1}^{n-1} e_{n,yy}^2(x,\tilde{y}_j)\rho_j + \epsilon_2(x),\end{aligned}$$

where $|\epsilon_2(x)| \le ce^{-\gamma_2 n}$. Then we get

$$\begin{aligned}\int_{-1}^{1}\int_{Y(x)} e_{n,yy}^2(x,y)\,dy\,dx &= \int_{-1}^{1} E_2(x)\,dx \\ &\le \frac{d-c}{2}\sum_{j=1}^{n-1}\left\|e_{n,yy}^2(\cdot,\tilde{y}_j)\right\|^2\rho_j + ce^{-\gamma_2 n} \\ &\le \int_{-1}^{1} K_2 e^{-2cn}\,dx \\ &\le 2K_2 e^{-2cn}, \end{aligned} \tag{3.81}$$

by (3.77). If $X(y)$ and $Y(x)$ consist of more than one interval, we sum the error over each interval.

Hence, by substituting (3.80) and (3.81) to (3.79), we get

$$\begin{aligned}\|\Delta e_n\|^2 &\le 4(K_1 e^{-2cn} + K_2 e^{-2cn}) = Ce^{-2cn}, \\ \|\Delta e_n\| &\le Ce^{-cn}. \end{aligned} \tag{3.82}$$

Now we show $\|\nabla e_n\|$ and $\|e_n\|$ also have an exponential decay. Multiply the error equation (3.75) by $e_n(x, y)$ and apply the Green's first identity:

$$\int_\Omega \nabla e_n \cdot \nabla e_n d\Omega = \int_\Omega (f - g_n) e_n d\Omega$$
$$\|\nabla e_n\|^2 = \int_\Omega (f - g_n) e_n d\Omega. \tag{3.83}$$

By Cauchy-Schwarz inequality,

$$\left| \int_\Omega (f - g_n) e_n d\Omega \right| \leq \|f - g_n\| \, \|e_n\| . \tag{3.84}$$

Using Poincaré inequality (since $e_n = 0$ on the boundary),

$$\|e_n\| \leq c \, \|\nabla e_n\| . \tag{3.85}$$

By (3.83),(3.84) and (3.85) we get,

$$\|\nabla e_n\|^2 \leq c \, \|f - g_n\| \, \|\nabla e_n\|$$
$$\|\nabla e_n\| \leq c \, \|f - g_n\|$$
$$\|\nabla e_n\| \leq Ce^{-cn} \quad \text{(By} \quad \text{(3.82))}. \tag{3.86}$$

Further, by (3.85) and (3.86) we get,

$$\|e_n\| \leq Ce^{-cn}.$$

□

Theorem 3.19. Let $u(x, y, t)$ and $f(x, y, t)$ be the solution and analytic non-homogeneous term of the 2-D Heat equation in the space-time domain $\Omega \times (-1, 1)$, where Ω is the irregular spatial domain. For any positive integer n, define $v_n(x, y, t)$ be solu-

tion of $(v_n)_t = \Delta v_n + g_n$ on $\widetilde{\Omega} \times (-1,1)$, where $\widetilde{\Omega}$ is the extended spatial domain and g_n is the Alternating non-periodic extension of f to $\widetilde{\Omega} \times (-1,1)$. At a fixed time $t \in [-1,1]$, the error between $u(x,y,t)$ and $v_n(x,y,t)$ on Ω can be defined as $e_n(x,y,t) = u(x,y,t) - v_n(x,y,t)|_\Omega$. Then $\|e_n(\cdot,\cdot,t)\| \leq Ce^{-cn}$, $t \in [-1,1]$.

Proof. Consider the 2-D Heat equation defined in the irregular domain $\Omega \times (-1,1)$ and the extended domain $\widetilde{\Omega} \times (-1,1)$. The spatial domain Ω is as in Figure (3.16) and the temporal domain is $(-1,1)$. Then

$$\begin{aligned} u_t &= \Delta u + f \quad \text{in } \Omega \times (-1,1), & (v_n)_t &= \Delta v_n + g_n \quad \text{in } \tilde{\Omega} = (-1,1)^2 \times (-1,1), \\ u &= 0 \quad \text{on } \partial\Omega \times (-1,1), & v_n &= 0 \quad \text{on } \partial\Omega \times (-1,1), \\ u(x,y,-1) &= 0. & 0 &= v_n(x,y,-1). \end{aligned}$$

By UCP (Theorem 3.12), v_n is well defined on $\tilde{\Omega} \times (-1,1)$. For a fixed t, the error function is defined as:

$$e_n(x,y,t) = u(x,y,t) - v_n(x,y,t)\Big|_\Omega.$$

Then

$$\begin{aligned} e_{n,t} - \Delta e_n &= f(x,y,t) - g_n(x,y,t)\Big|_\Omega \qquad (3.87) \\ \|(e_{n,t} - \Delta e_n)(\cdot,\cdot,t)\| &= \|f(\cdot,\cdot,t) - g_n(\cdot,\cdot,t)\|. \end{aligned}$$

In the Alternating Non-Periodic Extension, we first perform one non-periodic extension in the $x-$direction, followed by one in the $y-$direction. For fixed t, let the non-periodic extension in the $x-$direction be denoted by g^x. Therefore

$$\begin{aligned} \|e_{n,t} - \Delta e_n\|^2 &= \iint_\Omega (f - g_n)^2(x,y,t)dxdy \\ &= \iint_\Omega (f - g^x + g^x - g_n)^2(x,y,t)dxdy \end{aligned}$$

$$\leq 2\left(\iint_{\Omega}(f-g^x)^2(x,y,t)dxdy+\iint_{\Omega}(g^x-g_n)^2(x,y,t)dxdy\right). \quad (3.88)$$

By Theorem 3.16, for fixed t and y,

$$f(x_i,y,t)-g^x(x_i,y,t)=\sum_{k=n+1}^{\infty}a_k(y,t)T_k^h\left(\cos\frac{\pi x_i}{2}\right)+\sum_{k=n}^{\infty}b_k(y,t)U_k^h\left(\cos\frac{\pi x_i}{2}\right)\sin\frac{\pi x_i}{2}$$

$$\|f(x_i,\cdot,t)-g^x(x_i,\cdot,t)\|\leq c_{1,i}(t)e^{-c_{2,i}(t)n},$$

for some continuous positive functions $c_{1,i}(t)$ and $c_{2,i}(t)$ for $t\in[-1,1]$. Thus

$$\sum_{i=1}^{n-1}\|f(x_i,\cdot,t)-g^x(x_i,\cdot,t)\|^2\rho_i\leq\sum_{i=1}^{n-1}c_{1,i}^2(t)e^{-2c_{2,i}(t)n}\rho_i=C_1(t)e^{-2C_2(t)n}. \quad (3.89)$$

Now, using g^x, we perform the extension in the y direction to obtain g_n. Since this is a one-dimensional extension, the corresponding one-dimensional results hold. Therefore, for fixed t and x we get

$$g^x(x,y_j,t)-g_n(x,y_j,t)=\sum_{k=n+1}^{\infty}\tilde{a}_k(x,t)T_k^h\left(\cos\frac{\pi y_j}{2}\right)+\sum_{k=n}^{\infty}\tilde{b}_k(x,t)U_k^h\left(\cos\frac{\pi y_j}{2}\right)\sin\frac{\pi y_j}{2}$$

$$\|g^x(\cdot,y_j,t)-g_n(\cdot,y_j,t)\|\leq c_{3,j}(t)e^{-c_{4,j}(t)n},$$

for some continuous positive functions $c_{3,j}(t)$ and $c_{4,j}(t)$ for $t\in[-1,1]$. Thus

$$\sum_{j=1}^{n-1}\|g^x(\cdot,y_j,t)-g_n(\cdot,y_j,t)\|^2\rho_j\leq\sum_{j=1}^{n-1}c_{3,j}^2(t)e^{-2c_{4,j}(t)n}\rho_j=C_3(t)e^{-2C_4(t)n}. \quad (3.90)$$

For fixed t, and for a given y, define $X(y)\subset[-1,1]$ such that $(X(y),y)=\Omega\cap\{(x,y),x\in\mathbb{R}\}$. Similarly, for fixed t, and for a given x, define $Y(x)\subset[-1,1]$ such that $(x,Y(x))=\Omega\cap\{(x,y),y\in\mathbb{R}\}$. For each fixed t, extend the definition of $f-g^x$

and $g^x - g_n$ to $[-1,1]^2$ by extension by zero. Thus, by (3.88), we get

$$\|(e_{n,t} - \Delta e_n)(\cdot,\cdot,t)\|^2 \le 2\left(\int_{-1}^{1}\int_{X(y)} (f-g^x)^2(x,y,t)dxdy + \int_{-1}^{1}\int_{Y(x)} (g^x - g_n)^2(x,y,t)dydx\right). \tag{3.91}$$

Let $E_1(y,t) = \int_{X(y)}(f-g^x)^2(x,y,t)\,dx$ and $E_2(x,t) = \int_{Y(x)}(g^x-g_n)^2(x,y,t)\,dy$. Suppose $[a,b] = X(y)$ and $[c,d] = Y(x)$. Take $\tilde{x}_i = \left(\frac{b-a}{2}\right)x_i + \left(\frac{a+b}{2}\right)$ and $\tilde{y}_j = \left(\frac{d-c}{2}\right)y_j + \left(\frac{c+d}{2}\right)$. Thus

$$\begin{aligned} E_1(y,t) &= \int_{X(y)} (f-g^x)^2(x,y,t)\,dx \\ &= \frac{b-a}{2}\sum_{i=1}^{n-1}(f-g^x)^2(\tilde{x}_i,y,t)\rho_i + \epsilon_1(y,t), \end{aligned}$$

where $|\epsilon_1(y,t)| \le c_1(t)e^{-\gamma_1(t)n}$ for some positive γ_1. This implies that

$$\begin{aligned} \int_{-1}^{1}\int_{X(y)} (f-g^x)^2(x,y,t)\,dx\,dy &= \int_{-1}^{1} E_1(y,t)\,dy \\ &\le \frac{b-a}{2}\sum_{i=1}^{n-1}\|(f-g^x)(\tilde{x}_i,\cdot,t)\|^2\rho_i + c_1(t)e^{-\gamma_1(t)n} \\ &\le \int_{-1}^{1} K_1(t)e^{-2c_1(t)n}\,dy \\ &\le 2K_1(t)e^{-2c_1(t)n}, \end{aligned} \tag{3.92}$$

by (3.89). Similarly,

$$\begin{aligned} E_2(x,t) &= \int_{Y(x)} (g^x-g_n)^2(x,y,t)\,dy \\ &= \frac{d-c}{2}\sum_{j=1}^{n-1}(g^x-g_n)^2(x,\tilde{y}_j,t)\rho_j + \epsilon_2(x,t), \end{aligned}$$

where $|\epsilon_2(x,t)| \le c_2(t)e^{-\gamma_2(t)n}$. Then we get

$$\int_{-1}^{1}\int_{Y(x)} (g^x-g_n)^2(x,y,t)\,dy\,dx = \int_{-1}^{1} E_2(x,t)\,dx$$

$$\leq \frac{d-c}{2}\sum_{j=1}^{n-1}\left\|(g^x-g_n)(\cdot,\tilde{y}_j,t)\right\|^2\rho_j + c_2(t)e^{-\gamma_2(t)n}$$
$$\leq \int_{-1}^{1} K_2(t)e^{-2c_2(t)n}\,dx$$
$$\leq 2K_2(t)e^{-2c_2(t)n}, \tag{3.93}$$

by (3.90). Hence, by substituting (3.92)and (3.93) to 3.91, we get

$$\|e_{n,t}-\Delta e_n\|^2 \leq C(t)e^{-2c(t)n}$$
$$\|e_{n,t}-\Delta e_n\| \leq C(t)e^{-c(t)n}. \tag{3.94}$$

Thus, $\|e_{n,t}-\Delta e_n\| \leq Ce^{-cn}$ for some positive constants c and C where, $C = \sup_{t\in[-1,1]} C(t)$ and $c = \inf_{t\in[-1,1]} c(t)$. Now we need to show $\|e_n(\cdot,\cdot,t)\|$ also has an exponential decay for all $t \in [-1,1]$. For a fixed $t \in (-1,1)$, multiply the error equation (3.87) by $e_n(x,y,t)$ and integrate over the spatial domain Ω:

$$\int_\Omega (e_{n,t}-\Delta e_n)e_n(x,y,t)d\Omega = \int_\Omega (f-g_n)e_n(x,y,t)d\Omega. \tag{3.95}$$

$$\begin{aligned}\int_\Omega (e_{n,t}-\Delta e_n)e_n(x,y,t)d\Omega &= \int_\Omega e_{n,t}e_n d\Omega - \int_\Omega \Delta e_n e_n d\Omega \\ &= \frac{1}{2}\frac{d}{dt}\left\|e_n(\cdot,\cdot,t)\right\|^2 + \int_\Omega |\nabla e_n|^2 d\Omega \\ &= \frac{1}{2}\frac{d}{dt}\left\|e_n(\cdot,\cdot,t)\right\|^2 + \left\|\nabla e_n\right\|^2. \end{aligned}\tag{3.96}$$

Further, by Cauchy-Schwarz inequality,

$$\begin{aligned}\left|\int_\Omega (f-g_n)e_n(x,y,t)d\Omega\right| &\leq \|f(\cdot,\cdot,t)-g_n(\cdot,\cdot,t)\|\,\|e_n(\cdot,\cdot,t)\| \\ &\leq C(t)e^{-c(t)n}\,\|e_n(\cdot,\cdot,t)\| \quad (\text{By} \quad (3.94)) \\ &\leq Ce^{-cn}\,\|e_n(\cdot,\cdot,t)\|, \end{aligned}\tag{3.97}$$

where $C = \sup_{t\in[-1,1]} C(t)$ and $c = \inf_{t\in[-1,1]} c(t)$. By substituting (3.96) and (3.97) to (3.95) we get,

$$\frac{1}{2}\frac{d}{dt}\left\|e_n(\cdot,\cdot,t)\right\|^2 + \left\|\nabla e_n(\cdot,\cdot,t)\right\|^2 \leq Ce^{-cn}\left\|e_n(\cdot,\cdot,t)\right\|. \tag{3.98}$$

Let $E(t) = \int_\Omega |e_n(x,y,t)|^2 d\Omega$, so

$$\begin{aligned}
\frac{d}{dt}E(t) + 2\left\|\nabla e_n\right\|^2 &\leq 2Ce^{-cn}\sqrt{E(t)} \\
E'(t) &\leq 2Ce^{-cn}\sqrt{E(t)} \\
y'(t) &\leq Ce^{-cn} \quad \text{where} \quad y(t) = \sqrt{E(t)} \\
y(t) &\leq y(-1) + Ce^{-cn}t.
\end{aligned} \tag{3.99}$$

Since $y(-1) = 0$, $y(t) \leq Ce^{-cn}$ for each $t \in [-1,1]$,

$$\left\|e_n(\cdot,\cdot,t)\right\| \leq Ce^{-cn}. \tag{3.100}$$

□

Theorem 3.20. Let $u(x,y,t)$ and $f(x,y,t)$ be the solution and analytic non-homogeneous term of the 2-D Wave equation in the space-time domain $\Omega \times (-1,1)$, where Ω is the irregular spatial domain. For any positive integer n, define $v_n(x,y,t)$ be solution of $(v_n)_{tt} = \Delta v_n + g_n$ on $\widetilde{\Omega} \times (-1,1)$, where $\widetilde{\Omega}$ is the extended spatial domain and g_n is the Alternating non-periodic extension of f to $\widetilde{\Omega} \times (-1,1)$. At a fixed time $t \in [-1,1]$, the error between $u(x,y,t)$ and $v_n(x,y,t)$ on Ω can be defined as $e_n(x,y,t) = u(x,y,t) - v_n(x,y,t)|_\Omega$. Then $\|e_n(\cdot,\cdot,t)\| \leq Ce^{-cn}$, $\|e_{n,t}(\cdot,\cdot,t)\| \leq Ce^{-cn}$ and $\|\nabla e_n(\cdot,\cdot,t)\| \leq Ce^{-cn}$, $t \in [-1,1]$.

Proof. Consider the 2-D Wave equation defined in the irregular domain $\Omega \times (-1,1)$ and the extended domain $\widetilde{\Omega} \times (-1,1)$. The spatial domain Ω is as in Figure (3.16)

and the temporal domain is $(-1,1)$. Then

$$\begin{aligned} u_{tt} &= \Delta u + f \quad \text{in } \Omega \times (-1,1), & v_{n,tt} &= \Delta v_n + g_n \quad \text{in } \tilde{\Omega} = (-1,1)^2 \times (-1,1), \\ u &= 0 \quad \text{on } \partial\Omega \times (-1,1), & v_n &= 0 \quad \text{on } \partial\Omega \times (-1,1), \\ u(x,y,-1) &= 0, & 0 &= v_n(x,y,-1), \\ u_t(x,y,-1) &= 0. & 0 &= v_{n,t}(x,y,-1). \end{aligned}$$

By UCP (Theorem 3.13), v_n is well defined on $\tilde{\Omega} \times (-1,1)$. For a fixed t, the error function is defined as:

$$e_n(x,y,t) = u(x,y,t) - v_n(x,y,t)\Big|_{\Omega}.$$

Then

$$\begin{aligned} e_{n,tt} - \Delta e_n &= f(x,y,t) - g_n(x,y,t)\Big|_{\Omega} \\ \|(e_{n,tt} - \Delta e_n)(\cdot,\cdot,t)\| &= \|f(\cdot,\cdot,t) - g_n(\cdot,\cdot,t)\|. \end{aligned} \tag{3.101}$$

Following the same approach explained for the 2D Heat equation, we can obtain

$$\|e_{n,tt} - \Delta e_n\| \leq C(t)e^{-c(t)n}, \tag{3.102}$$

where $C(t)$ and $c(t)$ are continuous with the latter bounded away from zero.

Thus, $\|e_{n,tt} - \Delta e_n\| \leq Ce^{-cn}$ for some positive constants c and C where, $C = \sup_{t\in[-1,1]} C(t)$ and $c = \inf_{t\in[-1,1]} c(t)$. Now we need to show $\|\nabla e_n(\cdot,\cdot,t)\|$ and $\|e_n(\cdot,\cdot,t)\|$ also has an exponential decay for all $t \in [-1,1]$. Let

$$E(t) = \frac{1}{2}\int_{\Omega} (|e_{n,t}(x,y,t)|^2 + |\nabla e_n(x,y,t)|^2) dxdy.$$

Then

$$\begin{aligned}
E'(t) &= \int_\Omega e_{n,t}e_{n,tt}dxdy + \int_\Omega (\nabla e_n \cdot \nabla e_{n,t})dxdy \\
&= \int_\Omega e_{n,t}e_{n,tt}dxdy - \int_\Omega (e_{n,t}\Delta e_n)dxdy + \int_{\partial\Omega}\left(e_{n,t}\frac{\partial e_n}{\partial \nu}\right)ds \quad \text{(By Green's Identity)} \\
&= \int_\Omega e_{n,t}(e_{n,tt} - \Delta e_n)dxdy \\
&= \int_\Omega e_{n,t}(f - g_n)dxdy.
\end{aligned}$$

Further, by Cauchy-Schwarz inequality,

$$\begin{aligned}
|E'(t)| &\le \|f(\cdot,\cdot,t) - g_n(\cdot,\cdot,t)\| \, \|e_{n,t}(\cdot,\cdot,t)\| \\
&\le C(t)e^{-c(t)n} \|e_{n,t}(\cdot,\cdot,t)\| \quad \text{(By (3.102))} \\
&\le Ce^{-cn} \|e_{n,t}(\cdot,\cdot,t)\| . \qquad (3.103)
\end{aligned}$$

Since,

$$E(t) = \frac{1}{2}\|e_{n,t}\|^2 + \frac{1}{2}\|\nabla e_n\|^2 \ge \frac{1}{2}\|e_{n,t}\|^2,$$

implying $\|e_{n,t}\| \le \sqrt{2E(t)}$. Thus, by (3.103) we get

$$\begin{aligned}
E'(t) &\le Ce^{-cn}\sqrt{2E(t)} \le Ce^{-cn}\sqrt{E(t)} \\
\text{or} \quad y'(t) &\le Ce^{-cn}, \quad \text{where} \quad y(t) = \sqrt{E(t)}.
\end{aligned}$$

Consequently,

$$y(t) \le y(-1) + Ce^{-cn}t. \qquad (3.104)$$

Since $y(-1) = 0$, $y(t) \leq Ce^{-cn}$ for each $t \in [-1, 1]$,

$$\|e_{n,t}(\cdot, \cdot, t)\| \leq Ce^{-cn}, \quad \|\nabla e_n(\cdot, \cdot, t)\| \leq Ce^{-cn}. \tag{3.105}$$

Using Poincaré inequality (since $e_n = 0$ on the boundary),

$$\|e_n(\cdot, \cdot, t)\| \leq c \|\nabla e_n(\cdot, \cdot, t)\| \leq Ce^{-cn}.$$

□

Theorem 3.21. Let $\psi(x, y, t)$ and $f(x, y, t)$ be the solution and analytic non-homogeneous term of the stream function formulation of the 2-D Stokes equation in the space-time domain $\Omega \times (-1, 1)$, where Ω is the irregular spatial domain. For any positive integer n, define $\phi_n(x, y, t)$ be solution of $\Delta\phi_{n,t} = \Delta^2\phi_n + g_n$ on $\widetilde{\Omega} \times (-1, 1)$, where $\widetilde{\Omega}$ is the extended spatial domain and g_n is the Alternating non-periodic extension of f to $\widetilde{\Omega} \times (-1, 1)$. At a fixed time $t \in [-1, 1]$, the error between $\psi(x, y, t)$ and $\phi_n(x, y, t)$ on Ω can be defined as $e_n(x, y, t) = \phi(x, y, t) - \psi_n(x, y, t)|_\Omega$. Then $\|e_n(\cdot, \cdot, t)\| \leq Ce^{-cn}$ and $\|\nabla e_n(\cdot, \cdot, t)\| \leq Ce^{-cn}$, $t \in [-1, 1]$.

Proof. Consider the 2-D Stokes equation defined in the irregular domain $\Omega \times (-1, 1)$ and the extended domain $\widetilde{\Omega} \times (-1, 1)$. The spatial domain Ω is as in Figure (3.16) and the temporal domain is $(-1, 1)$. Then

$$\begin{aligned}
\Delta\psi_t = \Delta^2\psi + f(x, y, t) \quad \text{in } \Omega \times (-1, 1), \qquad & \Delta\phi_{n,t} = \Delta^2\phi_n + g_n(x, y, t) \quad \text{in } \tilde{\Omega} \times (-1, 1) \\
\psi(x, y, t) = 0 = \frac{\partial\psi}{\partial\nu} \quad \text{on } \partial\Omega \times (-1, 1), \qquad & \phi_n(x, y, t) = 0 = \frac{\partial\phi_n}{\partial\nu} \quad \text{on } \partial\Omega \times (-1, 1), \\
\psi(x, y, -1) = 0. \qquad & \phi_n(x, y, -1) = 0,
\end{aligned}$$

By UCP (Theorem 3.14), ϕ_n is well defined on $\tilde{\Omega} \times (-1, 1)$. For a fixed t, the error

function is defined as:

$$e_n(x,y,t) = \psi(x,y,t) - \phi_n(x,y,t)\Big|_\Omega.$$

Then

$$\Delta e_{n,t} - \Delta^2 e_n = f(x,y,t) - g_n(x,y,t)\Big|_\Omega \tag{3.106}$$
$$\|(\Delta e_{n,t} - \Delta^2 e_n)(\cdot,\cdot,t)\| = \|f(\cdot,\cdot,t) - g_n(\cdot,\cdot,t)\|.$$

Following the same approach explained for the 2D Heat equation, we can obtain

$$\|\Delta e_{n,t} - \Delta^2 e_n\| \le C(t)e^{-c(t)n}, \tag{3.107}$$

where $C(t)$ and $c(t)$ are continuous with the latter bounded away from zero.

Thus, $\|\Delta e_{n,t} - \Delta^2 e_n\| \le Ce^{-cn}$ for some positive constants c and C where, $C = \sup_{t\in[-1,1]} C(t)$ and $c = \inf_{t\in[-1,1]} c(t)$. Now we need to show $\|\nabla e_n(\cdot,\cdot,t)\|$ and $\|e_n(\cdot,\cdot,t)\|$ also has an exponential decay for all $t \in [-1,1]$. Multiply the error equation (3.106) by $e_n(x,y,t)$ and integrate over the spatial domain Ω:

$$\int_\Omega (\Delta e_{n,t} - \Delta^2 e_n)e_n(x,y,t)d\Omega = \int_\Omega (f - g_n)e_n(x,y,t)d\Omega. \tag{3.108}$$

$$\begin{aligned}
\int_\Omega (\Delta e_{n,t} - \Delta^2 e_n)e_n(x,y,t)d\Omega &= \int_\Omega \Delta e_{n,t}e_n d\Omega - \int_\Omega \Delta^2 e_n e_n d\Omega \\
&= -\int_\Omega \nabla e_{n,t}\nabla e_n d\Omega + \int_\Omega \nabla(\Delta e_n)\nabla e_n d\Omega \\
&= -\frac{1}{2}\frac{d}{dt}\int_\Omega |\nabla e_n|^2 d\Omega - \int_\Omega \Delta e_n \Delta e_n d\Omega + \int_{\partial\Omega} \Delta e_n \frac{\partial e_n}{\partial \nu} dS \\
&= -\frac{1}{2}\frac{d}{dt}\int_\Omega |\nabla e_n|^2 d\Omega - \int_\Omega |\Delta e_n|^2 d\Omega \\
&= -\frac{1}{2}\frac{d}{dt}\|\nabla e_n(\cdot,\cdot,t)\|^2 - \|\Delta e_n(\cdot,\cdot,t)\|^2 .
\end{aligned} \tag{3.109}$$

Further, by Cauchy-Schwarz inequality,

$$\begin{aligned}\left|\int_\Omega (f-g_n)e_n(x,y,t)d\Omega\right| &\le \|f(\cdot,\cdot,t)-g_n(\cdot,\cdot,t)\|\,\|e_n(\cdot,\cdot,t)\| \\ &\le C(t)e^{-c(t)n}\,\|e_n(\cdot,\cdot,t)\| \quad (\text{By} \quad (3.107)) \\ &\le Ce^{-cn}\,\|e_n(\cdot,\cdot,t)\|\,. \end{aligned} \tag{3.110}$$

By substituting (3.109) and (3.110) to (3.108) we get,

$$\begin{aligned}\frac{1}{2}\frac{d}{dt}\,\|\nabla e_n(\cdot,\cdot,t)\|^2 + \|\Delta e_n(\cdot,\cdot,t)\|^2 &\le Ce^{-cn}\,\|e_n(\cdot,\cdot,t)\| \\ &\le Ce^{-cn}\,\|\nabla e_n(\cdot,\cdot,t)\| \quad (\text{By Poincaré inequality}).\end{aligned} \tag{3.111}$$

Let $E(t)=\int_\Omega |\nabla e_n|^2 d\Omega$, so

$$\begin{aligned}\frac{d}{dt}E(t)+2\,\|\Delta e_n(\cdot,\cdot,t)\|^2 &\le 2Ce^{-cn}\sqrt{E(t)} \\ E'(t) &\le 2Ce^{-cn}\sqrt{E(t)} \\ y'(t) &\le Ce^{-cn} \quad \text{where} \quad y(t)=\sqrt{E(t)} \\ y(t) &\le y(-1)+Ce^{-cn}t.\end{aligned} \tag{3.112}$$

Since $y(-1)=0$, $y(t)\le Ce^{-cn}$ for each $t\in[-1,1]$,

$$\|\nabla e_n(\cdot,\cdot,t)\| \le Ce^{-cn}. \tag{3.113}$$

Using the Poincaré inequality (since $e_n=0$ on $\partial\Omega$),

$$\|e_n(\cdot,\cdot,t)\| \le c\,\|\nabla e_n(\cdot,\cdot,t)\| \le Ce^{-cn}. \tag{3.114}$$

□

4

Numerical Experiments

In this chapter, we demonstrate the accuracy and robustness of the proposed method through a broad set of numerical experiments involving a variety of domain shapes and model equations. All the irregular domains considered in this chapter have smooth boundaries to ensure that the solution is smooth. Spectral accuracy may deteriorate in the presence of geometric singularities, such as corners or cusps (e.g., lemniscate or teardrop shapes). In all figures, the error is measured as the absolute error in the infinity norm, evaluated at the collocation points.

This chapter is organized into two main parts according to the nature of the non-homogeneous term.

In section 4.1, we consider the elliptic and butterfly domains, where we implement the two-dimensional unsteady Stokes and Navier–Stokes equations, with the non-homogeneous term analytic and periodic in the extended domain.

Section 4.2 addresses the case where the non-homogeneous term is only known in the physical domain. It is further divided into two parts: periodic extensions and non-periodic extensions.

In section 4.2.1, we consider periodic extensions, where we implement the two-dimensional Poisson equation on the square domain using the Alternating Fourier

Extension method. Since the Alternating Fourier Extension method is not suitable for non-rectangular physical domains, we then proceed to non-periodic extensions.

In section 4.2.2, we consider non-periodic extensions. First, we consider two convex irregular domains. On these domains, we implement the two-dimensional Poisson equation, Heat equation, Wave equation, unsteady Stokes equation, Allen–Cahn equation, Nonlinear Schrödinger equation, and Navier–Stokes equations using the Alternating Non-periodic Extension method.

Next, we examine four non-convex irregular domains. The first is symmetric and non-convex, the second is symmetric and non-simply connected, while the third and fourth are non-symmetric and non-simply connected. The latter two domains are specifically designed to investigate whether shifting an internal hole from the center to a corner influences spectral convergence. This setup also allows us to examine how the loss of symmetry or the proximity of geometric irregularities to domain boundaries affects the performance of the method. For each of these domains, we implement the two-dimensional Poisson equation, unsteady Stokes equation, and unsteady Navier–Stokes equations.

4.1 Non-homogeneous term is analytic and periodic in the extended domain.

We have implemented spectral solvers for the 2D Poisson equation, Heat equation, unsteady Stokes equations, and Navier–Stokes equations defined in irregular domains. Here we consider two different irregular geometries. The first irregular boundary is an ellipse with axis lengths a, b and center at the origin ($\Gamma(x, y) = \frac{x^2}{a^2} + \frac{y^2}{b^2} - 1$). The second domain has the form of a butterfly with boundary $x = r\cos(\theta), y = r\sin(2\theta)$ parameterized by the polar angle θ.

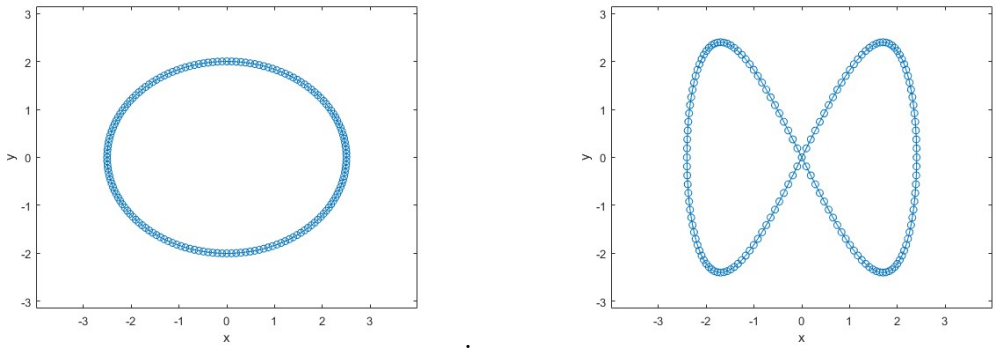

Figure 4.1: Elliptic domain with $a = 2.5$ and $b = 2$ and the butterfly domain with $r = 2.5$.

Spectral error convergence was observed in each instance. For steady problems, take f when the exact solution is $\psi(x, y) = e^{1+\sin(x+y)}$. For unsteady problems, take f corresponding to the exact solution $\psi(x, y, t) = e^{(1+t)+\sin(x+y)}$, with the initial condition $\psi(x, y, -1) = \psi_0(x, y)$. First, consider the numerical results for the Poisson equation defined in irregular geometries.

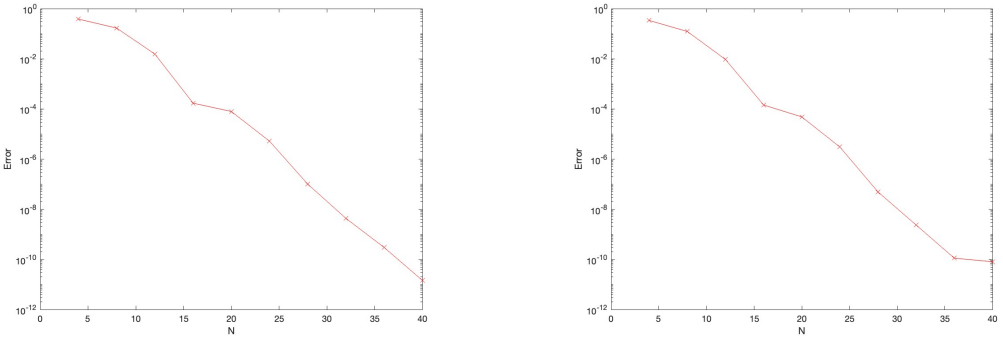

Figure 4.2: Spectral error convergence for the elliptic domain and the butterfly domain for the Poisson equation.

Now consider the numerical results for the stream function formulation of the 2D unsteady Stokes equation

$$(\psi_t)_{xx} + (\psi_t)_{yy} = (\psi_{xxxx} + \psi_{yyyy} + 2\psi_{xxyy}) + f,$$

defined in irregular geometries.

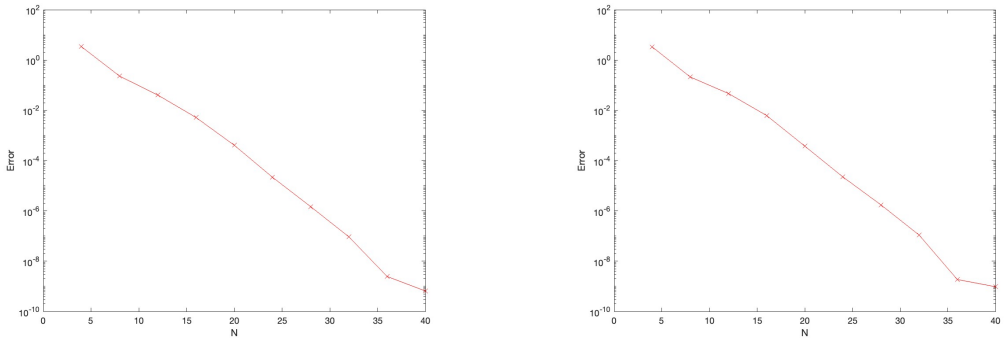

Figure 4.3: Spectral error convergence for the elliptic domain and the butterfly domain for the unsteady Stokes equation.

Next, we present numerical results for the nonlinear PDE, Navier–Stokes equation defined in irregular geometries. Here, we take zero function as the initial guess and apply a Picard iteration, terminating it whenever the infinity norm of the difference of two consecutive iterations is less than $\epsilon = 10^{-13}$. Here, we consider the stream function formulation of the unsteady Navier–Stokes equations

$$-\Delta\psi_t + \frac{1}{Re}\Delta^2\psi - \psi_y\psi_{xxx} + \psi_x\psi_{yyy} + \psi_x\psi_{yxx} - \psi_y\psi_{xyy} = f.$$

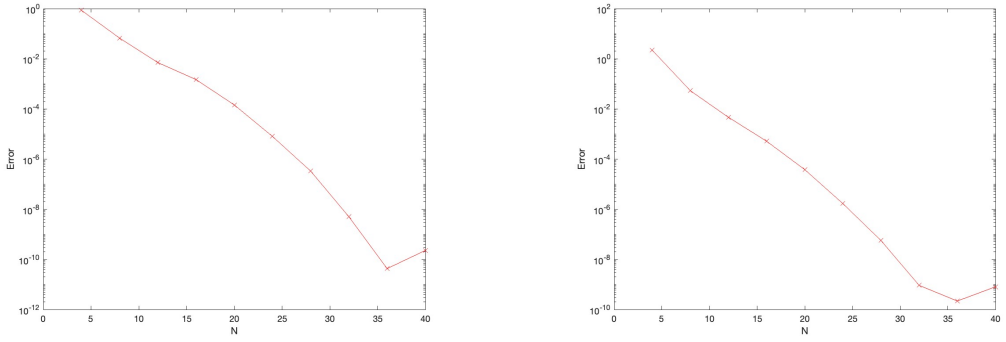

Figure 4.4: Spectral error convergence for the elliptic domain and the butterfly domain with $Re = 10$ for the unsteady Navier–Stokes equation.

4.2 Non-homogeneous term is only known in the physical domain.

4.2.1 Periodic Extensions

We have implemented 1D Poisson and Heat equations using the Fourier extension and observed spectral error convergence. To solve this PDE, we can use either Fourier or Chebyshev spectral collocation methods. Here, we use the Chebyshev spectral collocation. First, consider the numerical results for the 1D Poisson equation. Here, $f(x)$ is defined on the domain $[-1, 1]$ and extended it to the domain $[-2, 2]$ using Fourier extension. For the Poisson problem, take f when the exact solution is $u(x) = xe^x \sin(2x)$.

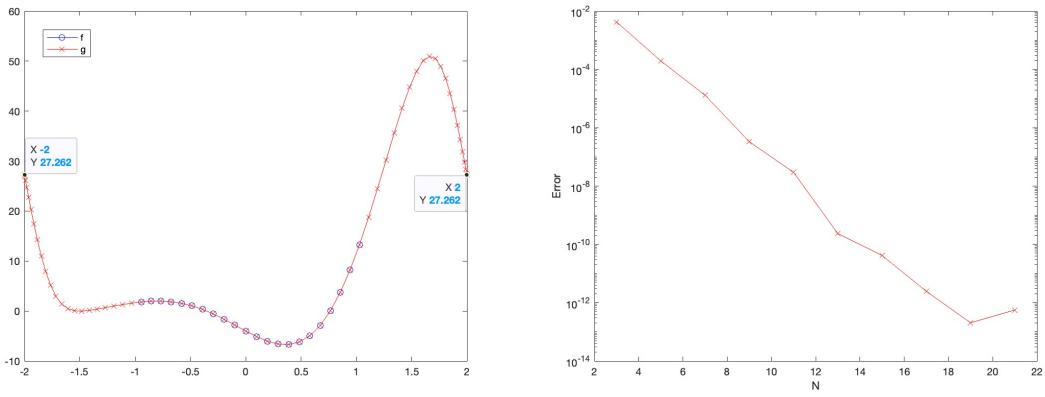

Figure 4.5: Fourier extension and spectral error convergence for the 1D Poisson equation.

Now consider the 1D Heat equation defined in the domain $[-1, 1] \times [-1, 1]$ and extend it to the domain $[-2, 2] \times [-1, 1]$. Here, take f when the exact solution is $u(x, t) = 6e^{t+x} \sin(\pi t/2) \sin(x)$.

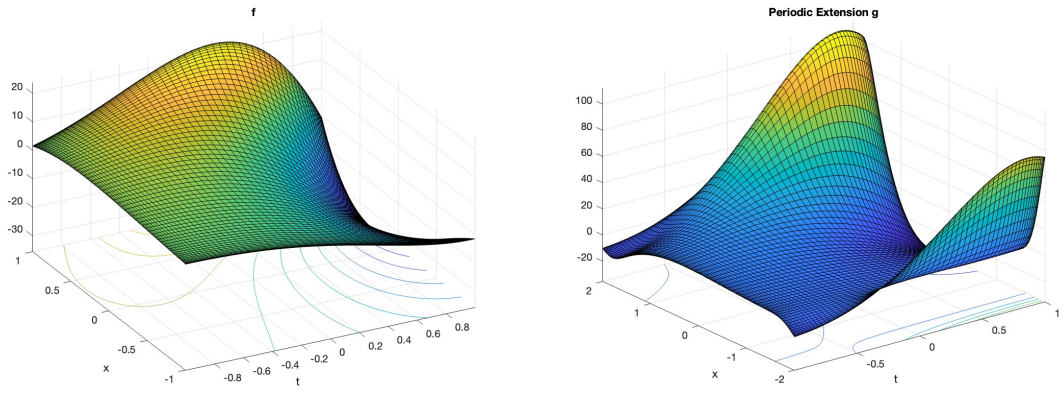

Figure 4.6: Fourier extension for the 1D Heat equation.

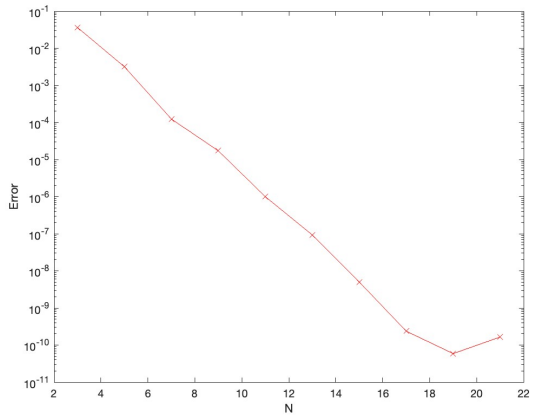

Figure 4.7: Spectral error convergence for the 1D Heat equation.

4.2.1.1 Alternating Fourier Extension method for the 2D Poisson equation

We implemented the 2D Poisson Equation defined on the square domain $R = (-1, 1)^2$, embedded it in a larger domain $R = (-2, 2)^2$, and then applied Alternating Fourier Extension method. Here we observed spectral error convergence.

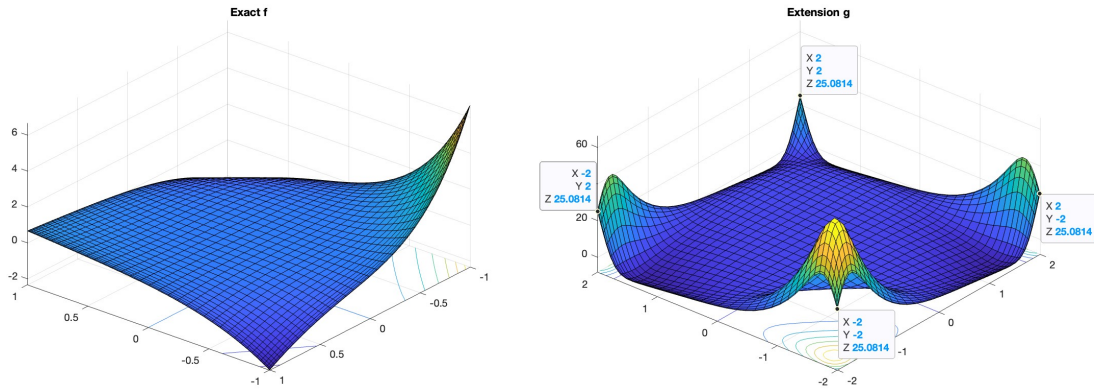

Figure 4.8: Fourier extension of a square domain for the 2D Poisson equation.

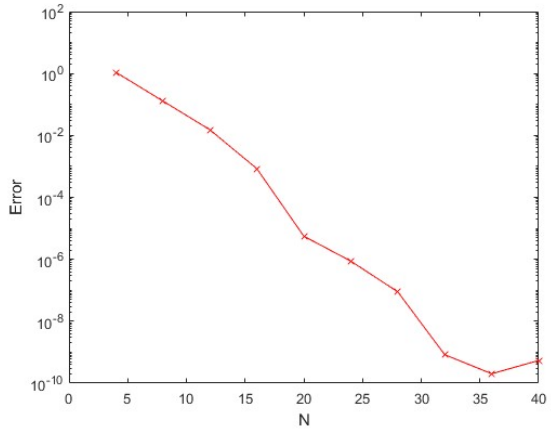

Figure 4.9: Error convergence for the 2D Poisson equation in a square domain.

4.2.2 Non-Periodic Extensions

4.2.2.1 Alternating Non-periodic Extension method for convex irregular domains

We have implemented the 2D Poisson equation, Heat equation, Wave equation, unsteady Stokes equation, Allen–Cahn equation, Nonlinear Schrödinger equation and Navier–Stokes equations defined in convex irregular domains. Here we consider two different irregular geometries. The first irregular boundary is $\Gamma(x,y) = \frac{x^4}{p^4} + \frac{y^2}{q^2} - 1$. The second domain is $\Gamma(x,y) = \frac{(x\cos(c)+y\sin(c))^2}{a^2} + \frac{(y\cos(c))^4}{b^2} - 1$.

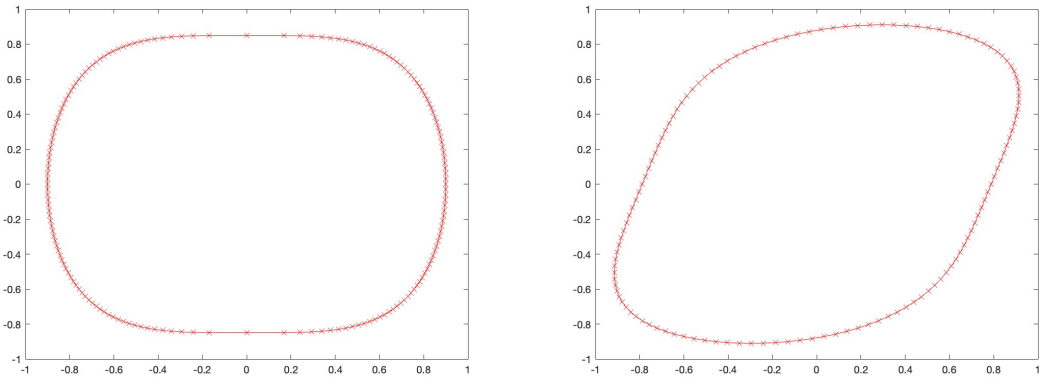

Figure 4.10: First irregular domain with $p = 0.9$ and $q = 0.85$ and the second irregular domain with $a = 0.75, b = 0.75$ and $c = -1.1\pi$.

Spectral error convergence was observed in each instance. For steady problems, take f when the exact solution is $e^{x+y+1}(x^2y^2 - x^2 - y^2 - 1)^2$ and for unsteady problems, take f when the exact solution is $e^{x+y+t+1}(x^2y^2 - x^2 - y^2 - 1)^2$. For unsteady problems, take the initial condition at $t = -1$, and perform the non-periodic extension for the initial condition as well. First, consider the numerical results for the Poisson equation defined in irregular geometries.

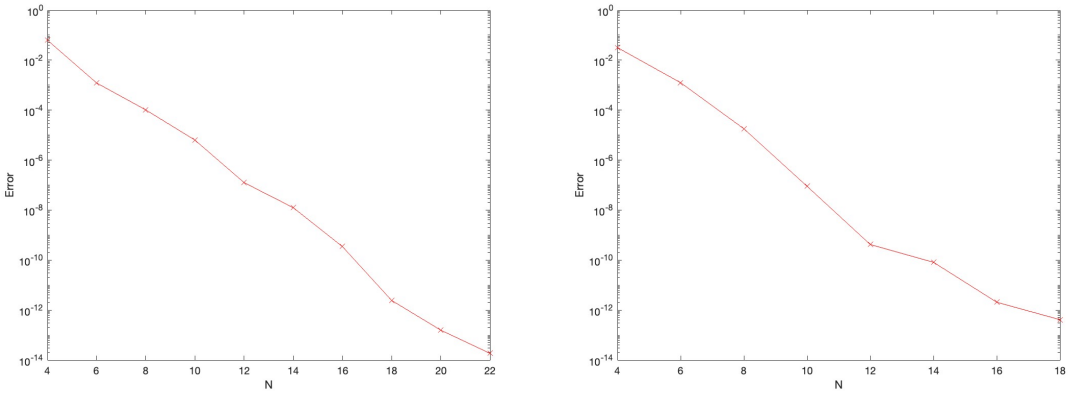

Figure 4.11: Spectral error convergence for the first and second irregular domains for the Poisson equation.

Now consider the numerical results for the 2D Wave equation $u_{tt} = \Delta u + f$ defined in irregular geometries with initial conditions $u(x, y, -1) = u_0(x, y)$ and $u_t(x, y, -1) = u_1(x, y)$.

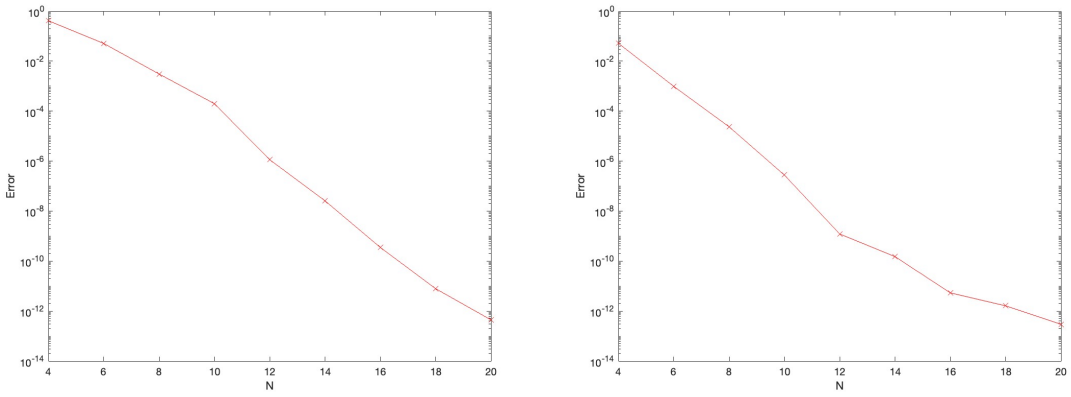

Figure 4.12: Spectral error convergence for the first and second domains for the Wave equation.

Next consider the numerical results for the stream function formulation of the 2D unsteady Stokes equation defined in irregular geometries.

$$(\psi_t)_{xx} + (\psi_t)_{yy} = (\psi_{xxxx} + \psi_{yyyy} + 2\psi_{xxyy}) + f.$$

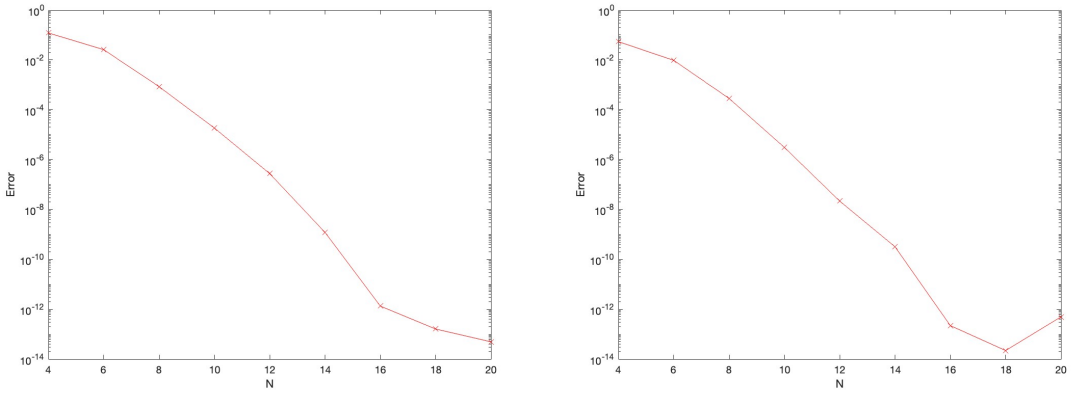

Figure 4.13: Spectral error convergence for the first and second domains for the unsteady Stokes equation.

Now, we present numerical results for the nonlinear PDEs, Allen–Cahn equation, Schrödinger equation and Navier–Stokes equation defined in irregular geometries. For all nonlinear PDEs, we take zero function as the initial guess and apply a Picard iteration, terminating it whenever the infinity norm of the difference of two

consecutive iterations is less than $\epsilon = 10^{-13}$.

Allen–Cahn equation:

$$u_t = \Delta u + au(1 - u^2) + f(x, y, t).$$

Nonlinear Schrödinger equation:

$$iu_t = -\Delta u + |u|^2 u + f(x, y, t).$$

Further, we consider the stream function formulation of the unsteady Navier–Stokes equations

$$-\Delta\psi_t + \frac{1}{Re}\Delta^2\psi - \psi_y\psi_{xxx} + \psi_x\psi_{yyy} + \psi_x\psi_{yxx} - \psi_y\psi_{xyy} = f.$$

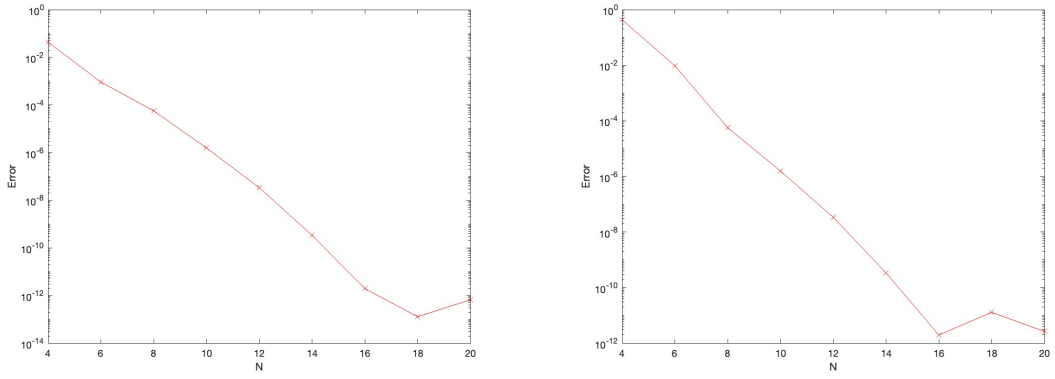

.

Figure 4.14: Spectral error convergence for the first and second domains with $a = 0.5$ for the Allen–Cahn equation.

	No of fixed-point iterations	
N	First Domain	Second Domain
4	8	10
8	7	9
12	10	12
16	14	19
20	18	19

Table 4.1: Number of fixed-point iterations for the Allen–Cahn equation on first and second domains for different values of N.

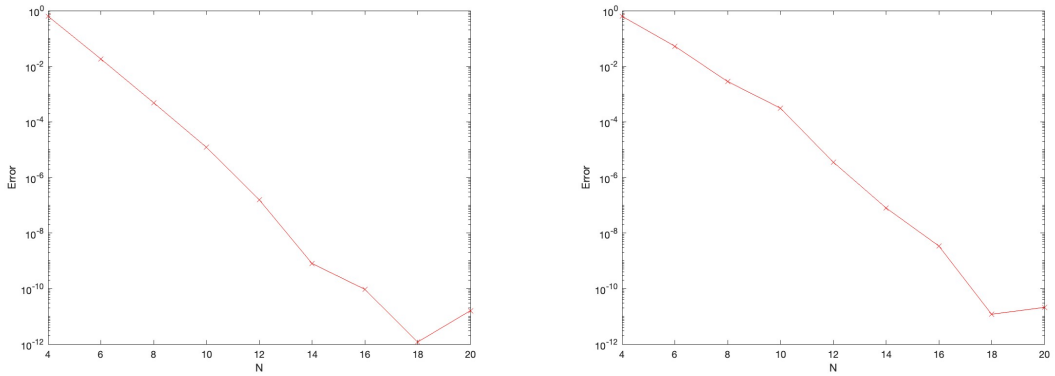

.

Figure 4.15: Spectral error convergence for the first and second domains for the nonlinear Schrödinger equation.

	No of fixed-point iterations	
N	First Domain	Second Domain
4	11	12
8	10	10
12	10	16
16	14	18
20	17	21

Table 4.2: Number of fixed-point iterations for the Schrödinger equation on first and second domains for different values of N.

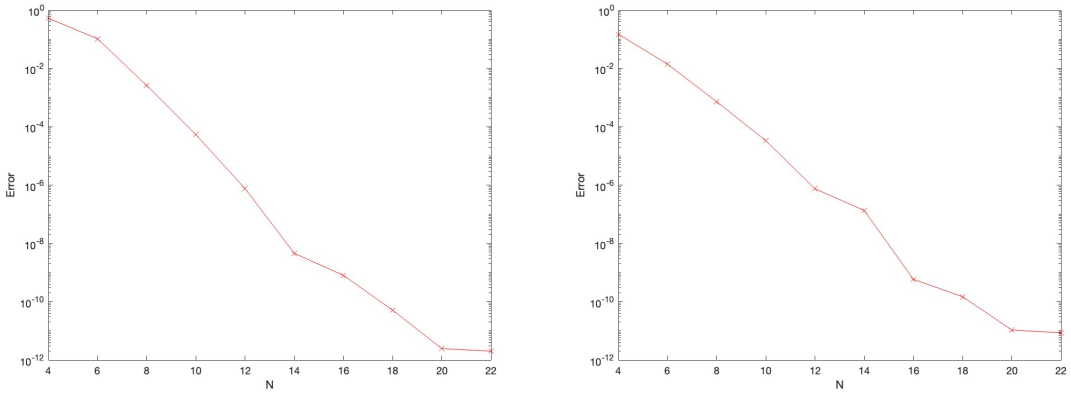

Figure 4.16: Spectral error convergence for the first and second domains with $Re = 10$ for the unsteady Navier–Stokes equation.

	No of fixed-point iterations	
N	First Domain	Second Domain
4	10	11
8	8	10
12	9	19
16	10	18
20	19	22

Table 4.3: Number of fixed-point iterations for the unsteady Navier–Stokes equation on first and second domains for different values of N.

4.2.2.2 Alternating Non-periodic Extension method for non-convex irregular domains

Now we consider PDEs defined in non-convex irregular domains. The first non-convex domain is $\Gamma(x, y) = x^2 + y^2 - (a + b\sin(cy))^2$. The second non-convex domain with a hole, whose inner boundary is defined as $\Gamma(x, y)_{inner} = \frac{y^4}{p^4} + \frac{x^2}{p^2} + y - 1$ and the outer boundary is defined as $\Gamma(x, y)_{outer} = \frac{y^4}{q^4} + \frac{x^2}{q^2} - 0.4y - 1$. In the third domain inner boundary is defined as $\Gamma(x, y)_{inner} = \frac{(x\cos(c_1)+y\sin(c_1))^2}{a_1^2} + \frac{(y\cos(c_1))^4}{b_1^2} - 1$ and the outer boundary is $\Gamma(x, y)_{outer} = \frac{(x\cos(c_2)+y\sin(c_2))^2}{a_2^2} + \frac{(y\cos(c_2))^4}{b_2^2} - 1$ where $a_1 = 0.2, b_1 = 0.2, c_1 = \frac{\pi}{6}$ and $a_2 = 0.75, b_2 = 0.75, c_2 = -1.1\pi$. Fourth domain inner boundary is defined as $\Gamma(x, y)_{inner} = \frac{(x-r)^4}{p^4} + \frac{(y-r)^2}{p^2} - 1$ and the outer boundary is

defined as $\Gamma(x,y)_{outer} = \frac{x^4}{q^4} + \frac{y^2}{q^2} - 1$.

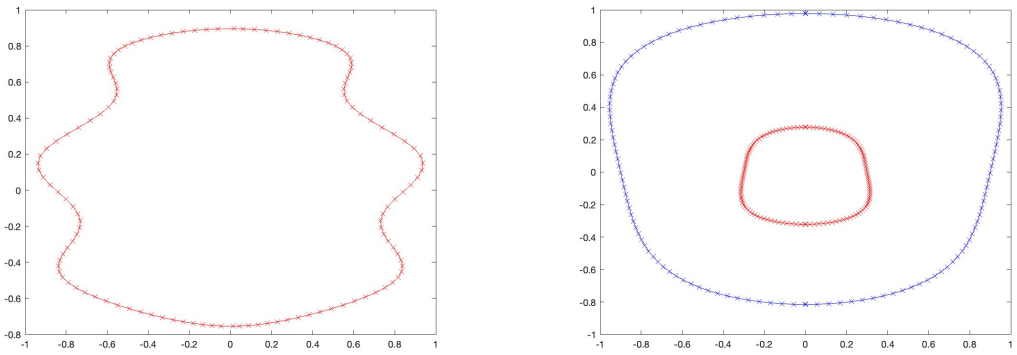

.

Figure 4.17: First irregular domain with $a = 0.85, b = 0.1, c = 10$ and the second irregular domain with $p = 0.3$ and $q = 0.9$.

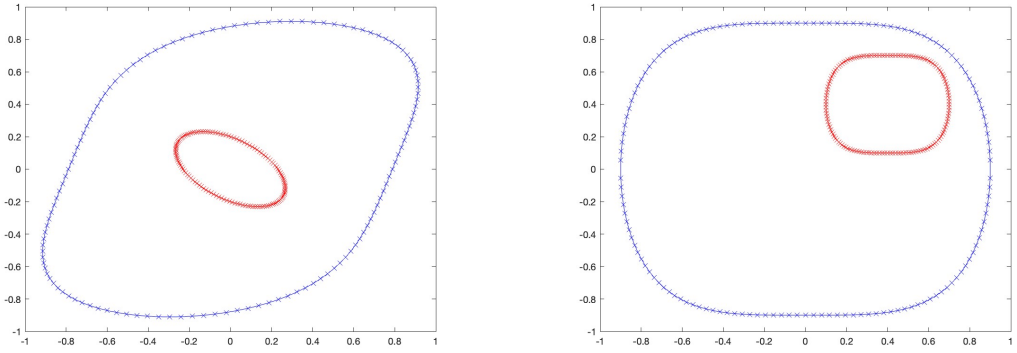

.

Figure 4.18: Third irregular domain with $a_1 = 0.2, b_1 = 0.2, c_1 = \frac{\pi}{6}$ and $a_2 = 0.75, b_2 = 0.75, c_2 = -1.1\pi$ and the fourth domain with $p = 0.3, q = 0.9$ and $r = 0.4$.

The first and second domains are symmetric non-convex domains, while the third and fourth domains are non-symmetric non-convex domains. The third and fourth domains were implemented to examine whether the position of an internal hole shifting from the center to a corner would impact spectral convergence. This setup allows us to investigate whether loss of symmetry or proximity of geometric irregularities to domain boundaries affects the performance of the method. However, based on the numerical results presented, we observe that such changes do not degrade spectral convergence, indicating robustness of the method even under those geometric changes.

First, consider the numerical results for the Poisson equation defined in non-convex irregular geometries.

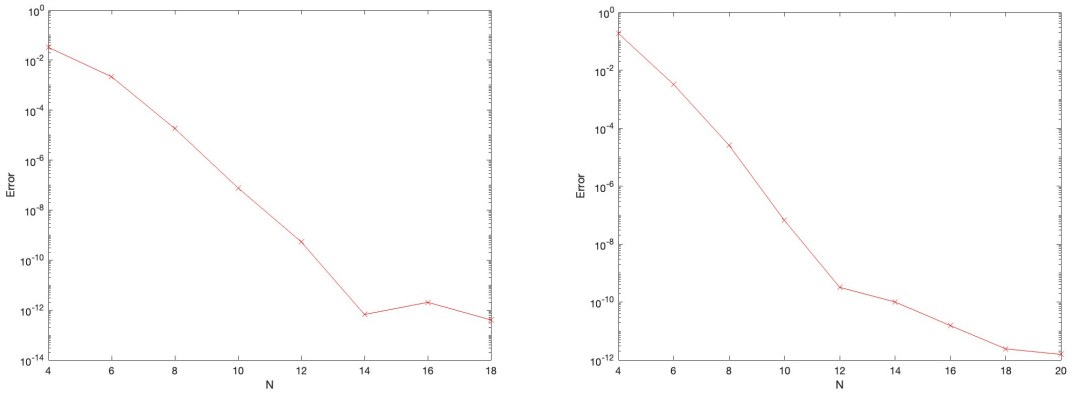

Figure 4.19: Spectral error convergence for the first and second non-convex domains for the Poisson equation.

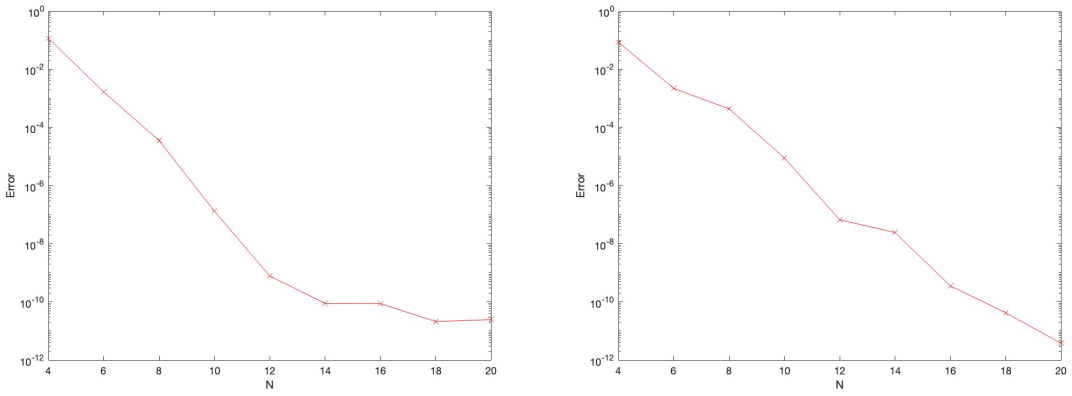

Figure 4.20: Spectral error convergence for the third and fourth non-convex domains for the Poisson equation.

Now consider the numerical results for the stream function formulation of the 2D unsteady Stokes equation defined in non-convex irregular geometries.

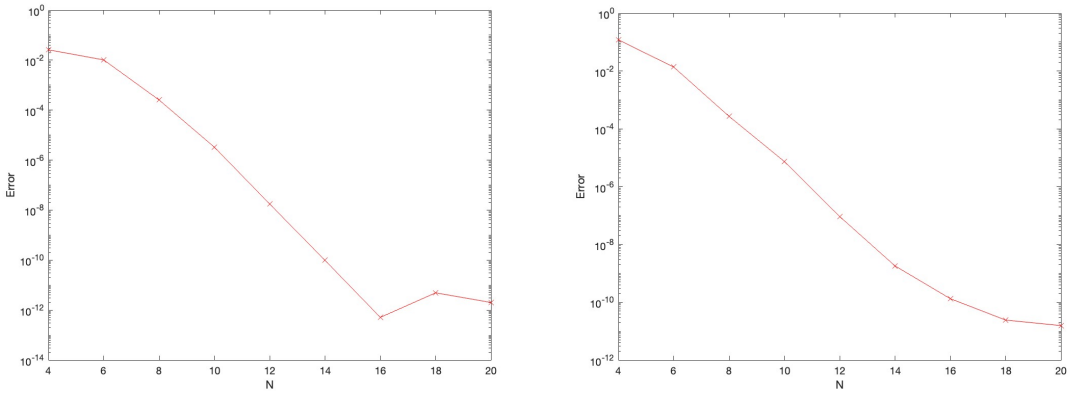

Figure 4.21: Spectral error convergence for the first and second non-convex domains for the unsteady Stokes equation.

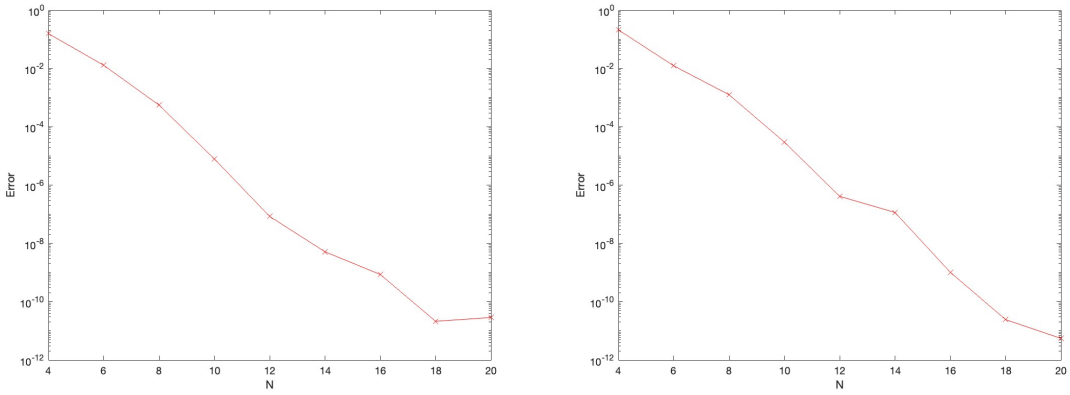

Figure 4.22: Spectral error convergence for the third and fourth non-convex domains for the unsteady Stokes equation.

Next, we present numerical results for the nonlinear PDE, Navier–Stokes equation defined in non-convex irregular geometries.

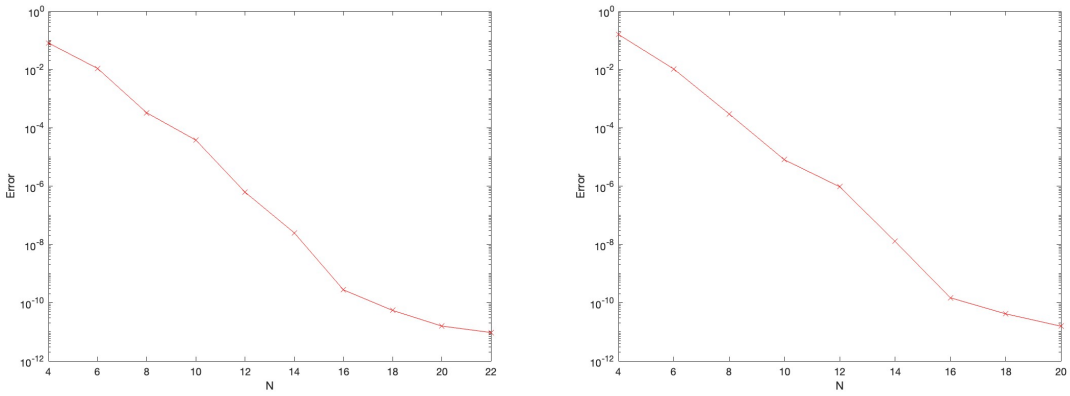

Figure 4.23: Spectral error convergence for the first and second non-convex domains with $Re = 10$ for the unsteady Navier–Stokes equation.

	No of fixed-point iterations	
N	First Domain	Second Domain
4	11	12
8	10	9
12	11	9
16	16	14
20	19	22

Table 4.4: Number of fixed-point iterations for the unsteady Navier–Stokes equation on first and second domains for different values of N.

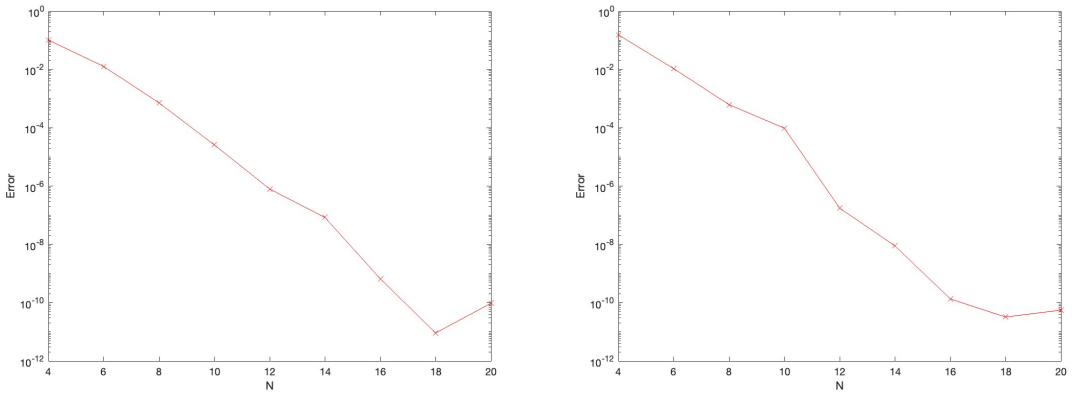

Figure 4.24: Spectral error convergence for the third and fourth non-convex domains with $Re = 10$ for the unsteady Navier–Stokes equation.

	No of fixed-point iterations	
N	Third Domain	Fourth Domain
4	12	14
8	10	12
12	14	21
16	21	25
20	21	24

Table 4.5: Number of fixed-point iterations for the unsteady Navier–Stokes equation on third and fourth domains for different values of N.

5

Conclusions

In this chapter, we provide a brief summary of main findings presented in Chapters 2 through 4 and outline potential directions for future research.

In Chapter 2, we focused on the analysis of space-time spectral methods for the stream function formulation of the unsteady Stokes equation. We proved the condition number estimate of the unsteady Stokes operator in Theorem 2.12 and the convergence analysis of the unsteady Stokes operator in Theorem 2.13.

In Chapter 3, we proposed a numerical method to approximate the solution of PDEs in irregular domains using space-time spectral collocation methods. The main idea is to embed the irregular domain in a regular one and extend the data from the physical domain to the larger regular domain. Initially, we assumed the non-homogeneous term is known, analytic, and periodic in the extended domain. We used the Fourier spectral method to solve the PDE on regular geometry and observed spectral error convergence in both linear and nonlinear PDEs. Then we assumed that the non-homogeneous term is only known in the physical domain and performed a periodic extension to the extended domain. We implemented Boyd's technique [15] for this Fourier extension and observed super-algebraic convergence only. Then we applied the method introduced by Huybrechs [58, 59] to extend

the non-homogeneous term of the PDE from the physical domain to the regular extended domain with exponential accuracy. We have implemented 1D Poisson and Heat equations using this Fourier extension and observed spectral error convergence.

Then, we introduced an algorithm, Alternating Fourier Extension, that can be used for the two-dimensional Fourier extension. In this method, we combined both techniques; 1D Fourier extension and domain embedding. The basic idea of this algorithm is to embed the complex geometry in a larger, regular (rectangular) domain and then apply Fourier extension in both the x and y directions separately until the periodicity error in both directions is very small. We implemented the 2D Poisson equation defined in the square physical domain $(-1,1)^2$, embedded it in a larger domain $(-2,2)^2$, and then applied Alternating Fourier Extension. Here we observed spectral error convergence.

However, we observed an issue; spikes at the corners of the extended domain when applying the Alternating Fourier Extension for a non-rectangular physical domain. We were able to overcome this issue, by implementing a non-periodic extension which we termed the Alternating Non-Periodic Extension. The basic concept of this new algorithm is very similar to the Alternating Fourier Extension. Here, we combined both techniques; 1D non-periodic extension (obtained by modifying the Huybrechs' method) and domain embedding. The basic idea of this algorithm is to embed the complex geometry in a larger, regular (rectangular) domain $(-1,1)^2$ and then apply non-periodic extensions in both the x and y directions once. This algorithm worked well for PDEs defined on both convex and non-convex irregular geometries. Further, we proved spectral convergence of the non-periodic extension for the 1D and 2D Poisson (Theorem 3.15, Theorem 3.18), 1D and 2D Heat (Theorem 3.16, Theorem 3.19), 1D and 2D Stokes (Theorem 3.17, Theorem 3.21) and 2D Wave equation (Theorem 3.20). In addition, we proved the uniqueness of the solution on the extended domain.

In chapter 4, we presented numerical experiments done in MATLAB to demonstrate the accuracy and efficiency of space-time spectral methods for solving PDEs in irregular geometry. First, we presented numerical results when non-homogeneous term is known, analytic, and periodic in the extended domain. Here, we observed spectral error convergence in both linear and nonlinear PDEs. Then we have presented numerical results when non-homogeneous term is only known in the physical domain. We have implemented the 2D Poisson equation, Heat equation, steady and unsteady Stokes equations, Allen–Cahn equation, Schrödinger equation and Navier–Stokes equations defined in convex as well as non-convex irregular domains using Alternating Non-Periodic Extension. Spectral error convergence is observed in each instance.

For our future works, we will continue our ongoing work to prove that every eigenvalue λ of B_4 is real ($\Im\lambda = 0$), a problem that has remained open for more than 20 years. This result is crucial for deriving condition number estimates for higher-order PDEs, such as the space-time beam operator, as it guarantees the stability and accuracy of spectral discretizations for such problems. Further, we hope to find an efficient solver using FFT to solve PDEs in irregular geometries using Alternating Non-Periodic Extension. Moreover, we hope to estimate the condition number for the non-periodic extension algorithm. We would also hope to develop an efficient numerical scheme for Delay PDEs based on the space-time spectral-collocation method, which can be used to significantly speed up the computation of numerical calculations. Since Delay PDEs depend on the solution at previous times, it is necessary to provide a history function that conveys the value of the solution prior to the initial time. Therefore, the space-time spectral method is really good for delay PDEs, especially with large delays. The development of such a numerical scheme for Delay PDEs will further enhance the significance of space-time spectral methods.

Bibliography

[1] D. Agress, P. Guidotti, D. Yan, *The smooth extension embedding method with Chebyshev polynomials*, Numer Methods Partial Differential Eq. 39, (2022), pp. 2355–2377.

[2] D. Agress, P. Guidotti, *The smooth extension embedding method*, SIAM J. Sci. Comput. 43 (2021), no. 1, pp. A446–A471.

[3] B. Adcock, D. Huybrechs, M. Vaquero, *On the numerical stability of Fourier extensions*, Found Comput Math 14, 635–687 (2014). https://doi.org/10.1007/s10208-013-9158-8.

[4] I. Ali, S.Khan, *Application of Legendre spectral collocation method to delay differential and stochastic delay differential equation*, AIP ADVANCES 8, 035301 (2018).

[5] L. Badea, P. Daripa, *On a boundary control approach to domain embedding methods*, SIAM J. Control Optim. 40 (2001), no. 2, pp. 421-449.

[6] L. Badea, P. Daripa, *On a Fourier method of embedding domains using an optimal distributed control*, Numer. Algorithms 32 (2–4) (2003), pp. 261–273.

[7] L. Badea, P. Daripa, *A domain embedding method using the optimal distributed control and a fast algorithm*, Numer. Algorithms 36 (2) (2004), pp. 95–112.

[8] A. Banerjee, N. Garofalo, R. Manna, *A strong unique continuation property for the heat operator with Hardy type potential*, The Journal of Geometric Analysis, 2020.

[9] C. Bernardi, Y. Maday, *Spectral Methods, Techniques of Scientific (Computing (Part 2), Handbook of Numerical Analysis*, Elsevier, 1997.

[10] R.H. Bartels, G.W. Stewart, *Solution of the matrix equation* $AX + XB = C$, Communications of the ACM, 15(9):820–826, 1972.

[11] M.J. Berger, J. Oliger, *Adaptive Mesh Refinement for Hyperbolic Partial Differential Equations*, Journal of Computational Physics, 53(3) (1984), pp. 484-512.

[12] K. Bingham, Y. Kurylev, E. Somersalo, *New analytic and geometric methods in inverse problems: Lectures given at the ems summer school and conference held in edinburgh, scotland 2000*, Springer Science and Business Media, 2013.

[13] J. Boyd, *Fourier embedded domain methods extending a function defined on an irregular region to a rectangle so that the extension is spatially periodic*, Applied Mathematics and Computation 161 (2005), pp. 591–597.

[14] J. Boyd, *A comparison of numerical algorithms for Fourier extension of the first, second, and third kinds*, J. Comput. Phys. 178 (1) (2002), pp. 118–160.

[15] J. Boyd, *Chebyshev and Fourier Spectral Methods*, 2nd ed., Dover, Mineola, New York, 2001.

[16] O. Bruno, *Fast, high-order, high-frequency integral methods for computational acoustics and electromagnetics*, in Topics in Computational Wave Propagation: Direct and Inverse Problems, M. Ainsworth, P. Davies, D. Duncan, P. Martin, and B. Rynne, eds., Lecture Notes Comput. Sci. Engrg. 31, Springer, New York, 2003, pp. 43–82.

[17] O. Bruno, Y. Han, M. Pohlman, *Accurate, high-order representation of complex three-dimensional surfaces via Fourier continuation analysis*, J. Comput. Phys 227 (2007), pp. 1094–1125.

[18] O. Bruno, M. Lyon, *High-order unconditionally stable FC-AD solvers for general smooth domains I. Basic elements*, Journal of Computational Physics 229 (2010), pp. 2009–2033.

[19] O. Bruno, M. Lyon, *High-order unconditionally stable FC-AD solvers for general smooth domains II. Elliptic, parabolic and hyperbolic PDEs; theoretical considerations*, Journal of Computational Physics 229 (2010), pp. 3358–3381.

[20] O. Bruno, J. Paul, *Two-dimensional Fourier Continuation and applications*, Computing and Mathematical Sciences, California Institute of Technology, Preprint, 2020.

[21] A. Bueno-Orovio, *Fourier embedded domain methods: Periodic and C^∞ extension of a function defined on an irregular region to a rectangle via convolution with Gaussian kernels*, Applied Mathematics and Computation 183 (2006), pp. 813–818.

[22] A. Bueno-Orovio, F. Fenton, V. Perez-Garcia, *Spectral Methods for Partial Differential Equations in Irregular Domains: The Spectral Smoothed Boundary Method*, SIAM J. Sci. Comput. 28 (2006), no. 3, pp. 886–900.

[23] A. Bueno-Orovio, V. Perez-Garcia, *Spectral smoothed boundary methods: The role of external boundary conditions*, Numerical Methods for Partial Differential Equations (2006), vol. 22, no. 2, pp. 435-448.

[24] M. Buffat, L. Le Penven, *A spectral fictitious domain method with internal forcing for solving elliptic PDEs*, Journal of Computational Physics, 230 (2011), pp. 2433–2450.

[25] M. Buffat, L. Le Penven, *On the spectral accuracy of a fictitious domain method for elliptic operators in multi-dimensions*, Journal of Computational Physics, 231 (2012), pp. 7893–7906.

[26] X. Cai, D. Keyes, *Nonlinearly Preconditioned Inexact Newton Algorithms*, SIAM J. SCI. COMPUT (2002), vol. 24, no. 1, pp. 183–200.

[27] X. Chen, L. Lin, *A spectral collocation method for elliptic PDEs in irregular domains with Fourier extension*, arXiv preprint arXiv:2101.01234, 2021.

[28] R. Chu, *Unique continuation property for harmonic functions via Carleman's method*, `https://www.math.ucla.edu/~rchu/UCP.pdf`, 2021.

[29] B. David, *Spectrally accurate solutions to inhomogeneous elliptic PDE in smooth geometries using function intension*, Journal of Computational Physics, 470 (2022), 111594.

[30] X. Dai, Y. Maday, *Stable Parareal in time method for first- and second-order hyperbolic systems*, SIAM Journal on Scientific Computing 35 (2013), no. 1, pp. 52–78.

[31] M. Deville, P. Fischer, E. Mund, *High-Order Methods for Incompressible Fluid Flow*, Cambridge University Press, 2002.

[32] V. Dolean, M. Gander, W. Kheriji, F. Kwok, R. Masson, *Nonlinear Preconditioning: How to use a Nonlinear Schwarz Method to Precondition Newton's Method*, SIAM J. Sci. Comput(2016), vol. 38, No. 6, pp. A3357-A3380.

[33] K.S. Eckhoff, C.E. Wasberg, *Solution of parabolic partial differential equations in Complex Geometries by a modified Fourier collocation method*, ICOSAHOM 95: Proceedings of the Third International Conference on Spectral and High Order Methods, 1995.

[34] A. Elghaoui, R. Pasquetti, *Mixed spectral-boundary element embedding algorithms for the Navier–Stokes equations in the vorticity-stream function formulation*, Journal of Computational Physics 153 (1999), pp. 82–100.

[35] A. Elghaoui, R. Pasquetti, *A spectral embedding method applied to the advection-diffusion equation*, Journal of Computational Physics 125 (1996), pp. 464–476.

[36] K.T. Elgindy, *A high-order embedded domain method combining a Predictor–Corrector-Fourier-Continuation-Gram method with an integral Fourier pseudospectral collocation method for solving linear partial differential equations in complex domains*, Journal of Computational and Applied Mathematics 361 (2019), pp. 372–395.

[37] M. Gander, *50 years of time parallel time integration, multiple shooting and time domain decomposition methods*, Contrib. Math. Comput. Sci. 9 (2015), pp. 69–113.

[38] M. Gander, V.T. Lunet, *Parallel-in-Time Integration Methods*, SIAM, 2024.

[39] M. Gander, S. Vandewalle, *Analysis of the parareal time-parallel time-integration method*, SIAM Journal on Scientific Computing 29 (2007), no. 2, pp. 556–578.

[40] R. Glowinski, T. Pan, J. Periaux, *A fictitious domain method for Dirichlet problem and applications*, Computer Methods in Applied Mechanics and Engineering 111 (1994), pp. 283-303.

[41] R. Glowinski, T. Pan, T. Hesla, D. Joseph, J. Periaux, *A fictitious domain approach to the direct numerical simulation of incompressible viscous flow past moving rigid bodies: application to particulate flow*, Journal of Computational Physics 169 (2001), pp. 363–426.

[42] R. Glowinski, Y. Kuznetsov, *Distributed Lagrange multipliers based on fictitious domain method for second order elliptic problems*, Computer Methods in Applied Mechanics and Engineering 196 (2007), pp. 1498-1506.

[43] D. Gottlieb and S. Orszag, *Numerical Analysis of Spectral Methods: Theory and Applications*, Society for Industrial and Applied Mathematics, Philadelphia, Pa., 1977.

[44] H. Golub, H. Welsch, *Calculation of Gauss Quadrature Rules*, (1969), Vol. 23, No. 106, pp. 221–230..

[45] H. Golub, S. Nash, C. Van Loan, *A Hessenberg Schur Method for the Problem* $AX + XB = C$, IEEE Transactions on Automatic Control, (1979), vol. 24, No. 6, pp. 909-913.

[46] B.E. Griffith, S. Qadeer, *The smooth forcing extension method: A high-order technique for solving elliptic equations on complex domains*, Journal of Computational Physics 439 (2021), 110390.

[47] B.E. Griffith, E. Nazockdast, S. Qadeer, *The projection extension method: A spectrally accurate technique for complex domains*, arXiv preprint arXiv:2110.12345, 2021.

[48] Y. Gu, J. Shen, *Accurate and efficient spectral methods for elliptic PDEs in complex domains*, J. Sci. Comput. 83(42), 2020.

[49] Y. Gu, J. Shen, *An efficient spectral method for elliptic PDEs in complex domains with circular embedding*, SIAM J. Sci. Comput. 43(1) (2021), pp. A309–A329.

[50] K. Gumerov, S. Rigg, R. M. Slevinsky, *Fast measure modification of orthogonal polynomials via matrices with displacment structure*,(2024), arXiv:2412.17663.

[51] B. Guo, *Spectral Methods and Their Applications*, World Scientific Publishing Co., Singapore, 1998.

[52] T. S. Gutleb, S. Olver, R. M. Slevinsky, *Polynomial and rational measure modifications of orthogonal polynomials via infinite-dimensional banded matrix factorizations*, Found. Comput. Math. (2024), pp. 1–43.

[53] R. D. Guy, D. B. Stein, B. Thomases, *A Fourier spectral method for solving PDEs in complex geometries with smooth extension*, Journal of Computational Physics 335 (2017), pp. 155–178.

[54] R. D. Guy, D. B. Stein, B. Thomases, *Spectrally accurate solution of PDEs in arbitrary smooth domains using extension methods*, Journal of Computational Physics 469 (2022), Article 111594.

[55] R.D. Guy, D.B. Stein, B. Thomases, *Immersed boundary smooth extension - A high-order method for solving PDEs on arbitrary smooth domains using Fourier spectral methods*, Journal of Computational Physics, 304 (2016), pp. 252-274.

[56] L. Hörmander, *The analysis of linear partial differential operators III: Pseudo-differential operators*, Grundlehren der mathematischen Wissenschaften, vol. 274, Springer-Verlag, Berlin, 1985.

[57] G. Horton, S. Vandewalle, *A space-time multigrid method for parabolic partial differential equations*, SIAM J. Sci. Comput. 16 (1995), No. 4, pp. 848–864.

[58] D. Huybrechs, *On the Fourier extension of nonperiodic functions*, SIAM Journal on Numerical Analysis, (2010), vol. 47, No. 6, pp. 4326–4355.

[59] R. Matthysen, D. Huybrechs, *Fast Algorithms for the Computation of Fourier Extensions of Arbitrary Length*, SIAM J. Sci. Comput, (2016), vol. 38, No. 2, pp. A899–A922.

[60] Z. Jackiewicz, B. Zubik-Kowal, *Spectral collocation and waveform relaxation methods for nonlinear delay partial differential equations*, Applied Numerical Mathematics 56 (2006), pp. 433–443.

[61] G.E. Karniadakis, S.J. Sherwin, *Spectral/hp Element Methods for CFD*, Oxford University Press, New York, 1999.

[62] D. A. Kopriva, J. L. Thomas, *A spectral method for solving elliptic problems in complex geometries using smooth extension*, J. Comput. Phys., 335 (2017), pp. 497–515.

[63] K. Korczak, A. Patera, *An isoparametric spectral element method for solution of the Navier–Stokes equations in complex geometry*, J. Comput. Phys., 62 (1986), pp. 361–382.

[64] G.P. Koomullil, Z.U.A. Warsi, *Numerical Mapping of Arbitrary domains using spectral methods*, J. Comput. Phys., 104 (1993), pp. 251–262.

[65] J. Le Rousseau, G. Lebeau, *On Carleman estimates for elliptic and parabolic operators. Applications to unique continuation and control of parabolic equations*, ESAIM: Control, Optimisation and Calculus of Variations, 18 (2012), no. 3, pp. 712–747.

[66] X. Li, J. Lowengrub, A. Ratz, A. Voigt, *Solving pdes in complex geometries: A diffuse domain approach*, Commun. Math. Sci.7 (2009), no. 1, pp. 81-107.

[67] W. Liu, J. Sun, B. Wu, *Space-time spectral collocation method for the one-dimensional Sine-Gordon equation*, Numerical Methods for Partial Differential Equations 31 (2015), no. 3, pp. 670–690.

[68] M. Lyon, *Sobolev smoothing of SVD-based Fourier continuations*, Applied Mathematics Letters 25 (2012), pp. 2227–2231.

[69] M. Lyon, *A fast algorithm for Fourier continuation*, SIAM J. Sci. Comput. 33 (6) (2011), pp. 3241–3260.

[70] A. Kaur, S. Lui, *Space-time spectral method for the Stokes problem*, Applied Numerical Mathematics, 187 (2023), pp. 206–234.

[71] A. Kaur, S. Lui, *New lower bounds on the minimum singular value of a matrix*, Linear Algebra and its Applications, 666 (2023), pp. 62–95.

[72] S. Lui, *Spectral Domain embedding for Elliptic PDEs in Complex Geometry*, J. Comput. and Appl. Math. 225 (2009), pp541-557.

[73] S. Lui, *Legendre spectral collocation in space and time for PDEs*, Numer. Math., 136 (2017), pp. 75-99.

[74] S. Lui, S. Nataj, *Chebyshev spectral collocation in space and time for the heat equation*, Elect. Trans. Numer. Anal., 52 (2020), pp. 295-319.

[75] S. Lui, S. Nataj, *Spectral collocation in space and time for linear PDEs*, J. Comput. Phys., 424 (2021) 109843.

[76] M. Lyon, *Sobolev smoothing of SVD-based Fourier continuations*, Applied Mathematics Letters 62 (2012), pp. 1790–1803.

[77] M. Lyon, *Approximation error in regularized SVD-based Fourier continuations*, Applied Mathematics Letters 25 (2012), pp. 2227–2231.

[78] J. Mead, B. Zubik-Kowal, *An iterated pseudospectral method for delay partial differential equations*, Applied Numerical Mathematics 55 (2005), pp. 227–250.

[79] S. Olver, R. M. Slevinsky, A. Townsend, *Fast algorithms using orthogonal polynomials*, Acta Numerica, 29(2020), pp. 573–699.

[80] B. Orel, A. Perne, *Computations with half-range Chebyshev polynomials*, J. Comput. and Appl. Math., 236 (2012), pp. 1753–1765.

[81] S. Orszag, *Spectral methods for problems in complex geometries*, J. Comput. Phys., 37 (1980), pp. 70–92.

[82] W.L.C. Piyasundara, *MSc Thesis: Space-time spectral collocation methods for the magnetohydrodynamics equations*, `http://hdl.handle.net/1993/35927`, 2021.

[83] S.C. Reddy, J.A.C. Weideman, *The accuracy of the Chebyshev differencing method for analytic functions*, SIAM J. Numer. Anal. 42(5) (2005), pp. 2176–2187.

[84] M. Salo, *Unique continuation for elliptic equations*, Lectures on Inverse Problems (Chapter on UCP), University of Jyväskylä, 2014.

[85] J. Shen, T. Tang, L.Wang, *Spectral Methods*, Springer-Verlag, Berlin, Heidelberg, 2011.

[86] D. Shirokoff, J.C. Nave, *A sharp interface active penalty method for the Incompressible Navier–Stokes Equations*, J. Sci. Comput. 62 (2015), pp. 53–77.

[87] H. Tal-Ezer, *Spectral methods in time for parabolic problems*, SIAM Journal on Numerical Analysis 26 (1989), no. 1, pp. 1-11.

[88] H. Tal-Ezer, *Spectral methods in time for hyperbolic equations*, SIAM Journal on Numerical Analysis 23 (1986), no. 1, pp. 11-26.

[89] T. Tang, X. Xu, *Accuracy enhancement using spectral post-processing for differential equations and integral equations*, Commun. Comput. Phys. 5 (2009), no. 2, pp. 779–792.

[90] D. Tataru, *Unique continuation for solutions to PDEs; between Hörmander's theorem and Holmgren's theorem*, Communications in Partial Differential Equations, 20 (1995), no. 5-6, pp. 855–884.

[91] L. Trefethen, J. Weideman, *The eigenvalues of second-order spectral differentiation matrices*, SIAM J. Numer. Anal. 25 (6) (1988), pp. 1279–1298.

[92] S. Vessella, *Unique Continuation Properties for Partial Differential Equations: Introduction to the Stability Estimates for Inverse Problems*, Birkhäuser Advanced Texts Basler Lehrbücher, Springer Nature Switzerland, 2025.

[93] J.C. Wheeler, *Modified moments and Gaussian quadratures, in: Proceedings of the International Conference of Padé Approximants, Continued Fractions and Related Topics*, Univ. Colorado, Boulder, (4) (1974), pp. 287–296.

[94] J. Zhu, Y. Ma, *Fictitious domain method with penalty for an incompressible fluid*, Numer. Methods Partial Differential Equations 26 (1) (2010), pp. 229–238.

[95] S. Zhang, *A domain embedding method for mixed boundary value problems*, C. R. Math. 343 (4) (2006), pp. 287–290.

[96] ____, *Legendre spectral collocation method for second-order nonlinear ordinary partial differential equations*, Discrete and Continuous Dynamical Systems 19 (2014), pp. 299–322.

[97] ____, *A Legendre spectral method in time for first-order hyperbolic equations*, Applied Numerical Mathematics 57 (2007), no. 1, pp. 1-11.